

UNIVERSITÄTSKLINIKUM HAMBURG-EPPENDORF

Zentrum für Onkologie
Strahlentherapie und Radioonkologie

Direktorin: Prof. Dr. med. Cordula Petersen

DNA damage response and double strand break repair in prostate cancer: From mechanisms to clinical application

Dissertation

zur Erlangung des Doktorgrades PhD
an der Medizinischen Fakultät der Universität Hamburg

vorgelegt von:

Mohamed Elsayed Elsayed Mohamed Elsesy (M.Sc.)
Aus Sharkia, Ägypten

Hamburg 2023

**Angenommen von der
Medizinischen Fakultät der Universität Hamburg am: 07.11.2023**

**Veröffentlicht mit Genehmigung der
Medizinischen Fakultät der Universität Hamburg.**

Prüfungsausschuss, der/die Vorsitzende: Prof. Dr. Kai Rothkamm

Prüfungsausschuss, zweite/r Gutachter/in: Prof. Dr. Gunhild von Amsberg

Printed with the support of the German Academic Exchange Service (DAAD)

1.	Synopsis.....	1
1.1.	Introduction	1
1.1.1.	Cancer of the prostate	1
1.1.2.	Management of prostate cancer	1
1.1.3.	Castration resistant prostate cancer	6
1.1.4.	DDR defects in prostate cancer	8
1.1.5.	Molecular therapeutic targeting of DNA repair in prostate cancer.....	10
1.2.	Aim of the work.....	13
1.3.	Materials and Methods.....	14
1.3.1.	Patient sample collection	14
1.3.2.	Prostate tumour tissue processing and organoid establishment	14
1.3.3.	Tissue slice cultures.....	14
1.3.4.	<i>Ex-vivo</i> induction of castration resistance	15
1.3.5.	Cell culture, drugs, and X-irradiation	15
1.3.6.	Whole genome sequencing (WGS) and RNA-sequencing (RNA-SEQ).....	15
1.3.7.	DNA methylation profiling	15
1.3.8.	Proliferation assay.....	16
1.3.9.	Colony formation assay (2D and 3D).....	16
1.3.10.	Migration assay	16
1.3.11.	Western blot.....	17
1.3.12.	Immunofluorescence	17
1.3.13.	Histology and imaging	17
1.3.14.	Cell cycle analysis and apoptosis quantification	18
1.3.15.	Graphs and statistics	18
1.4.	Summary of results	19
1.4.1.	Second-generation antiandrogen therapy radiosensitizes prostate cancer regardless of castration state through inhibition of DNA double strand break repair.....	19
1.4.2.	Pre-clinical patient-derived modelling of castration resistant prostate cancer facilitates individualized assessment of homologous recombination repair deficient disease.....	20
1.5.	Discussion.....	22
1.5.1.	AHT as radiosensitising agents	22
1.5.2.	Pre-clinical 3D models for precision medicine in PCa	23
1.5.3.	Future direction.....	24
2.	List of abbreviations.....	26
3.	References	28
4.	Publication list.....	35
4.1.	Publication 1	35
4.2.	Publication 2	63
5.	Zusammenfassung	88
6.	Summary	91
7.	Erklärung des Eigenanteils an den Publikationen.....	93
8.	Acknowledgement	94
9.	Curriculum Vitae (CV).....	95
10.	Eidesstattliche Erklärung.....	98

1. Synopsis

1.1. Introduction

1.1.1. Cancer of the prostate

Prostate cancer (PCa) is a complex global health problem that is known to be the most frequently diagnosed cancer in 105 countries. In Europe, it is the most common non-cutaneous cancer affecting men. Also, it is considered the third most common cause of cancer-related death (Marhold, Kramer et al. 2022). As a disease entity, PCa is marked by extensive molecular inter- and intra-tumoural heterogeneity, which creates a continuing clinical paradox. The clinical variance of this tumour can range widely from indolent with low-risk to advanced status which can be either organ-confined but with therapy resistance or highly invasive with metastasis, mainly in bones and pelvic lymph nodes, which are the most common reservoirs for disseminated prostate tumour cells.

1.1.2. Management of prostate cancer

There are three main therapeutic pillars known in the management of PCa namely surgery, radiotherapy (RT), and androgen deprivation therapy (ADT) or different anti-hormonal therapies (AHTs) as shown in Fig. 1. A very safe and effective method that was developed since more than 40 years is the anatomic approach for radical prostatectomy (RP). RP aims to remove all PCa with negative surgical margins, so it is usually prescribed for early-stage patients with organ-confined cancer (Walsh 1998), while with high-risk patients, monotherapy will not be adequate to fully eradicate microscopic nests of tumour cells in the prostate bed. Therefore, either adjuvant or salvage therapy is always required (Yossepowitch, Eggener et al. 2008, Ma, Lilleby et al. 2020). The factors such as pathologic findings and Gleason score in the surgical biopsies as well as serum prostate specific antigen (PSA) level before surgery determine progression rates after RP. Post-RP, either local or distant relapse in high proportion of patients is expected. Patients with local recurrence should be treated with salvage RT and/or ADT, while for those with distant recurrence, ADT is combined with either chemotherapeutics such as docetaxel and cabazitaxel, or novel AHTs such as abiraterone, enzalutamide, apalutamide, and darolutamide (Paschalis and de Bono 2020).

Introduction

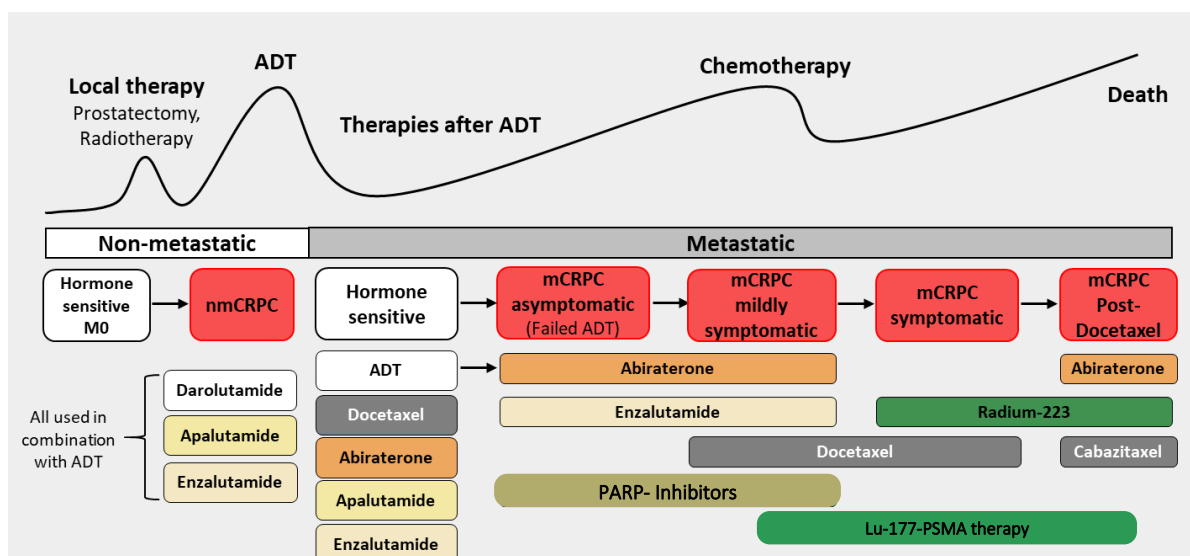


Fig. 1. Clinical course and management of prostate cancer. The figure illustrates different episodes from therapy response followed by relapse during the lifetime of prostate cancer patient. Prostatectomy and/or radiotherapy are the optimum treatment approaches when the tumour is localized. At this phase, the tumour depends on androgens and therefore amenable to androgen deprivation therapy (ADT), however the majority of these patients will progress within 2 years to the incurable lethal stage castration resistant prostate cancer (CRPC). Several therapeutic regimens are used to manage this stage, such as antiandrogens including enzalutamide, apalutamide, and darolutamide; the selective cytochrome P450 17A1 (CYP17A1) inhibitor abiraterone acetate; and the two taxane-based chemotherapies docetaxel and cabazitaxel offering a short progression-free survival. The targeted alpha therapy, radium- 223 and beta particle emitting therapy, Lu-177-PSMA are particularly indicated in case of metastases. This figure was modified from (Merseburger, Alcaraz et al. 2016, Paschalis and de Bono 2020).

RT which is the second pillar in the management of localized PCa cases can be either as ablative therapy for curative approaches or as salvage therapy for recurrent cases post-RP. Over the years, various image guided techniques along with efficient treatment planning systems contributed to a significant advance in the precision of administering radiation doses. This was achieved through shortening the overall exposure time with different planning regimens of dose fractionation meantime achieving ultimate oncological control with minimal damage to nearby normal structures (Higgins, McLaren et al. 2006). RT is usually administered either by external beam (EBRT) or brachytherapy techniques. EBRT is a standard mode of treatment delivery for localized PCa patients with different treatment schedules of dose fractionation. Conventional EBRT delivers daily doses or 1.8-2.0 Gy fractions over 39–45 treatment sessions (Kupelian, Thakkar et al. 2005). The low alpha/beta ratio ranging from 1.5 to 3.1 implied in PCa - unlike many other tumour entities and similar to or below normal tissues (Strouthos, Tselis et al. 2018) - supports the benefits gained from administering higher radiation doses per session with moderate hypofractionation regimens which utilize daily (2.4 to 4 Gy) fraction sizes over 20–30 treatment sessions. A modern approach termed stereotactic

Introduction

body RT employs ultrahypofractionation regimens that deliver ≥ 5 Gy per fraction for 3-5 fractions. Such ultrahypofractionation RT regimens paved the way for a favorable safety and toxicity profile with remarkable biochemical tumour control outcomes for localized PCa patients (Patel, Switchenko et al. 2020). Prostate brachytherapy is an alternative to EBRT that requires radioactive source implantation in the prostate as a source of radiation. Two forms are known for brachytherapy, namely, low dose rate (LDRBT) brachytherapy and high dose rate brachytherapy (HDRBT) (Henry, Pieters et al. 2022). LDRBT approach utilizes permanent interstitial implantation of radioactive seeds within the prostate to release radiation slowly over several months. On the other hand, HDRBT involves temporary placement of high-activity radiation sources (e.g., iridium-192) within the prostate (Edgren, Ekelund et al. 2006). According to the National Comprehensive Cancer Network (NCCN) guidelines by 2020, HDRBT is the standard of care option for very low, and intermediate risk subgroups of localized PCa patients (Mohler, Antonarakis et al. 2019).

ADT is the mainstay for therapeutic interventions through either surgical or chemical castration. ADT relies on depleting androgens or inhibiting signaling through androgen receptor (AR) signaling axis (Chen, Clegg et al. 2009). Synthesis of androgens is regulated through Hypothalamic–Pituitary–Gonadal Axis (Fig. 2). The hypothalamus secretes gonadotropin-releasing hormone (GnRH) which acts on the pituitary gland to release luteinizing hormone (LH) that acts on Leydig cells in the testicles to control androgen biosynthesis. Upon binding of AR to its native ligands as testosterone or the much more potent form 5α -dihydrotestosterone (DHT), it will be then translocated to the nucleus, where the AR dimers bind to androgen response elements (AREs) in the promoter regions of different target genes eliciting transcription networks that maintain not only growth and survival but also genomic stability and DNA repair, which all together in PCa will end with deregulated cell homeostasis (Tan, Li et al. 2015).

Dysregulated AR signaling axis remains to be the prominent hallmark of PCa as AR signaling axis will continue to be the backbone for PCa pathogenesis and a key regulator in the initiation and progression of PCa disease. This dependence of PCa cells on the sustained AR activity provided a strong mechanistic rationale for different therapeutic strategies, including surgical castration, GnRH analogues (e.g., leuprolide and goserelin), antiandrogens (e.g., nilutamide, flutamide, and bicalutamide), novel AR-directed therapies (e.g., apalutamide, enzalutamide, and darolutamide), and androgen biosynthesis inhibitors (e.g., abiraterone acetate) (Bambury

Introduction

and Rathkopf 2016). It was firstly showed by Huggins and Hodges in the 1940s that the removal of testicles by surgical castration provided a prominent success in prostate tumour regression (Huggins and Hodges 1972). Although ADT through orchiectomy can reduce circulating testosterone to more than 90% within 24 h with promptly shrinking tumour mass, it is usually accompanied with psychological problems derived mainly from erectile dysfunction as well impaired libido in most cases. Surgical castration remained the standard care until in the 1980s where GnRH agonist was firstly introduced. These GnRH analogues prolong the activation of GnRH receptors and accordingly leads to desensitization, which will eventually result in suppression of gonadotrophin secretion and suppression of circulating testosterone to the castrate level. In the same era, antiandrogens were introduced which act differently by preventing the androgens from binding to the AR. Unlike nonsteroidal antiandrogens (NSAAs) (e.g., bicalutamide), steroidal antiandrogens (SAAs) (e.g., spironolactone and oxendolone) had limited clinical applications because of their many unwanted side effects as well as limited clinical efficacy. Flutamide was the first widely used NSAA followed by nilutamide for treatment of PCa patients. Many undesired side effects including gynecomastia resulted in rapid withdrawal of flutamide. Also, visual problems, alcohol intolerance and respiratory disturbances resulted in limited use of nilutamide in treatment of PCa. Bicalutamide which was firstly approved by FDA in 1995, showed higher efficacy with less side effects compared to previous NSAAs. Unfortunately, in 2-3 years posttreatment patients acquire resistance against bicalutamide that was rationalized by accumulated mutations in the AR (Guo, Yeh et al. 2017).

Improving efficacy, selectivity as well as overcoming the acquired resistance that is the inevitable event seen with all different antiandrogens resulted in the appearance of novel antiandrogens. Because of its higher binding affinity to AR, enzalutamide shows better efficacy compared to all previous NSAAs. Moreover, enzalutamide not only prevents androgens from binding to AR but also impairs binding of AR to AREs, which induces apoptosis and impairs cellular proliferation (Tran, Ouk et al. 2009, Bennett and Ingason 2014). Another common second-generation antiandrogen is apalutamide or commonly known as ARN-509. ARN-509 is structurally and mechanistically analogous to enzalutamide. ARN-509 shows higher potency than enzalutamide which allowed the use of lower doses than enzalutamide to achieve equal efficacy, resulting in less toxicity. ARN-509 is well tolerated with fewer toxic effects due to its

Introduction

lower central nervous system distribution and hence lower risk of seizures and other central side effects (Rathkopf, Morris et al. 2013).

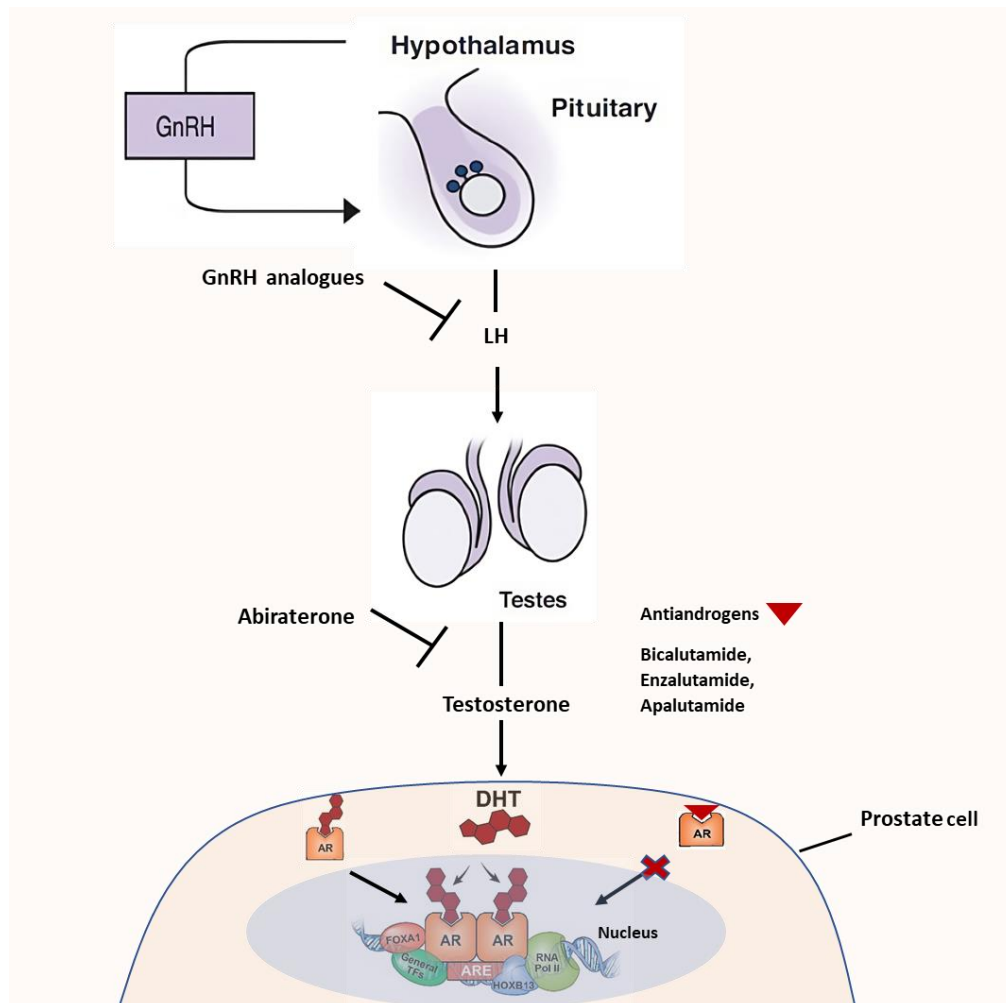


Fig. 2. Androgen signalling axis and its inhibitors in prostate cancer. The synthesis of androgen is epically regulated by the hypothalamic-pituitary-gonadal axis through secretion of gonadotropin-releasing hormone (GnRH) and luteinising hormone (LH). GnRH analogues suppress the production of systemic testosterone. Other agents including bicalutamide, enzalutamide, apalutamide block the binding between androgens and androgen receptor (AR). Abiraterone inhibits androgen biosynthesis.

Depletion of circulating androgens or blocking the AR using the different available anti androgens might be not enough to completely shut down AR signaling axis in some cases. In such scenario, intratumorally de novo testosterone synthesis from cholesterol is seen or even from other weak adrenal androgens through sequential steps mediated by cytochrome P450 enzymes such as CYP11A1 and CYP17A1. Abiraterone acetate (AA), which was introduced in the clinical setting in 2011 showed promising results in reducing androgen levels to the

castrate level within the PCa itself. Unlike ketoconazole which was used firstly in such cases with non-specific and weak inhibitory effect on CYP family, AA showed better safety profile by selectively inhibiting CYP17 complex with more clinical effectiveness manifested by higher potency up to 30 folds compared to ketoconazole (Montgomery, Mostaghel et al. 2008, Vasaitis, Bruno et al. 2011). Remarkably, AA showed more potent anti-tumour activity which is explained by its dual mechanism of action. Besides its well-known mode of action of inhibiting androgen biosynthesis intratumorally, abiraterone metabolite named Δ^4 -abiraterone (D4A) acts through competitive AR antagonism providing comparable potency seen with enzalutamide (Li, Bishop et al. 2015).

For better efficacy with prolonging overall survival and delaying acquired resistance, androgens/AR modulating agents are rarely used as monotherapy, instead they are usually combined with other anti-androgens especially in advanced cases. Another favourable treatment combination, which is a standard-of-care in PCa management is combining RT with ADTs or anti-androgens (Ghashghaei, Kucharczyk et al. 2019). It is based on the observation that the DNA repair machinery is fueled by AR signaling (Bartek, Mistrik et al. 2013). As a transcription factor, activated AR was reported to activate the transcription of varieties of key components of DNA repair machinery (Goodwin, Schiewer et al. 2013). As hyperactivated AR signaling is a manifest of PCa, RT alone would end up with resistance through this enhanced DNA repair capacity. Suppression of AR signaling in advance to RT through ADTs or AHTs have been representing a golden therapeutic strategy in PCa (Böhmer, Wirth et al. 2016).

1.1.3. Castration resistant prostate cancer

Drugs that deprive androgens in the blood circulation of PCa patients or other AR blockers play a paramount role in controlling the disease providing immediate palliative benefits. Unfortunately, some of these patients within 2-3 years present with primary or acquired resistance to these agents and progress to an incurable stage of disease termed castration resistant prostate cancer (CRPC) (Morote, Aguilar et al. 2022). In the last decade, many studies tried to describe the different mechanisms responsible for inducing resistance. These mechanisms include some non-AR-related and several AR-related pathways, such as amplification or mutation of AR, expression of AR splice variants, intratumoural androgen biosynthesis, and increased steroidogenesis (Waltering, Urbanucci et al. 2012). The continued activation of the AR signaling axis represents a distinctive mechanism of resistance.

Introduction

Overexpression of AR as a result of AR gain or amplification causes hypersensitivity to even very low levels of androgens, leading to resistance to AR blockers (Aggarwal, Thomas et al. 2015). In addition, post-translational modifications in the AR including methylation, ubiquitylation, and phosphorylation were found to mediate resistance to AHTs through enhancement of the AR transcriptional activity (Gioeli and Paschal 2012). Although PCa is known to carry a low mutational burden, some mutations in AR are implicated also in the resistance induction process. Different hotspot mutations were described in AR, which lead to differential response to AHTs in PCa patients. For example, mutations in exon 8 lead to conformational changes in the AR binding domain, forcing the AR blockers to act as an agonist. Moreover, T877A AR mutation has been proposed to confer resistance against abiraterone, while F876L mutation results in enzalutamide and ARN-509 to act as partial agonists in PCa patients (Taplin, Bublely et al. 1999, Korpai, Korn et al. 2013). A more prominent resistance mechanism to AR blockers is the expression of splice variants of AR such as AR-V7 that lacks a ligand binding domain and therefore is constitutively active even in the absence of androgens (Dehm and Tindall 2011, Cao, Qi et al. 2014). Increased steroidogenesis is also a well-known mechanism for resistance against AR-targeted therapy. In such patients and after ADT, there is an increased intratumoral testosterone and DHT synthesis from weak androgens produced by adrenal gland. This results in AR reactivation that also can be through the overexpression of CYP17A1 and de novo synthesis of androgens from cholesterol (Mostaghel, Marck et al. 2011). A very aggressive stage arises with progression of disease to neuroendocrine carcinoma of the prostate where those patients show a loss of AR and hence a resistance status to all agents that modulate the AR signaling pathway (Conteduca, Oromendia et al. 2019). Furthermore, there are other AR independent pathways implicated in the resistance process. The activation of different signaling pathways, such as the phosphatidylinositol 3-kinase (PI3K)/protein kinase B (Akt), nuclear factor kappa-light-chain-enhancer of activated B cells (NF- κ B), and glucocorticoid receptor, trigger cell survival and proliferation and mediate resistance against AR-targeted agents. It was reported that the two oncogenic pathways AR and PI3K-AKT are involved in reciprocal feedback regulation, which means that inhibition of one of them will activate the other. The sustained activation of PI3K signaling provides a potential mechanism of resistance to AR inhibitors (Rotinen, You et al. 2018).

Eventually, the progression from hormone-naïve to hormone-resistant status is the inevitable fate. This lethal stage of disease still represents the most vexing problem facing PCa patients

as well as medical oncologists. Up to date the ideal treatment plan, including best first choice, timing, and the best following treatment option in case of resistance to one therapy remains controversial. Further deep understanding to the mechanisms that play the hidden role in the progression to this aggressive stage will facilitate more the way to re-delineate the ideal treatment sequencing pathway.

1.1.4. DDR defects in prostate cancer

Genome stability is continuously challenged by many DNA lesions arising from either endogenous genotoxic insults, which result as a consequence of normal cellular metabolism such as reactive oxygen intermediates, or exogenously after the exposure to DNA targeting agents such as various cytotoxic chemicals or IR. Defects in DNA-repair after the exposure to any of these DNA insults can cause genomic instability and subsequently lead to cancer susceptibility or cell death (Negrini, Gorgoulis et al. 2010). Cells are guarded by very tight and complicated checkpoint mechanisms to control any DNA lesions which are then repaired by a series of repair pathways such as nucleotide excision repair, base excision repair, or double-strand break (DSB) repair. DSBs are the most deleterious form of DNA damage. Unlike single strand breaks, DSBs have no complementary DNA strand to be used as a template for repair. DSBs are particularly lethal as, if incorrectly repaired or unrepaired, they can cause various genomic rearrangements such as deletions, translocations, and fusions in the DNA (Elliott and Jasin 2002). Two classical pathways are known to be used by the cells to repair DSBs namely, non-homologous DNA end joining (NHEJ) and homologous recombination (HR) pathways (Helleday, Lo et al. 2007). The NHEJ is the dominant DNA repair pathway as it is active throughout the cell cycle. This system repairs DSBs through the re-ligation of the DNA ends in a flexible manner without relying on a homologous template, therefore it is much more prone to frequent mutation errors (Chang, Pannunzio et al. 2017). On the other hand, the HRR system is restricted to S and G2 phases of the cell cycle as it requires a homologous sequence as a template to guide the repair. The coordination between the checkpoint machinery implemented in the S and G2 phases and different key mediators of HRR including, among many others, RAD51, RAD51 paralogs, BRCA1, BRCA2, and PALB2 proteins, provides a very efficient repair system with high fidelity and error-free mode (Wright, Shah et al. 2018). However, the maintenance of the genome stability is guided by the balance between both pathways. Despite all of these intricate repair mechanisms, variable genomic aberrations have been frequently observed with PCa progression. The characterization of the genomic and

Introduction

transcriptomic landscape of PCa through different comprehensive molecular analysis studies of primary prostate carcinomas as well as advanced cases nourished this research area with the molecular underpinnings that might play a pivotal role in PCa initiation and progression (Cancer-Genome-Atlas-Research-Network. 2015, Fraser, Sabelnykova et al. 2017, Das, Sjöström et al. 2021, De Vargas Roditi, Jacobs et al. 2022, Song, Weinstein et al. 2022).

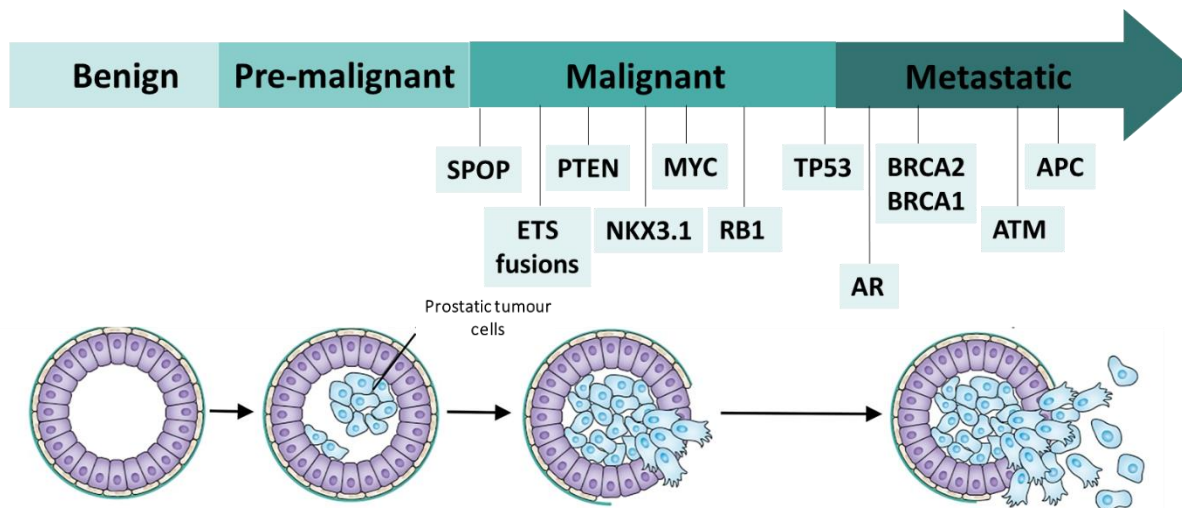


Fig. 3. Common genomic lesions in prostate cancer according to their enrichment during disease progression. Inter- and intra-tumour heterogeneity with variable genetic alterations is a usual attribute to PCa. For example, the transmembrane protease serine 2:v-ets erythroblastosis virus E26 oncogene homolog (*TMPRSS2:ERG*) gene fusion, tumour protein P53 (TP53) mutation, phosphatase and tensin homolog (PTEN) and retinoblastoma 1 (RB1) deletion, amplification of the proto-oncogene MYC are common genetic lesions seen in all PCa stages. This contrasts with the early event, speckle-type POZ protein (SPOP) mutation that usually seen in early PCas. The deletion or the loss of function of the homeobox protein NKX3.1 occurs also early in PCa but remarkably with an increase in its incidence with disease progression. While AR amplification and mutations in homologous recombination repair (HRR) genes such as breast cancer 1,2 (BRCA1,2,) and ataxia telangiectasia mutated (ATM) are enriched in metastatic castration resistant prostate cancer (mCRPC). This figure was modified from (Mills 2014, Rebello, Oing et al. 2021).

Genetic susceptibility has long been known as prime risk factor for PCa (Fig. 3). Unlike other cancers, PCa is known with limited mutational burden, which is approximately 1 per megabase (MB) with primary disease and approximately 4 per Mb in mCRPC. Usually, these alterations are markedly common in either oncogenes or tumour suppressor genes, which eventually results in functional defects through dysregulation of discrete biological pathways like cell cycle progression, PI3K–AKT signaling, wnt pathway and much more importantly DNA damage repair (Rebello, Oing et al. 2021). The transmembrane protease serine 2:v-ets erythroblastosis virus E26 oncogene homolog (*TMPRSS2:ERG*) gene fusion is the most frequent rearrangement in PCa, which results in ERG overexpression. A very common early event seen in primary PCa is the mutated tumour suppressor gene Speckle-type POZ protein (SPOP) and the loss of its

function. SPOP is also an adaptor of the cullin 3-based ubiquitin ligase, which is responsible for degradation of several proteins including AR. This will eventually result in high levels of androgen signaling and oncogenic transcriptional activity.

One of the other key genetic alterations which is also seen in PCa is deletion and/or mutation of PTEN and TP53. PTEN loss will provoke the hyperactivation of the PI3K–AKT signaling cascade driving oncogenic changes. Interestingly, almost all of the aforementioned alterations have previously been linked to DNA repair defects (Brenner, Ateeq et al. 2011, Chatterjee, Choudhary et al. 2015, Kari, Mansour et al. 2016, Hjorth-Jensen, Maya-Mendoza et al. 2018, Mansour, Tennstedt et al. 2018, Hamid, Gray et al. 2019). A seminal molecular analysis of 19% of 333 primary prostate tumours by The Cancer Genome Atlas (TCGA) revealed aberrations in different DNA damage response and repair (DDR) genes including ATM, BRCA2, BRCA1, CDK12, RAD51C and mismatch repair (MMR)-related genes (MSH2, MSH6 and PMS2) (Cancer-Genome-Atlas-Research-Network. 2015). Amplifications or mutations of AR are not commonly seen with primary prostate carcinomas but more prevailing with advanced cases with poor outcome and therapy resistance. With disease progression, AR is prone to post-translational modifications or variable genomic aberrations which include different mutations, and copy number amplification or even complete loss seen with neuroendocrine cancer of the prostate that usually has very bad prognosis and very limited drug options. Usually, these different alterations have a tight role in therapeutic resistance (Kwan and Wyatt 2022).

1.1.5. Molecular therapeutic targeting of DNA repair in prostate cancer

It was tightly reported the intimate relationship between AR signaling and the DNA damage response (DDR) machinery (Fig. 4). Polkinghorn and colleagues (Polkinghorn, Parker et al. 2013) demonstrated that DNA repair capacity is enhanced through activated androgen signaling axis. Such intriguing interplay between AR-DDR machineries was demonstrated by lower expression of a large subset of DDR-related genes after the antiandrogen ARN-509 treatment in CRPC xenograft. Interestingly, AR ChIP-seq showed enrichment of AR in the enhancers of 32 of the DNA repair genes after synthetic androgen treatment in LNCaP cells. Goodwin and colleagues (Goodwin, Schiewer et al. 2013) further investigated this positive regulatory circuit, as they demonstrated that AR activates the transcription of numerous DNA repair genes such as DNA-PKcs and KU70 (Key components in NHEJ repair pathway) as well as other repair genes involved in other pathways such as HR (RAD51 paralogs) and mismatch

Introduction

repair (MSH2/6). Notably, many of these genes are stimulated through the direct binding of AR to their enhancer regions. This cross talk between both machineries can explain why genetic aberrations in DNA repair genes are frequently seen with a significant proportion of patients with advanced PCa (Jividen, Kedzierska et al. 2018).

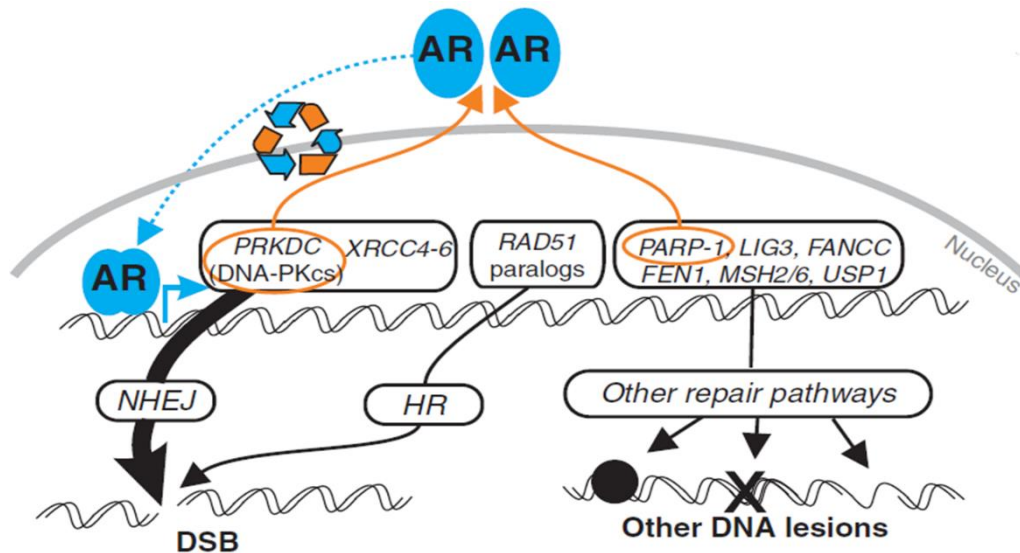


Fig. 4. Schematic model depicts the AR-DNA repair circuit. Hormone signalling initiated by AR activates the expression of several genes involved in DNA repair machinery. Among these genes are key components in (i) non-homologous end joining (NHEJ) such as KU70/80 (XRCC6/5) and DNA protein kinases (DNA-PKcs), (ii) homologous recombination (HR) including RAD51 paralogs (XRCC2 and XRCC3). In addition, AR also relocates to the promoters and regulates the expression of other repair genes such as poly (ADP-ribose) polymerase-1 (PARP-1), DNA Ligase 3 (LIG3), MSH2/6 that are involved in other repair pathways. DNA-PKcs and PARP-1 were also shown to potentiate AR function creating a positive regulatory circuit between AR-DNA repair response (DRR) machineries. This figure was modified from (Bartek, Mistrik et al. 2013).

On one side, this PCa progression can end with the aggressive phenotype CRPC, but the other bright side that around 60 % of such patients show clinically actionable molecular alterations in AR-independent pathways providing a weakness for this entity. However, deep insights into the genome of these advanced cases revealed that 19-27 % of them show deleterious mutations in different DDR genes. This can be exploited, and such patients can get great benefits from drugs targeting the DDR pathway or with genotoxic treatments, such as chemotherapy or RT. In advanced stages and specifically with patients showing castration resistant phenotype, mutations in BRCA1/2, and ATM are most commonly seen and usually HR deficiency is reported. Furthermore, around 3% of advanced PCa also show microsatellite instability due to the loss-of-function mutations in MSH2 and MSH6 (Pritchard, Morrissey et

Introduction

al. 2014, Wu, Liang et al. 2021). Especially mutations in HRR genes reduce the ability to effectively repair single and double strand DNA breaks. Taking this advantage, patients harboring these mutations can be targeted by Poly (ADP-ribose) polymerase (PARP) inhibitors. PARP is an enzyme which is involved in DNA single-strand breaks (SSBs) repair. Trapping PARP on the DNA using PARPi will accumulate SSBs and subsequently unrepaired DSBs especially in tumour-specific HRR deficiency.

Several clinical trials in the last few years, tested several PARPis in the management of mCRPC patients who showed mutations in any of the pre-specified HR repair genes. As shown in Table 1, all clinical trials showed promising results regarding PARPi sensitivity especially with BRCA mutated patients. Therefore, and based on the PROFOUND trial, olaparib was approved from FDA for those patients with restriction to those with BRCA mutations. Furthermore, TOPARP-A and PROpel trials showed that the benefits from olaparib is not only restricted to BRCA mutations carriers but also for patients with other mutations in HRR genes such as ATM. The restriction for using PARPis to BRCA-mutated patients might miss a potentially larger proportion of responding patients.

Table 1 | Characteristics of different clinical trials assessing different PARPis in PCa.

Clinical TRIAL	Study design	Outcome
TOPARP-B (Mateo, Porta et al. 2020)	Single arm → Olaparib	Favours [Olaparib] mPFS BRCA1/2 > ATM > others
TRITON2 (Abida, Campbell et al. 2020)	Single arm → Rucaparib	Favours [Rucaparib] rPFS >>BRCA alteration
TALAPRO-1 (de Bono, Mehra et al. 2021)	Single arm → Talazoparib	Favours [Talazoparib] rPFS BRCA1/2 > ATM > others
PROfound (de Bono, Mateo et al. 2020)	Arm1→ Olaparib Arm2→ Enzalutamide or abiraterone	Favours [Olaparib]
PROpel (Saad, Armstrong et al. 2022)	Arm1→ Olaparib + Abiraterone Arm2→ Abiraterone	Favours [Olaparib + Abiraterone]
MAGNITUDE (Chi, Rathkopf et al. 2022)	Arm1→ Niraparib + Abiraterone Arm2→ Abiraterone	Favours [Niraparib + Abiraterone]

1.2. Aim of the work

The current work aims to provide the rationale for some potential treatment options to achieve better response in PCa especially in CRPC patients.

In general, two strategies have been tested in the current study to achieve the ultimate goal:

Strategy 1: Combination of the second generation AHTs including abiraterone, enzalutamide or apalutamide with IR, seeking a radiosensitization effect.

Rationale: Based on the previous reports showing that AR regulates the expression of several DNA DSB repair genes (Bartek, Mistrik et al. 2013, Goodwin, Schiewer et al. 2013, Polkinghorn, Parker et al. 2013, Mills 2014, Li, Karanika et al. 2017), we hypothesized that blocking AR would induce an inhibitory effect on DNA DSB repair and hence cause radiosensitization.

Strategy 2: Development of robust pre-clinical models from naive and castration resistant PCa patients that support a valid assay that functionally detects HRR-defects. This individualized PARPi screening allows immediate translation of treatment sensitivities into tailored clinical therapy recommendations to the clinic.

Rationale: Mutation analysis of HRR genes is currently used to identify PCa patients that benefit from PARP-inhibition. In addition to the fact that mutation analysis is time-intensive and expensive, it predicts response to a given therapy rather than providing a concrete functional response, hence, it remains challenging to be routinely incorporated into clinical practice. Therefore, we sought in this strategy to develop robust pre-clinical models to detect HRR defects functionally and guide treatment with PARPis.

1.3. Materials and Methods

1.3.1. Patient sample collection

From PCa patients with high-risk score according to D'Amico risk stratification, PCa tissues were derived after radical prostatectomy at Martini-Klinik, Prostate Cancer Center Hamburg, Germany. From palpable tumour, 1–2 punch biopsies were usually obtained in culture medium and then directly brought to the laboratory where these fresh tumour biopsy specimens were processed within 30 minutes.

1.3.2. Prostate tumour tissue processing and organoid establishment

Fresh tumour tissue samples were collected in adDMEM/F-12 +++; Advanced DMEM/F-12 medium supplemented with 1x GlutaMAX, 10mM HEPES and penicillin/streptomycin. The samples were firstly washed three times with PBS and then mechanically dissected using scalpel into very small pieces which further digested enzymatically by incubation in 37 °C shaker for 30 – 90 minutes in 5 mg/ml Collagenase type II dissolved in adDMEM/F-12 +++ supplemented with 10 µM ROCK inhibitor. The single cells or cell clusters were then extracted from the disrupted extracellular matrix using 50 µm cell strainer and finally suspended in cold Cultrex Basement Membrane Extract (BME). Upon gelation of the Matrigel after around 30 minutes, 500 µL of complete organoid medium was added. The culture was replenished every 4 days with fresh medium. During passaging, each 4-6 weeks, tumoroids were passaged by mechanical shearing of BME droplets through P1000 pipet tip and then for a maximum of 5 min at 37 °C, the mixture was incubated with TrypLE Express containing 10 µM ROCK inhibitor. The resulting cell clusters and single cells were washed and re-plated, following the protocol described above.

1.3.3. Tissue slice cultures

Using the McIlwain Tissue Chopper, the received tumour tissues were cut to 300 µm slices and then one of each placed onto Millicell® cell culture inserts (0.4 µm, 30 mm diameter), which were inserted in tissue culture dishes (35 mm) containing 1 ml Dulbecco's modified Eagle medium (DMEM) supplemented with 10 % fetal calf serum (FCS) and incubated at 37°C. The dissected tissues were left overnight before *ex-vivo* treatment to help for re-oxygenation and recovery. To track down hypoxia, all slices were additionally treated 2 hrs. before fixation with 200 µM pimonidazole.

1.3.4. *Ex-vivo* induction of castration resistance

Only tumour tissues which derived from hormone sensitive PCa patients with no evidence for resistance to any of the androgen deprivation therapies were employed here. Using the *ex-vivo* assay, tumour slices were cultured for up to 6 weeks in either hormone proficient condition (DMEM supplemented with 10% FCS) or androgen-depleted medium (DMEM supplemented with charcoal-stripped serum in the presence of the antihormonal therapy, 10 μ M abiraterone).

1.3.5. Cell culture, drugs, and X-irradiation

LNcaP PCa cells (ATCC, Manassas, VA, USA) were grown in DMEM supplemented with 10% FCS, 100 U/ml penicillin and 100 mg/ml streptomycin at 37 °C with 10% CO₂. LNcaP-ARN509, LNcaP-Bic, LNcaP-abi, and C4-2B-Enza cells were maintained in medium containing the corresponding drug to which they are resistant. Abiraterone acetate, apalutamide and enzalutamide were kindly provided by Janssen Cilag GmbH, Neuss, Germany. LNcaP-abl cells (a gift from Prof. Culig, Medical University Innsbruck, Austria) were grown in DMEM supplemented with 10% Charcoal Stripped FBS. All cell lines tested negative for mycoplasma contamination. Irradiation was performed as previously described (200 kV, 15 mA, additional 0.5mm Cu filter at a dose rate of 0.8 Gy/min) (Tepper, Foote et al. 2021).

1.3.6. Whole genome sequencing (WGS) and RNA-sequencing (RNA-SEQ)

Total DNA and RNA was extracted from PCa cells using DNeasy Blood and tissue kit (Qiagen, 69504) and RNEASY MINI KIT (Qiagen, 74106), respectively. DNA and RNA were then sent to Novogene (Sacramento, CA) for WGS and RNA-SEQ libraries preparation and sequencing. Data analysis was performed by Novogene and further validated in Bioinformatics core facility at UKE.

1.3.7. DNA methylation profiling

Total DNA was isolated using DNeasy Blood and tissue kit (Qiagen, 69504) from tumoroids derived from PCa patients. The genome-wide DNA methylation patterns in these tumoroids were analyzed using Illumina HumanMethylation450 BeadChip (450K) arrays. Only sites covered by at least 3 reads were considered for analysis. For each sample, the percentage of methylation per site (beta value) was computed. Average hierarchical clustering of samples

was performed by “1-Pearson’s correlation coefficient” as distance measure on the n= 10,000 CpG sites showing the highest standard deviation across the cohort.

1.3.8. Proliferation assay

For all resistant sublines, cells were seeded without the inhibitor to which the cells are resistant. For each treatment, cells were cultured in triplicate in 6-well plates. To determine the effect of the different treatment regimens, cells were treated as indicated, and harvested at 3-, 6-, and 10-days post-treatment and the cell number was determined via Beckman Coulter cell counter (Life Science, Germany). For all 10-day cell growth studies, medium with or without drugs were changed on day 3 and 6 during the treatment course.

1.3.9. Colony formation assay (2D and 3D)

To determine cellular survival, 2D CFA was used where the cells were plated at density of 200 cells/well in 6-well plates, and directly treated with 10 μ M bicalutamide or 5 μ M abiraterone acetate for 24 hrs. The cells were then X-irradiated (RS225 research system, GLUMAY MEDICAL, UK at 200 kV, 15 mA). After 2–3 weeks, colonies were fixed using 70% ethanol and stained with 0.1% crystal violet. Colonies containing at least 50 cells were only considered for cellular survival analysis. 3D CFA was performed in either agarose or matrigel based system. For agarose CFA, cells at density of 10000 cells/well were mixed with 0.3% agarose in DMEM with 10% FCS and plated onto 6-well plates containing a solidified bottom layer (0.6% agarose the same growth medium). Two weeks later, colonies were stained with 0.5 mg/mL MTT. For matrigel based CFA, cell pellets from cell lines or harvested and sheared cells derived from tumoroids were seeded at density of 2000 - 4000 cell/dome, respectively. The cells were then mixed with cold reduced growth factor basement membrane extract (RGF BME) type 2. Upon completed gelation of the matrigel containing cells, medium was added containing the specific drug at the indicated concentrations. After 3-4 weeks, colonies (3D cell cultures or tumoroids) were stained with 0.5 mg/mL MTT for 1.5h. Colonies were then harvested using Cultrex™ Organoid Harvesting Solution. All MTT stained colonies were photographed using REBEL Microscopy (ECHO, San-Diego, CA, USA) and analyzed using Image-J. Surviving fractions (SFs) were calculated by normalization to the plating efficiency of the untreated control. DMSO was used as a control at the same concentration.

1.3.10. Migration assay

Using 24-well Transwell plate with 8µm pore-size (Corning® BioCoat®, 354578), chemotaxis assay was performed. In FBS-free DMEM, either LNCaP or LNCaP-ARN509 were seeded at density of 2×10^5 cells into the transwell chamber. DMEM containing 10% FBS was used as cell attractant in the lower chamber. After 36 hr., the inserts were thereafter fixed in 70% ethanol and stained in 0.1% crystal violet. Using ImageJ, cell migration was analyzed by counting the numbers of migrated cells.

1.3.11. Western blot

RAD51 Immunoblot analysis was performed with the rabbit anti-RAD51 (Merck, Cat#PC130). Beta-actin was immunoblotted by mouse anti-beta-actin (Sigma) and used as a loading control. Goat-anti-mouse IgG-AlexaFluor 594 (Molecular Probes, Cat#A11005) and Goat-anti-rabbit IgG-AlexaFluor 488 (Molecular Probes, Cat#A11008) secondary antibodies were used. Membranes were developed and analyzed using LiCor Biosciences at room temperature.

1.3.12. Immunofluorescence

Cells were grown on coverslips until 50–60% confluence, followed by treatment of drug of interest. After time of incubation, cells on coverslips were washed three times, fixed in 4% para-formaldehyde/PBS for 10 min, permeabilized with 0.2% Triton X-100/PBS on ice for 5 min, washed twice with PBS, and blocked in 3% BSA/PBS for 1 h. Cells were labeled with primary antibodies (anti-phospho-S139-H2AX and anti-53BP1 or anti-RAD51 for 1 h at 1:500 dilution in 1% BSA/PBS, followed by incubation for 1h with anti-mouse Alexa-fluor594 (1:500) and anti-rabbit Alexa-fluor488 (1:600) secondary antibodies. Cells were counterstained with 4'-6-diamidino-2-phenylindole (DAPI, 10ng/ml) and visualized with Zeiss AxioObserver.Z1 microscope. For cultured tumour tissue, tissue slices were fixed for 1 h in 4% PFA/PBS and washed twice each 1 h with 25% sucrose/PBS. Samples were freezed in TissueTek® (Serva) and stored at -80 °C. Cryoslices (5 µm) were prepared using the Cryo Star NX70 Microtome. The fixed cryoslices were permeabilized with 1% SDS/PBS and blocked with 3% BSA/PBS for 1 h. Labeling the respective proteins were performed as illustrated above with cells. For DSB analysis fields of view were taken per time point or treatment with a minimum of 100 cells (cell lines) or 50 cells (tumour tissue). DSBs were analyzed using ImageJ and DAPI-based image masks and normalized to single nucleus values.

1.3.13. Histology and imaging

Histological analysis was performed by standard hematoxylin and eosin (H&E) staining and percentage of cancer cells and Gleason score was determined by a pathologist. Immunohistochemistry was performed using antibodies against AMACR (Thermo Scientific, PA5-82739, 1:250), and Ki67 (Abcam, ab15580, 1:250). Images were acquired using ZEISS Axio Scan.Z1 Slide Scanner and photos were then processed using netScope® Viewer.

1.3.14. Cell cycle analysis and apoptosis quantification

For cell cycle analysis, treated cells were harvested and fixed with 80% cold ethanol ($-20\text{ }^{\circ}\text{C}$). After washing, the DNA was stained with propidium iodide solution containing RNase A. Cell cycle distribution was monitored by flow cytometry (FACS CANTO 2, BD Bioscience Systems, Heidelberg, Germany) and analyzed using Mod-Fit software.

Apoptosis was investigated by detection of caspase activity utilizing the FAMFLICA™ Poly Caspases Assay Kit (Immunochemistry Technologies, Bloomington, MN, USA), according to the manufacturer's instructions. Flow cytometric analysis was performed on a FACS Canto with FACS Diva Software (Becton Dickinson, Toronto, ON, Canada).

1.3.15. Graphs and statistics

Statistical analyses, data fitting and graphics were performed with the GraphPad Prism 9.0 program (GraphPad Software). The IDAT files of the samples were loaded, filtered, and normalized with the package limma (version 3.40.0) in R (version 3.6.0). By using multiple datasets containing different numbers of CpG sites, our samples are reduced to 450k sites. In addition, a correction was made for possible batch effects related to chip size using the limma package.

1.4. Summary of results

1.4.1. Second-generation antiandrogen therapy radiosensitizes prostate cancer regardless of castration state through inhibition of DNA double strand break repair

In the current study, we provided a rationale for the use of the second-generation antiandrogens abiraterone acetate, apalutamide and enzalutamide as radiosensitising agents.

The findings of the current study can be summarized as following:

- The aforementioned antiandrogens increased the cytotoxic effect of 2Gy as demonstrated by significant (i) suppression of cell growth and (ii) increase of the doubling times.
- This radiosensitising effect was reported in both hormone-responsive LNCaP and castration-resistant C4-2B cells.
- Indeed, these findings were further validated in sublines resistant to (i) hormone ablation (LNCaP-abl), (ii) abiraterone acetate (LNCaP-abi), (iii) apalutamide (LNCaP-ARN509), (iv) enzalutamide (C4-2B-ENZA) and in castration-resistant 22-RV1 cells.
- Importantly, the radiosensitization effect was not observed using the first-generation antiandrogen bicalutamide.
- Furthermore, the radiosensitization effect of second-generation antiandrogens was attributed to the inhibition of DNA DSB repair, as demonstrated by a significant increase in residual γ H2AX and 53BP1 foci numbers at 24 h post-IR.
- DSB repair inhibition was further recapitulated in 22 patient-derived tumour slice cultures treated with abiraterone acetate and 2 Gy in *ex vivo* settings.

In conclusion, these data show that second-generation antiandrogens can enhance radiosensitivity in PCa through DSB repair inhibition, regardless of their hormonal status. Translated into clinical practice, our results may help to find additional strategies to improve the effectiveness of RT in localized PCa, paving the way for a clinical trial.

1.4.2. Pre-clinical patient-derived modelling of castration resistant prostate cancer facilitates individualized assessment of homologous recombination repair deficient disease

The use of mutation analysis of homologous-recombination-repair (HRR) genes to estimate the response of PCa patients to drugs such as PARP inhibitors or cisplatin may miss a larger proportion of responding patients. The current study provides pre-clinical models for PCa – especially the CRPC subtype – that can be used to functionally test for HRR-defects and hence better predict the response of PCa patients to the aforementioned drugs.

These models include:

- (i) Established *in vitro* sublines from the hormone sensitive LNCaP cells, harboring resistance towards hormone ablation (LNCaP-abl), abiraterone acetate (LNCaP-abi), apalutamide (LNCaP-ARN509), bicalutamide (LNCaP-BICA).
- (ii) *Ex vivo* tumour slice cultures established from CRPC patients or *ex vivo*-induced castration resistance through culturing the tumour slices from HSPC patients in castration resistant conditions (hormone ablation in the presence of abiraterone).
- (iii) Patient-derived organoids (PDOs) established from CRPC patients.

The findings of the current study can be summarized as following:

- *In vitro* CRPC LNCaP sublines revealed a HRR-defect and enhanced sensitivity to olaparib and cisplatin due to impaired RAD51 expression and recruitment.
- *Ex-vivo*-induced castration resistant tumour slice cultures or tumour slice cultures derived directly from CRPC-patients showed increased olaparib- or cisplatin-associated enhancement of residual IR-induced γ H2AX/53BP1 foci.
- A robust protocol for PDO cultures from CRPC patients was established maintaining the morphological similarities between the PDOs and their primary tumours. Furthermore, using methylome profiling, the established PDOs were genetically clustered with PCa but not with normal prostate or other tumour entities.
- Importantly, an enhanced sensitivity of the PDOs established from CRPC-patients to olaparib and cisplatin compared to those established from HSPC patients was validated.

Summary of results

- Olaparib but not cisplatin was found to selectively inhibit the migration rate of mCRPC cells.

These pre-clinical models allow individualized functional assessment of HRR deficient disease and provide immediate use to select PCa patients for the treatment with the aforementioned drugs in the clinical settings.

1.5. Discussion

PCa is a complex multifaceted and biologically heterogeneous disease, with often low-risk disease, but also aggressive phenotypes with treatment resistance. Significant progress has been achieved in delineating the treatment landscape based on the clinical stage. Despite this progress, advanced PCa is still associated with poor outcomes, with CRPC remaining an incurable disease with limited treatment options.

In the current study, we worked in two strategies to help improve the treatment options of advanced PCa patients: (1), Combining second generation AHTs with RT to achieve better disease control, and (2) establishing robust pre-clinical models for PCa to predict the response to specific therapy such as olaparib or cisplatin.

1.5.1. AHT as radiosensitising agents

One of the most extensively used treatment combinations for the management of localized PCa patients is ADT plus RT. Taking advantage of the functional interplay between AR and DNA repair machinery (Abida, Cyrta et al. 2019), suppression of endogenous testosterone production through ADTs can enhance the radiotherapeutic effect. This combination of RT and ADT was a subject to different clinical studies. In the RTOG 94-08 clinical trial, four months ADT administration prior to and during RT could increase overall survival for intermediate but not for low-risk patients (McGowan, Hunt et al. 2010). In line with this study, the prospective trial EORTC 22863 revealed a survival advantage for patients with locally advanced PCa, favoring the combined treatment approach. Except for high-risk patients, this survival benefit for the combined arm was not recapitulated in other studies (Hanks, Pajak et al. 2003, Horwitz, Bae et al. 2008).

At our institution, the UKE Department of Radiotherapy & Radiooncology, a total of 203 patients with localized PCa were included in a retrospective study. All patients had received radiotherapy, but only 65 of these patients had received ADT as well. There was a modest but non-significant enhancement in the biochemical failure-free survival in the patients who had received the combination regimen compared to those who had only received RT.

In addition to different endocrine therapies, the antiandrogen bicalutamide combined with radiation was also a subject for different pre-clinical and clinical studies for the treatment of PCa. Employing the androgen sensitive LNCaP cells to test efficacy of bicalutamide before, during and after IR revealed an antagonistic effect when they are used in close temporal

proximity (Quéro, Giocanti et al. 2010). On the other hand, a combination of this castration therapy with RT showed a significant improvement in overall survival, PFS and PSA-PFS in patients with locally advanced disease compared to those receiving RT alone (See and Tyrrell 2006).

On a genome-wide level, AR ChIP-seq was performed by Asangani et al. to assess AR localization after bicalutamide or the newer generation AR blocker enzalutamide. As expected, the highest enrichment of AR across AR binding sites was seen with DHT-treated VCaP cells. Interestingly, enzalutamide markedly attenuated this AR enrichment compared to bicalutamide (Asangani, Dommeti et al. 2014).

In terms of the cross talk between both machineries; DDR and AR signaling, and in light of the higher potency previously reported with the newer generation enzalutamide evidenced by extensive impairment of genome-wide AR recruitment to AREs as well as the aforementioned controversial clinical trials, we demonstrated in the current work a higher radiosensitivity in PCa preclinical models mediated by the second-generation antiandrogens (Elsesy, Oh-Hohenhorst et al. 2020). This radiosensitization effect was attributed to inhibition of DNA DSB repair capacity. These data validate the previously reported tight crosstalk between AR signaling and DNA repair mechanisms (Bartek, Mistrik et al. 2013, Goodwin, Schiewer et al. 2013, Böhmer, Wirth et al. 2016).

1.5.2. Pre-clinical 3D models for precision medicine in PCa

Research in the PCa field is hampered by the limited number of such pre-clinical models that recapitulate the in-vivo tumour. In the current study, we developed robust in vitro and ex-vivo pre-clinical models that help represent the human disease seen in the clinic. Currently, the most frequently used PCa models are cell lines isolated from patients for cell culture. Cell lines have been (and still are) very useful in understanding molecular functions, as well as providing a first clue for developing new targeted therapies for PCa, as they can easily be genetically or pharmacologically manipulated. However, these cell lines were kept for several years in culture and have likely accumulated several mutations that are not present in the tumours they were originally established from. Furthermore, most of these cell lines were established from metastatic origins (Mai, Chin et al. 2022), therefore, they do not appropriately represent the primary tumours. Furthermore, the pharmacological landscape of PCa has substantially evolved especially after discovering the second-generation anti-androgens. The currently

available cell lines have mostly been obtained from patients treated with ADTs or the first-generation anti-androgens but not the second-generation antiandrogens. Thus, the development of more reliable PCa models for pre-clinical studies is required to reflect changes in the clinical landscape of this disease.

In the current study, we presented robust pre-clinical models that resemble the tumour *in-vivo*, including tumour slice cultures and PDOs. *Ex vivo* tumour slice cultures are a very powerful technique as they preserve the cell repertoire and immune components and provide a quick assessment of therapeutic efficacy. We could keep these slices in culture under optimum conditions for up to 6 weeks with no effect on proliferation or oxygenation rate (Köcher, Beyer et al. 2019). We employed this model to predict the response of PCa patients to IR either alone or combined with either cisplatin or olaparib. This response was presented by an index that indicates the enhancement ratio of the number of residual IR-induced DSBs mediated by olaparib (PiER-index) or for example cisplatin (CisER-index).

Moreover, we present in the current study a very robust protocol for establishment of PDOs from PCa patients (Elsesy, Oh-Hohenhorst et al. 2023). These PDOs showed similarities to the primary tumours they were established from and are epigenetically clustered within PCa but not with any other tumour entities or normal prostate. Importantly, we could show that PDOs can serve as a reliable tool to stratify therapeutic responders from nonresponders and select the optimal standard-of-care treatment regimens for personalized medicine. For example, we employed these pre-clinical models to functionally predict HRR defects in PCa patients to stratify them according to their response to drugs such as olaparib or cisplatin (Elsesy, Oh-Hohenhorst et al. 2023).

This indeed is expected to become a potent platform and even the gold standard for anticancer drug screening of individualization in the future.

1.5.3. Future direction

Patient-derived models can indeed better represent the *in-vivo*-tumour than *in-vitro* cell lines, but also have some limitations. Although the *ex-vivo* tumour slice culture enables many analyses, it has some disadvantages. For example, it can only be maintained for up to 6 weeks (in our hands) and cannot reliably be stored for future analysis. A further challenging disadvantage of this model is its inability to directly analyse the effect on cell survival and clonogenicity, but it rather enables monitoring the effect on DSB repair as an indirect

Discussion

surrogate marker for survival. Currently, some modifications are being tested in our lab to (i) enable the preservation of tumour slices for future analysis, (ii) establish immunostaining of some death markers and (iii) establish some survival assays.

In comparison to the *ex-vivo* tumour slice cultures, PDOs present a more robust pre-clinical cancer model for better translational research, however with some limitations and improving potentials. Indeed, we present here a high success rate (approximately 60%) for establishing PDOs from advanced PCa samples. This high success rate can be attributed to the aggressiveness of this tumour which enables higher proliferation rate and more cancer stem cells within the sample. A question being addressed currently in our lab is whether we can achieve such a high rate also with primary, hormone-naive low risk PCa samples. In addition, PDOs are still considered *ex-vivo* cultures that miss the tumour environment, including immune components. Therefore, there is still space for future improvement for the PDOs as a pre-clinical cancer model. It is important, for instance, to establish co culturing conditions with the missing tumour microenvironmental elements such as blood vessels, immune cells, and other stroma cells.

Collectively, all the pre-clinical models presented here, from cell lines to *ex-vivo* tumour slices and PDO cultures, are useful complementary models to have an improved understanding of PCa biology. Limitations of each model have to be considered to properly translate research from bench to bed side.

2. List of abbreviations

μ	Micro (10^{-6})
53BP1	p53 binding protein 1
AA	Abiraterone acetate
ADT	Androgen deprivation therapy
AHT	Anti-hormonal therapy
AR	Androgen receptor
AREs	Androgen response elements
ATM	Ataxia telangiectasia mutated
ATMi	ATM inhibitor
BRCA1	Breast cancer 1
BRCA2	Breast cancer 2
CDK12	Cyclin-dependent kinase 12
CNA	Copy number alterations
CRPC	Castration resistant prostate cancer
DAPI	4',6-Diamidino-2-phenylindole
DDR	DNA-damage-response
DHT	5 α -dihydrotestosterone
DMEM	Dulbecco's modified Eagle's medium
DMSO	Dimethyl sulfoxide
DNA	Deoxyribonucleic acid
DNA-PK	DNA-dependent protein kinase
DSB	Double strand break
dsDNA	Double stranded DNA
EBRT	External beam radiotherapy
EDTA	Ethylene diamine tetra acetic acid
FACS	Fluorescence-activated cell sorting
GnRH	Gonadotropin-releasing hormone
HDRBT	High dose rate brachytherapy
HR	Homologous recombination
IR	Ionizing radiation
LDRBT	Low dose rate brachytherapy
LH	Luteinizing hormone
m	Milli (10^{-3})
M	Molar
MB	Megabase
mCRPC	Metastatic castrate resistant prostate cancer
MMR	Mismatch repair
mRNA	Messenger ribonucleic acid
n	Nano (10^{-9})
NCCN	National Comprehensive Cancer Network
NHEJ	Nonhomologous end-joining

Abbreviations

NSAAs	Nonsteroidal antiandrogens
PARP1	Poly (ADP-ribose) polymerase 1
PARPi	PARP inhibitor
PBS	Phosphate buffered saline
PCa	Prostate cancer
PMSF	Phenyl methyl sulfonyl fluoride
PSA	Prostate specific antigen
RAD51	Recombination protein RAD51
RNA	Ribonucleic acid
Rpm	Rotations per minute
RP	Radical prostatectomy
RT	Room temperature
SAAs	Steroidal antiandrogens
SDS	Sodium dodecyl sulphate
SPOP	Speckle-type POZ protein
TCGA	The Cancer Genome Atlas
Tween 20	Polyoxyethylen-sorbitanmonolaurate 20
UV	Ultraviolet
V	Volts
γH2AX	Phosphorylated histone variant H2AX at S139

3. References

- Abida, W., D. Campbell, A. Patnaik, J. D. Shapiro, B. Sautois, N. J. Vogelzang, E. G. Voog, A. H. Bryce, R. McDermott, F. Ricci, J. Rowe, J. Zhang, J. M. Piulats, K. Fizazi, A. S. Merseburger, C. S. Higano, L. E. Krieger, C. J. Ryan, F. Y. Feng, A. D. Simmons, A. Loehr, D. Despain, M. Dowson, F. Green, S. P. Watkins, T. Golsorkhi and S. Chowdhury (2020). "Non-BRCA DNA Damage Repair Gene Alterations and Response to the PARP Inhibitor Rucaparib in Metastatic Castration-Resistant Prostate Cancer: Analysis From the Phase II TRITON2 Study." *Clin Cancer Res* **26**(11): 2487-2496.
- Abida, W., J. Cyrta, G. Heller, D. Prandi, J. Armenia, I. Coleman, M. Cieslik, M. Benelli, D. Robinson, E. M. Van Allen, A. Sboner, T. Fedrizzi, J. M. Mosquera, B. D. Robinson, N. De Sarkar, L. P. Kunju, S. Tomlins, Y. M. Wu, D. Nava Rodrigues, M. Loda, A. Gopalan, V. E. Reuter, C. C. Pritchard, J. Mateo, D. Bianchini, S. Miranda, S. Carreira, P. Rescigno, J. Filipenko, J. Vinson, R. B. Montgomery, H. Beltran, E. I. Heath, H. I. Scher, P. W. Kantoff, M. E. Taplin, N. Schultz, J. S. deBono, F. Demichelis, P. S. Nelson, M. A. Rubin, A. M. Chinnaiyan and C. L. Sawyers (2019). "Genomic correlates of clinical outcome in advanced prostate cancer." *Proc Natl Acad Sci U S A* **116**(23): 11428-11436.
- Aggarwal, R. R., G. Thomas, J. Youngren, A. Foye, S. Olson, P. Paris, T. M. Beer, C. J. Ryan, O. Witte, C. P. Evans, M. E. Gleave, J. Stuart, J. J. Alumkal, A. Toschi, N. Zona, R. E. Reiter, P. Lara, K. N. Chi and E. J. Small (2015). "Androgen receptor (AR) amplification in patients (pts) with metastatic castration resistant prostate cancer (mCRPC) resistant to abiraterone (Abi) and enzalutamide (Enz): Preliminary results from the SU2C/PCF/AACR West Coast Prostate Cancer Dream Team (WCDT)." *Journal of Clinical Oncology* **33**(15_suppl): 5068-5068.
- Asangani, I. A., V. L. Dommeti, X. Wang, R. Malik, M. Cieslik, R. Yang, J. Escara-Wilke, K. Wilder-Romans, S. Dhanireddy, C. Engelke, M. K. Iyer, X. Jing, Y. M. Wu, X. Cao, Z. S. Qin, S. Wang, F. Y. Feng and A. M. Chinnaiyan (2014). "Therapeutic targeting of BET bromodomain proteins in castration-resistant prostate cancer." *Nature* **510**(7504): 278-282.
- Bambury, R. M. and D. E. Rathkopf (2016). "Novel and next-generation androgen receptor-directed therapies for prostate cancer: Beyond abiraterone and enzalutamide." *Urol Oncol* **34**(8): 348-355.
- Bartek, J., M. Mistrik and J. Bartkova (2013). "Androgen receptor signaling fuels DNA repair and radioresistance in prostate cancer." *Cancer Discov* **3**(11): 1222-1224.
- Bennett, L. L. and A. Ingason (2014). "Enzalutamide (Xtandi) for patients with metastatic, resistant prostate cancer." *Ann Pharmacother* **48**(4): 530-537.
- Böhmer, D., M. Wirth, K. Miller, V. Budach, A. Heidenreich and T. Wiegel (2016). "Radiotherapy and Hormone Treatment in Prostate Cancer." *Dtsch Arztebl Int* **113**(14): 235-241.
- Brenner, J. C., B. Ateeq, Y. Li, A. K. Yocum, Q. Cao, I. A. Asangani, S. Patel, X. Wang, H. Liang, J. Yu, N. Palanisamy, J. Siddiqui, W. Yan, X. Cao, R. Mehra, A. Sabolch, V. Basrur, R. J. Lonigro, J. Yang, S. A. Tomlins, C. A. Maher, K. S. Elenitoba-Johnson, M. Hussain, N. M. Navone, K. J. Pienta, S. Varambally, F. Y. Feng and A. M. Chinnaiyan (2011). "Mechanistic rationale for inhibition of poly(ADP-ribose) polymerase in ETS gene fusion-positive prostate cancer." *Cancer Cell* **19**(5): 664-678.
- Cancer-Genome-Atlas-Research-Network. (2015). "The Molecular Taxonomy of Primary Prostate Cancer." *Cell* **163**(4): 1011-1025.
- Cao, B., Y. Qi, G. Zhang, D. Xu, Y. Zhan, X. Alvarez, Z. Guo, X. Fu, S. R. Plymate, O. Sartor, H. Zhang and Y. Dong (2014). "Androgen receptor splice variants activating the full-length

References

- receptor in mediating resistance to androgen-directed therapy." *Oncotarget* **5**(6): 1646-1656.
- Chang, H. H. Y., N. R. Pannunzio, N. Adachi and M. R. Lieber (2017). "Non-homologous DNA end joining and alternative pathways to double-strand break repair." *Nat Rev Mol Cell Biol* **18**(8): 495-506.
- Chatterjee, P., G. S. Choudhary, T. Alswillah, X. Xiong, W. D. Heston, C. Magi-Galluzzi, J. Zhang, E. A. Klein and A. Almasan (2015). "The TMPRSS2-ERG Gene Fusion Blocks XRCC4-Mediated Nonhomologous End-Joining Repair and Radiosensitizes Prostate Cancer Cells to PARP Inhibition." *Mol Cancer Ther* **14**(8): 1896-1906.
- Chen, Y., N. J. Clegg and H. I. Scher (2009). "Anti-androgens and androgen-depleting therapies in prostate cancer: new agents for an established target." *Lancet Oncol* **10**(10): 981-991.
- Chi, K. N., D. E. Rathkopf, M. R. Smith, E. Efsthathiou, G. Attard, D. Olmos, J. Y. Lee, E. J. Small, A. J. Gomes, G. Roubaud, M. Saad, B. Zurawski, V. Sakalo, G. Mason, A. d. Corral, G. C. Wang, D. Wu, B. Diorio, A. M. L.-. Gitlitz and S. K. Sandhu (2022). "Phase 3 MAGNITUDE study: First results of niraparib (NIRA) with abiraterone acetate and prednisone (AAP) as first-line therapy in patients (pts) with metastatic castration-resistant prostate cancer (mCRPC) with and without homologous recombination repair (HRR) gene alterations." *Journal of Clinical Oncology* **40**(6_suppl): 12-12.
- Conteduca, V., C. Oromendia, K. W. Eng, R. Bareja, M. Sigouros, A. Molina, B. M. Faltas, A. Sboner, J. M. Mosquera, O. Elemento, D. M. Nanus, S. T. Tagawa, K. V. Ballman and H. Beltran (2019). "Clinical features of neuroendocrine prostate cancer." *Eur J Cancer* **121**: 7-18.
- Das, R., M. Sjöström, R. Shrestha, C. Yogodzinski, E. A. Egusa, L. N. Chesner, W. S. Chen, J. Chou, D. K. Dang, J. T. Swinderman, A. Ge, J. T. Hua, S. Kabir, D. A. Quigley, E. J. Small, A. Ashworth, F. Y. Feng and L. A. Gilbert (2021). "An integrated functional and clinical genomics approach reveals genes driving aggressive metastatic prostate cancer." *Nature Communications* **12**(1): 4601.
- de Bono, J., J. Mateo, K. Fizazi, F. Saad, N. Shore, S. Sandhu, K. N. Chi, O. Sartor, N. Agarwal, D. Olmos, A. Thiery-Vuillemin, P. Twardowski, N. Mehra, C. Goessl, J. Kang, J. Burgents, W. Wu, A. Kohlmann, C. A. Adelman and M. Hussain (2020). "Olaparib for Metastatic Castration-Resistant Prostate Cancer." *New England Journal of Medicine* **382**(22): 2091-2102.
- de Bono, J. S., N. Mehra, G. V. Scagliotti, E. Castro, T. Dorff, A. Stirling, A. Stenzl, M. T. Fleming, C. S. Higano, F. Saad, C. Buttigliero, I. M. van Oort, A. D. Laird, M. Mata, H. C. Chen, C. G. Healy, A. Czibere and K. Fizazi (2021). "Talazoparib monotherapy in metastatic castration-resistant prostate cancer with DNA repair alterations (TALAPRO-1): an open-label, phase 2 trial." *Lancet Oncol* **22**(9): 1250-1264.
- De Vargas Roditi, L., A. Jacobs, J. H. Rueschoff, P. Bankhead, S. Chevrier, H. W. Jackson, T. Hermanns, C. D. Fankhauser, C. Poyet, F. Chun, N. J. Rupp, A. Tschaebunin, B. Bodenmiller and P. J. Wild (2022). "Single-cell proteomics defines the cellular heterogeneity of localized prostate cancer." *Cell Reports Medicine* **3**(4).
- Dehm, S. M. and D. J. Tindall (2011). "Alternatively spliced androgen receptor variants." *Endocr Relat Cancer* **18**(5): R183-196.
- Edgren, M., A. M. Ekelund, P. Albertsson, L. M. Lundberg, A. Ullen, S. Levitt, S. Nilsson and B. Lennernäs (2006). "High dose-rate brachytherapy of prostate cancer utilising Iridium-192 after-loading technique: technical and methodological aspects." *Int J Oncol* **29**(6): 1517-1524.

References

- Elliott, B. and M. Jasin (2002). "Double-strand breaks and translocations in cancer." Cell Mol Life Sci **59**(2): 373-385.
- Elsesy, M. E., S. J. Oh-Hohenhorst, A. Löser, C. Oing, S. Mutiara, S. Köcher, S. Meien, A. Zielinski, S. Burdak-Rothkamm, D. Tilki, H. Huland, R. Schwarz, C. Petersen, C. Bokemeyer, K. Rothkamm and W. Y. Mansour (2020). "Second-Generation Antiandrogen Therapy Radiosensitizes Prostate Cancer Regardless of Castration State through Inhibition of DNA Double Strand Break Repair." Cancers (Basel) **12**(9).
- Elsesy, M. E., S. J. Oh-Hohenhorst, C. Oing, A. Eckhardt, S. Burdak-Rothkamm, M. Alawi, C. Müller, U. Schüller, T. Maurer, G. von Amsberg, C. Petersen, K. Rothkamm and W. Y. Mansour (2023). "Preclinical patient-derived modeling of castration-resistant prostate cancer facilitates individualized assessment of homologous recombination repair deficient disease." Mol Oncol.
- Fraser, M., V. Y. Sabelnykova, T. N. Yamaguchi, L. E. Heisler, J. Livingstone, V. Huang, Y. J. Shiah, F. Yousif, X. Lin, A. P. Masella, N. S. Fox, M. Xie, S. D. Prokopec, A. Berlin, E. Lalonde, M. Ahmed, D. Trudel, X. Luo, T. A. Beck, A. Meng, J. Zhang, A. D'Costa, R. E. Denroche, H. Kong, S. M. Espiritu, M. L. Chua, A. Wong, T. Chong, M. Sam, J. Johns, L. Timms, N. B. Buchner, M. Orain, V. Picard, H. Hovington, A. Murison, K. Kron, N. J. Harding, C. P'ng, K. E. Houlahan, K. C. Chu, B. Lo, F. Nguyen, C. H. Li, R. X. Sun, R. de Borja, C. I. Cooper, J. F. Hopkins, S. K. Govind, C. Fung, D. Waggott, J. Green, S. Haider, M. A. Chan-Seng-Yue, E. Jung, Z. Wang, A. Bergeron, A. Dal Pra, L. Lacombe, C. C. Collins, C. Sahinalp, M. Lupien, N. E. Fleshner, H. H. He, Y. Fradet, B. Tetu, T. van der Kwast, J. D. McPherson, R. G. Bristow and P. C. Boutros (2017). "Genomic hallmarks of localized, non-indolent prostate cancer." Nature **541**(7637): 359-364.
- Ghashghaei, M., M. Kucharczyk, S. Elakshar, T. Muanza and T. Niazi (2019). "Combining prostate cancer radiotherapy with therapies targeting the androgen receptor axis." Curr Oncol **26**(5): e640-e650.
- Gioeli, D. and B. M. Paschal (2012). "Post-translational modification of the androgen receptor." Mol Cell Endocrinol **352**(1-2): 70-78.
- Goodwin, J. F., M. J. Schiewer, J. L. Dean, R. S. Schrecengost, R. de Leeuw, S. Han, T. Ma, R. B. Den, A. P. Dicker, F. Y. Feng and K. E. Knudsen (2013). "A hormone-DNA repair circuit governs the response to genotoxic insult." Cancer Discov **3**(11): 1254-1271.
- Guo, C., S. Yeh, Y. Niu, G. Li, J. Zheng, L. Li and C. Chang (2017). "Targeting androgen receptor versus targeting androgens to suppress castration resistant prostate cancer." Cancer Lett **397**: 133-143.
- Hamid, A. A., K. P. Gray, G. Shaw, L. E. MacConaill, C. Evan, B. Bernard, M. Loda, N. M. Corcoran, E. M. Van Allen, A. D. Choudhury and C. J. Sweeney (2019). "Compound Genomic Alterations of TP53, PTEN, and RB1 Tumor Suppressors in Localized and Metastatic Prostate Cancer." Eur Urol **76**(1): 89-97.
- Hanks, G. E., T. F. Pajak, A. Porter, D. Grignon, H. Brereton, V. Venkatesan, E. M. Horwitz, C. Lawton, S. A. Rosenthal, H. M. Sandler and W. U. Shipley (2003). "Phase III trial of long-term adjuvant androgen deprivation after neoadjuvant hormonal cytoreduction and radiotherapy in locally advanced carcinoma of the prostate: the Radiation Therapy Oncology Group Protocol 92-02." J Clin Oncol **21**(21): 3972-3978.
- Helleday, T., J. Lo, D. C. van Gent and B. P. Engelward (2007). "DNA double-strand break repair: from mechanistic understanding to cancer treatment." DNA Repair (Amst) **6**(7): 923-935.
- Henry, A., B. R. Pieters, F. André Siebert and P. Hoskin (2022). "GEC-ESTRO ACROP prostate brachytherapy guidelines." Radiotherapy and Oncology **167**: 244-251.

References

- Higgins, G. S., D. B. McLaren, G. R. Kerr, T. Elliott and G. C. Howard (2006). "Outcome analysis of 300 prostate cancer patients treated with neoadjuvant androgen deprivation and hypofractionated radiotherapy." Int J Radiat Oncol Biol Phys **65**(4): 982-989.
- Hjorth-Jensen, K., A. Maya-Mendoza, N. Dalgaard, J. O. Sigurðsson, J. Bartek, D. Iglesias-Gato, J. V. Olsen and A. Flores-Morales (2018). "SPOP promotes transcriptional expression of DNA repair and replication factors to prevent replication stress and genomic instability." Nucleic Acids Res **46**(18): 9484-9495.
- Horwitz, E. M., K. Bae, G. E. Hanks, A. Porter, D. J. Grignon, H. D. Brereton, V. Venkatesan, C. A. Lawton, S. A. Rosenthal, H. M. Sandler and W. U. Shipley (2008). "Ten-year follow-up of radiation therapy oncology group protocol 92-02: a phase III trial of the duration of elective androgen deprivation in locally advanced prostate cancer." J Clin Oncol **26**(15): 2497-2504.
- Huggins, C. and C. V. Hodges (1972). "Studies on prostatic cancer. I. The effect of castration, of estrogen and androgen injection on serum phosphatases in metastatic carcinoma of the prostate." CA Cancer J Clin **22**(4): 232-240.
- Jividen, K., K. Z. Kedzierska, C. S. Yang, K. Szlachta, A. Ratan and B. M. Paschal (2018). "Genomic analysis of DNA repair genes and androgen signaling in prostate cancer." BMC Cancer **18**(1): 960.
- Kari, V., W. Y. Mansour, S. K. Raul, S. J. Baumgart, A. Mund, M. Grade, H. Sirma, R. Simon, H. Will, M. Dobbstein, E. Dikomey and S. A. Johnsen (2016). "Loss of CHD1 causes DNA repair defects and enhances prostate cancer therapeutic responsiveness." EMBO Rep **17**(11): 1609-1623.
- Köcher, S., B. Beyer, T. Lange, L. Nordquist, J. Volquardsen, S. Burdak-Rothkamm, T. Schlomm, C. Petersen, K. Rothkamm and W. Y. Mansour (2019). "A functional ex vivo assay to detect PARP1-EJ repair and radiosensitization by PARP-inhibitor in prostate cancer." Int J Cancer **144**(7): 1685-1696.
- Korpai, M., J. M. Korn, X. Gao, D. P. Rakiec, D. A. Ruddy, S. Doshi, J. Yuan, S. G. Kovats, S. Kim, V. G. Cooke, J. E. Monahan, F. Stegmeier, T. M. Roberts, W. R. Sellers, W. Zhou and P. Zhu (2013). "An F876L mutation in androgen receptor confers genetic and phenotypic resistance to MDV3100 (enzalutamide)." Cancer Discov **3**(9): 1030-1043.
- Kupelian, P. A., V. V. Thakkar, D. Khuntia, C. A. Reddy, E. A. Klein and A. Mahadevan (2005). "Hypofractionated intensity-modulated radiotherapy (70 Gy at 2.5 Gy per fraction) for localized prostate cancer: long-term outcomes." Int J Radiat Oncol Biol Phys **63**(5): 1463-1468.
- Kwan, E. M. and A. W. Wyatt (2022). "Androgen receptor genomic alterations and treatment resistance in metastatic prostate cancer." Prostate **82 Suppl 1**: S25-s36.
- Li, L., S. Karanika, G. Yang, J. Wang, S. Park, B. M. Broom, G. C. Manyam, W. Wu, Y. Luo, S. Basourakos, J. H. Song, G. E. Gallick, T. Karantanos, D. Korentzelos, A. K. Azad, J. Kim, P. G. Corn, A. M. Aparicio, C. J. Logothetis, P. Troncoso, T. Heffernan, C. Toniatti, H. S. Lee, J. S. Lee, X. Zuo, W. Chang, J. Yin and T. C. Thompson (2017). "Androgen receptor inhibitor-induced "BRCAness" and PARP inhibition are synthetically lethal for castration-resistant prostate cancer." Sci Signal **10**(480).
- Li, Z., A. C. Bishop, M. Alyamani, J. A. Garcia, R. Dreicer, D. Bunch, J. Liu, S. K. Upadhyay, R. J. Auchus and N. Sharifi (2015). "Conversion of abiraterone to D4A drives anti-tumour activity in prostate cancer." Nature **523**(7560): 347-351.
- Ma, T. M., O. Lilleby, W. A. Lilleby and A. U. Kishan (2020). "Ablative Radiotherapy in Prostate Cancer: Stereotactic Body Radiotherapy and High Dose Rate Brachytherapy." Cancers (Basel) **12**(12).

References

- Mai, C. W., K. Y. Chin, L. C. Foong, K. L. Pang, B. Yu, Y. Shu, S. Chen, S. K. Cheong and C. W. Chua (2022). "Modeling prostate cancer: What does it take to build an ideal tumor model?" Cancer Lett **543**: 215794.
- Mansour, W. Y., P. Tennstedt, J. Volquardsen, C. Oing, M. Kluth, C. Hube-Magg, K. Borgmann, R. Simon, C. Petersen, E. Dikomey and K. Rothkamm (2018). "Loss of PTEN-assisted G2/M checkpoint impedes homologous recombination repair and enhances radio-curability and PARP inhibitor treatment response in prostate cancer." Sci Rep **8**(1): 3947.
- Marhold, M., G. Kramer, M. Krainer and C. Le Magnen (2022). "The prostate cancer landscape in Europe: Current challenges, future opportunities." Cancer Lett **526**: 304-310.
- Mateo, J., N. Porta, D. Bianchini, U. McGovern, T. Elliott, R. Jones, I. Syndikus, C. Ralph, S. Jain, M. Varughese, O. Parikh, S. Crabb, A. Robinson, D. McLaren, A. Birtle, J. Tanguay, S. Miranda, I. Figueiredo, G. Seed, C. Bertan, P. Flohr, B. Ebbs, P. Rescigno, G. Fowler, A. Ferreira, R. Riisnaes, R. Pereira, A. Curcean, R. Chandler, M. Clarke, B. Gurel, M. Crespo, D. Nava Rodrigues, S. Sandhu, A. Espinasse, P. Chatfield, N. Tunariu, W. Yuan, E. Hall, S. Carreira and J. S. de Bono (2020). "Olaparib in patients with metastatic castration-resistant prostate cancer with DNA repair gene aberrations (TOPARP-B): a multicentre, open-label, randomised, phase 2 trial." Lancet Oncol **21**(1): 162-174.
- McGowan, D. G., D. Hunt, C. U. Jones, M. Amin, M. H. Leibenhaut, S. M. Husian, M. Rotman, L. Souhami, H. Sandler and W. U. Shipley (2010). "Short-term Endocrine Therapy Prior to and during Radiation Therapy Improves Overall Survival in Patients with T1b-T2b Adenocarcinoma of the Prostate and PSA ≥ 20; 20: Initial Results of RTOG 94-08." International Journal of Radiation Oncology, Biology, Physics **77**(1): 1.
- Merseburger, A. S., A. Alcaraz and C. A. von Klot (2016). "Androgen deprivation therapy as backbone therapy in the management of prostate cancer." Onco Targets Ther **9**: 7263-7274.
- Mills, I. G. (2014). "Maintaining and reprogramming genomic androgen receptor activity in prostate cancer." Nat Rev Cancer **14**(3): 187-198.
- Mohler, J. L., E. S. Antonarakis, A. J. Armstrong, A. V. D'Amico, B. J. Davis, T. Dorff, J. A. Eastham, C. A. Enke, T. A. Farrington, C. S. Higano, E. M. Horwitz, M. Hurwitz, J. E. Ippolito, C. J. Kane, M. R. Kuettel, J. M. Lang, J. McKenney, G. Netto, D. F. Penson, E. R. Plimack, J. M. Pow-Sang, T. J. Pugh, S. Richey, M. Roach, S. Rosenfeld, E. Schaeffer, A. Shabsigh, E. J. Small, D. E. Spratt, S. Srinivas, J. Tward, D. A. Shead and D. A. Freedman-Cass (2019). "Prostate Cancer, Version 2.2019, NCCN Clinical Practice Guidelines in Oncology." J Natl Compr Canc Netw **17**(5): 479-505.
- Montgomery, R. B., E. A. Mostaghel, R. Vessella, D. L. Hess, T. F. Kalhorn, C. S. Higano, L. D. True and P. S. Nelson (2008). "Maintenance of intratumoral androgens in metastatic prostate cancer: a mechanism for castration-resistant tumor growth." Cancer Res **68**(11): 4447-4454.
- Morote, J., A. Aguilar, J. Planas and E. Trilla (2022). "Definition of Castrate Resistant Prostate Cancer: New Insights." Biomedicines **10**(3).
- Mostaghel, E. A., B. T. Marck, S. R. Plymate, R. L. Vessella, S. Balk, A. M. Matsumoto, P. S. Nelson and R. B. Montgomery (2011). "Resistance to CYP17A1 inhibition with abiraterone in castration-resistant prostate cancer: induction of steroidogenesis and androgen receptor splice variants." Clin Cancer Res **17**(18): 5913-5925.
- Negrini, S., V. G. Gorgoulis and T. D. Halazonetis (2010). "Genomic instability--an evolving hallmark of cancer." Nat Rev Mol Cell Biol **11**(3): 220-228.
- Paschalis, A. and J. S. de Bono (2020). "Prostate Cancer 2020: "The Times They Are a'Changing"." Cancer Cell **38**(1): 25-27.

References

- Patel, S. A., J. M. Switchenko, B. Fischer-Valuck, C. Zhang, B. S. Rose, R. C. Chen, A. B. Jani and T. J. Royce (2020). "Stereotactic body radiotherapy versus conventional/moderate fractionated radiation therapy with androgen deprivation therapy for unfavorable risk prostate cancer." Radiation Oncology **15**(1): 217.
- Polkinghorn, W. R., J. S. Parker, M. X. Lee, E. M. Kass, D. E. Spratt, P. J. Iaquinta, V. K. Arora, W. F. Yen, L. Cai, D. Zheng, B. S. Carver, Y. Chen, P. A. Watson, N. P. Shah, S. Fujisawa, A. G. Goglia, A. Gopalan, H. Hieronymus, J. Wongvipat, P. T. Scardino, M. J. Zelefsky, M. Jasin, J. Chaudhuri, S. N. Powell and C. L. Sawyers (2013). "Androgen receptor signaling regulates DNA repair in prostate cancers." Cancer Discov **3**(11): 1245-1253.
- Pritchard, C. C., C. Morrissey, A. Kumar, X. Zhang, C. Smith, I. Coleman, S. J. Salipante, J. Milbank, M. Yu, W. M. Grady, J. F. Tait, E. Corey, R. L. Vessella, T. Walsh, J. Shendure and P. S. Nelson (2014). "Complex MSH2 and MSH6 mutations in hypermutated microsatellite unstable advanced prostate cancer." Nat Commun **5**: 4988.
- Quéro, L., N. Giocanti, C. Hennequin and V. Favaudon (2010). "Antagonistic interaction between bicalutamide (Casodex) and radiation in androgen-positive prostate cancer LNCaP cells." Prostate **70**(4): 401-411.
- Rathkopf, D. E., M. J. Morris, J. J. Fox, D. C. Danila, S. F. Slovin, J. H. Hager, P. J. Rix, E. Chow Maneval, I. Chen, M. Gönen, M. Fleisher, S. M. Larson, C. L. Sawyers and H. I. Scher (2013). "Phase I study of ARN-509, a novel antiandrogen, in the treatment of castration-resistant prostate cancer." J Clin Oncol **31**(28): 3525-3530.
- Rebello, R. J., C. Oing, K. E. Knudsen, S. Loeb, D. C. Johnson, R. E. Reiter, S. Gillissen, T. Van der Kwast and R. G. Bristow (2021). "Prostate cancer." Nat Rev Dis Primers **7**(1): 9.
- Rotinen, M., S. You, J. Yang, S. G. Coetzee, M. Reis-Sobreiro, W. C. Huang, F. Huang, X. Pan, A. Yáñez, D. J. Hazelett, C. Y. Chu, K. Steadman, C. M. Morrissey, P. S. Nelson, E. Corey, L. W. K. Chung, S. J. Freedland, D. Di Vizio, I. P. Garraway, R. Murali, B. S. Knudsen and M. R. Freeman (2018). "ONECUT2 is a targetable master regulator of lethal prostate cancer that suppresses the androgen axis." Nat Med **24**(12): 1887-1898.
- Saad, F., A. J. Armstrong, A. Thiery-Vuillemin, M. Oya, E. Loreda, G. Procopio, J. J. d. Menezes, G. C. Giroto, C. Arslan, N. Mehra, F. Parnis, E. Brown, F. Schlürmann, J. Y. Joung, M. Sugimoto, C. H. Poehlein, E. Harrington, C. Desai, J. Kang and N. Clarke (2022). "PROpel: Phase III trial of olaparib (ola) and abiraterone (abi) versus placebo (pbo) and abi as first-line (1L) therapy for patients (pts) with metastatic castration-resistant prostate cancer (mCRPC)." Journal of Clinical Oncology **40**(6_suppl): 11-11.
- See, W. A. and C. J. Tyrrell (2006). "The addition of bicalutamide 150 mg to radiotherapy significantly improves overall survival in men with locally advanced prostate cancer." J Cancer Res Clin Oncol **132** Suppl 1: S7-16.
- Song, H., H. N. W. Weinstein, P. Allegakoen, M. H. Wadsworth, J. Xie, H. Yang, E. A. Castro, K. L. Lu, B. A. Stohr, F. Y. Feng, P. R. Carroll, B. Wang, M. R. Cooperberg, A. K. Shalek and F. W. Huang (2022). "Single-cell analysis of human primary prostate cancer reveals the heterogeneity of tumor-associated epithelial cell states." Nature Communications **13**(1): 141.
- Strouthos, I., N. Tselis, G. Chatzikonstantinou, S. Butt, D. Baltas, D. Bon, N. Milickovic and N. Zamboglou (2018). "High dose rate brachytherapy as monotherapy for localised prostate cancer." Radiother Oncol **126**(2): 270-277.
- Tan, M. H., J. Li, H. E. Xu, K. Melcher and E. L. Yong (2015). "Androgen receptor: structure, role in prostate cancer and drug discovery." Acta Pharmacol Sin **36**(1): 3-23.

References

- Taplin, M. E., G. J. Bubley, Y. J. Ko, E. J. Small, M. Upton, B. Rajeshkumar and S. P. Balk (1999). "Selection for androgen receptor mutations in prostate cancers treated with androgen antagonist." Cancer Res **59**(11): 2511-2515.
- Tepper, J. E., R. L. Foote and J. M. Michalski (2021). Gunderson & Tepper's Clinical Radiation Oncology, Elsevier.
- Tran, C., S. Ouk, N. J. Clegg, Y. Chen, P. A. Watson, V. Arora, J. Wongvipat, P. M. Smith-Jones, D. Yoo, A. Kwon, T. Wasielewska, D. Welsbie, C. D. Chen, C. S. Higano, T. M. Beer, D. T. Hung, H. I. Scher, M. E. Jung and C. L. Sawyers (2009). "Development of a second-generation antiandrogen for treatment of advanced prostate cancer." Science **324**(5928): 787-790.
- Vasaitis, T. S., R. D. Bruno and V. C. Njar (2011). "CYP17 inhibitors for prostate cancer therapy." J Steroid Biochem Mol Biol **125**(1-2): 23-31.
- Walsh, P. C. (1998). "Anatomic radical prostatectomy: evolution of the surgical technique." J Urol **160**(6 Pt 2): 2418-2424.
- Waltering, K. K., A. Urbanucci and T. Visakorpi (2012). "Androgen receptor (AR) aberrations in castration-resistant prostate cancer." Mol Cell Endocrinol **360**(1-2): 38-43.
- Wright, W. D., S. S. Shah and W. D. Heyer (2018). "Homologous recombination and the repair of DNA double-strand breaks." J Biol Chem **293**(27): 10524-10535.
- Wu, K., J. Liang, Y. Shao, S. Xiong, S. Feng and X. Li (2021). "Evaluation of the Efficacy of PARP Inhibitors in Metastatic Castration-Resistant Prostate Cancer: A Systematic Review and Meta-Analysis." Front Pharmacol **12**: 777663.
- Yossepowitch, O., S. E. Eggener, A. M. Serio, B. S. Carver, F. J. Bianco, Jr., P. T. Scardino and J. A. Eastham (2008). "Secondary therapy, metastatic progression, and cancer-specific mortality in men with clinically high-risk prostate cancer treated with radical prostatectomy." Eur Urol **53**(5): 950-959.

4. Publication list

4.1. Publication 1



Article

Second-Generation Antiandrogen Therapy Radiosensitizes Prostate Cancer Regardless of Castration State through Inhibition of DNA Double Strand Break Repair

Mohamed E. Elsesy ^{1,2} , Su Jung Oh-Hohenhorst ^{3,4}, Anastassia Löser ¹, Christoph Oing ^{5,6} , Sally Mutiara ¹, Sabrina Köcher ¹, Stefanie Meien ^{1,6}, Alexandra Zielinski ¹, Susanne Burdak-Rothkamm ¹ , Derya Tilki ^{3,7}, Hartwig Huland ³, Rudolf Schwarz ¹, Cordula Petersen ¹, Carsten Bokemeyer ⁵, Kai Rothkamm ¹ and Wael Y. Mansour ^{1,2,6,*}

- ¹ Department of Radiotherapy and Radiooncology, University Medical Center Hamburg-Eppendorf, 20246 Hamburg, Germany; m.elsesy@uke.de (M.E.E.); an.loeser@uke.de (A.L.); sally.mutiara@gmail.com (S.M.); s.koecher@uke.de (S.K.); s.meien@uke.de (S.M.); a.zielinski@uke.de (A.Z.); s.burdak-rothkamm@uke.de (S.B.-R.); r.schwarz@uke.de (R.S.); cor.petersen@uke.de (C.P.); k.rothkamm@uke.de (K.R.)
- ² Department of Tumor Biology, National Cancer Institute, Cairo University, Cairo 11796, Egypt
- ³ Martini-Klinik Prostate Cancer Center, University Medical Center Hamburg-Eppendorf, 20246 Hamburg, Germany; s.oh-hohenhorst@uke.de (S.J.O.-H.); d.tilki@uke.de (D.T.); h.huland@uke.de (H.H.)
- ⁴ Institute of Anatomy and Experimental Morphology, University Medical Center Hamburg-Eppendorf, 20246 Hamburg, Germany
- ⁵ Department of Oncology, Hematology and Bone Marrow Transplantation with Section of Pneumology, University Medical Center Hamburg-Eppendorf, 20246 Hamburg, Germany; c.oing@uke.de (C.O.); cbokemeyer@uke.de (C.B.)
- ⁶ Mildred Scheel Cancer Career Center HaTriCS4, University Medical Center Hamburg-Eppendorf, 20246 Hamburg, Germany
- ⁷ Department of Urology, University Medical Center Hamburg-Eppendorf, 20246 Hamburg, Germany
- * Correspondence: wmansour@uke.de; Tel.: +49-40-7410-53831; Fax: +49-40-7410-55139

Received: 10 August 2020; Accepted: 27 August 2020; Published: 31 August 2020



Simple Summary: The combination of RT and the first generation AR blockers to improve the outcome in prostate cancer remain a matter of controversial debate in clinical trials. In the current study we aim to investigate the effect of three FDA approved second-generation antiandrogens (abiraterone acetate, apalutamide and enzalutamide), as more potent inhibitors of the AR signaling, on the cytotoxicity of RT in pre-clinical models. In vitro and ex vivo analyses revealed a strong radiosensitising effect for the second-generation antiandrogens, regardless of the castration state. The first-generation AR-blocker bicalutamide failed to show any radiosensitising effect. The radiosensitising effect of the second-generation antiandrogens was attributed to the inhibition of DSB repair. Together, we provide a proof-of-principle pre-clinical evidence to rationalize the clinical use of the second-generation antiandrogens to enhance the effect of IR as a potential strategy to improve the outcomes of PCa patients with localized disease who undergo ablative RT.

Abstract: (1) *Background:* The combination of the first-generation antiandrogens and radiotherapy (RT) has been studied extensively in the clinical setting of prostate cancer (PCa). Here, we evaluated the potential radiosensitizing effect of the second-generation antiandrogens abiraterone acetate, apalutamide and enzalutamide. (2) *Methods:* Cell proliferation and agarose-colony forming assay were used to measure the effect on survival. Double strand break repair efficiency was monitored using immunofluorescence staining of γ H2AX/53BP1. (3) *Results:* We report retrospectively a minor benefit for PCa patients received first-generation androgen blockers and RT compared

to patients treated with RT alone. Combining either of the second-generation antiandrogens and 2Gy suppressed cell growth and increased doubling time significantly more than 2Gy alone, in both hormone-responsive LNCaP and castration-resistant C4-2B cells. These findings were recapitulated in resistant sub-clones to (i) hormone ablation (LNCaP-abl), (ii) abiraterone acetate (LNCaP-abi), (iii) apalutamide (LNCaP-ARN509), (iv) enzalutamide (C4-2B-ENZA), and in castration-resistant 22-RV1 cells. This radiosensitization effect was not observable using the first-generation antiandrogen bicalutamide. Inhibition of DNA DSB repair was found to contribute to the radiosensitization effect of second-generation antiandrogens, as demonstrated by a significant increase in residual γ H2AX and 53BP1 foci numbers at 24h post-IR. DSB repair inhibition was further demonstrated in 22 patient-derived tumor slice cultures treated with abiraterone acetate before ex-vivo irradiation with 2Gy. (4) *Conclusion:* Together, these data show that second-generation antiandrogens can enhance radiosensitivity in PCa through DSB repair inhibition, regardless of their hormonal status. Translated into clinical practice, our results may help to find additional strategies to improve the effectiveness of RT in localized PCa, paving the way for a clinical trial.

Keywords: abiraterone acetate; apalutamide; enzalutamide; DNA double strand break repair; prostate cancer; radiosensitization

1. Introduction

Prostate cancer (PCa) remains one of the most frequent cancers, and a leading cause of cancer death [1]. Treatment modalities for localized disease include radical prostatectomy, radiation therapy (RT) with or without androgen deprivation therapy (ADT), and active surveillance [1]. Conventional ADT acts by either inhibiting the testosterone production within the testicular stroma through interfering with luteinizing hormone releasing hormone (LHRH) from the pituitary gland or a direct blockade of androgen binding to the androgen receptor (AR). Both approaches block AR signaling, which is the major driver of PCa growth and progression [2]. Currently, various classes of ADT drugs are available, including LHRH agonists and antagonists, and androgen receptor inhibitors (ARIs), such as bicalutamide, flutamide or cyproterone acetate [3,4]. Eventually, ADT prevents the activation and subsequent translocation of the AR to the nucleus, where it acts as a transcription factor, regulating the expression of many target genes that promote prostatic epithelial cell survival and proliferation [4]. ADT has been shown to induce symptom relief and biochemical and objective responses in PCa patients, highlighting the pivotal role of androgens in PCa evolution [5]. Despite the immediate palliative benefits that can be achieved by ADT, the majority of patients relapse within a few years, due to alternative mechanisms of AR signaling, AR amplification or alternative splicing, intratumoral androgen production, or adrenal gland testosterone production. Rising prostate-specific antigen (PSA) values or detectable disease progression despite the appropriate suppression of systemic testosterone levels characterize castration resistance, a major driver of PCa-associated mortality [6,7]. Androgens are still of utmost importance for the growth of castration-resistant PCa (CRPC); that is why CRPC treatment strategies involve novel, second-generation antiandrogenic agents. These differ from LHRH analogues, by blocking specific aspects of extra-gonadal androgen-synthesis and tumoral AR signaling. First-generation antiandrogens established androgen receptor blockade as a therapeutic strategy, but do not completely abrogate androgen receptor activity. Efficacy and potency have been improved by the development of second-generation antiandrogen therapies. These exhibit increased specificity to the AR over other steroidal receptors, act at a higher affinity than the first generation, are exclusively antagonistic to the AR, and in turn, elicit no androgen withdrawal syndrome.

Several second-generation anti-androgens are currently approved by the Food and Drug Administration (FDA), including the androgen biosynthesis inhibitor abiraterone acetate, which suppresses the CYP17 enzyme, and direct AR blockers, such as enzalutamide, apalutamide and darolutamide,

which block AR with 6–9-fold greater affinity than that of the first-generation agent bicalutamide. Notably, abiraterone was found to act as an AR antagonist, which leads to a dose dependent decrease in the AR levels [8,9].

Radiotherapy (RT) is one of the genotoxic modalities that induces various forms of DNA damage. Double strand breaks (DSBs) are considered the most important and toxic lesions induced by ionizing radiation (IR), which, if not repaired or inappropriately repaired, can eventually result in genomic instability and subsequent cell death. A sophisticated DNA-damage response (DDR) machinery, represented by the two main pathways, homologous recombination (HR) and nonhomologous end joining (NHEJ), can ensure fast and appropriate repair of the DSBs. Importantly, tumors with a collapse in the DNA repair capacity of either the HR or NHEJ pathways which can be due to mutations in DDR genes can provide more benefit after radiotherapy [10].

RT is an effective local therapy which is used as a curative treatment of localized intermediate or high risk PCa [11]. However, up to 30% of PCa patients show signs of treatment failure within 5 years [12]. The risk of failure of local treatment approaches can be estimated by the D’Amico risk classification stratifying patients as low, intermediate or high risk, based on the known prognostic factors: PSA, Gleason score (GS), and T stage. Moreover, factors associated with intrinsic tumor radioresistance or micro metastatic disease may also contribute to relapses following ablative radiotherapy [13,14]. Possible alternatives to improve RT results include higher radiation doses and agents that optimize the radiation effect [15].

Preclinical studies have demonstrated a radiosensitizing role of androgen suppression, arguing towards the combination of RT together with ADT to enhance the therapeutic effect. Despite several clinical studies, the timing and duration of ADT in relation to ablative radiotherapy remain a matter of controversial debate, but ADT has been adopted as a central companion treatment for patients undergoing curative RT for localized disease. For high-risk prostate cancer, long-term ADT for 18 months has been shown to be better than 6 months of ADT in terms of local treatment failure, biochemical relapse rates, distant metastasis-free survival and overall survival (OS) in a large randomized clinical trial [16]. Interestingly, 18 months of ADT were equally effective to 36 months of ADT in the same setting in another large clinical trial [17]. As a consequence, duration (and timing) of ADT in relation to ablative radiotherapy and the mechanisms behind ADT acting as a radiosensitizing treatment need to be further elucidated.

This study aimed to investigate the ability of second generation antiandrogens to enhance the cytotoxic effects and therapeutic ratio of IR, and to determine potential mechanisms underlying this effect. Findings revealed that, regardless of the castration state, second generation antiandrogens, such as abiraterone acetate, apalutamide, and enzalutamide efficiently radiosensitize PCa cells through the inhibition of DNA DSB repair capacity. Our observations provide a mechanistic rationale to study the combination of second generation androgens and locally ablative RT in the clinical setting, to further improve outcomes for patients with localized disease.

2. Results

2.1. ADT Plus RT Confers a Slight but Not Significant Increase in the Biochemical Relapse-Free Survival of Patients with Intermediate- and High-Risk PCa

Due to the increasing interest for the use of combined antiandrogenic therapy with RT in the management of PCa, we performed a retrospective analysis, employing a cohort of 166 PCa patients treated with RT with or without ADT, between 2008 and 2016 at our institution. The median follow-up was 40 months (range 12–116) and the median age of patients was 73 years old (range 53–80). Further clinicopathological characteristics of the patients are described in Table 1.

Table 1. Patient characteristics.

Characteristics	n	%	Mean (±SD)/Median (Range)
Age (years)	166	100	73 (53–80)
Baseline PSA-value (ng/mL)	166	100	8 (2.1–165)
<10	100	60.2	6 (2.1–9.85)
10–20	47	28.3	12.58 (10–20)
>20	19	11.4	39 (21.5–165)
Post-therapeutic PSA-nadir (ng/mL)	164	100	0.1 (0–13.5)
Gleason-Score	166	100	7 (6–10)
<7	19	11.4	6
7	112	67.5	7
>7	35	21.1	8 (8–10)
T stage *	165 *	100	-
T1c	39	23.6	-
T2a-b	53	32.1	-
T2c-T3a/b	71	43	-
Tx	2	1.2	-
Risk categories *	166	100	-
Low risk	5	3	-
Intermediate risk	104	62.7	-
High risk	57	34.3	-
Androgen deprivation therapy	166	100	-
Yes	46	27.7	-
No	120	72.2	-
Target volume (EBRT)	166	100	-
Prostate and seminal vesicles	125	75.3	-
Additional irradiation of pelvic lymph nodes	41	24.7	-
Charlson Comorbidity Index	165	100	4 (1–9)

* For defining risk categories, classification according to NCCN was applied. Thus, the worst/highest parameter was leading in defining the underlying risk group. EBRT: External Beam Radiation Therapy; NCCN: National Comprehensive Cancer Center.

The patients were classified as treated with RT alone (without ADT) or with ADT plus RT (+ADT). Biochemical relapse-free as well as OS were compared in both arms. Neither overall nor biochemical relapse-free survival showed a benefit for the combined treatment compared to the RT alone (Figure 1a,b).

While the patients with high-risk cancer generally responded worse to RT than those with intermediate cancer as shown in Figure 1c, patients treated with RT and ADT showed a moderate tendency towards increased BCR-free survival in both risk groups. However, we failed to identify any statistical difference between the two groups (±ADT) for either intermediate or high-risk patients ($p = 0.25$). In terms of therapy-related side effects, 59.9% of patients ($n = 94/155$) suffered from low grades (1–2) of acute gastrointestinal toxicity (GIT), while 87.7% ($n = 136/155$) exhibited symptoms of genitourinary toxicity (GUT). There was no significant difference between the two treatment groups regarding the occurrence of GIT (Table 2, $p = 0.34$), and only modest significance regarding GUT (Table 3, $p = 0.06$).

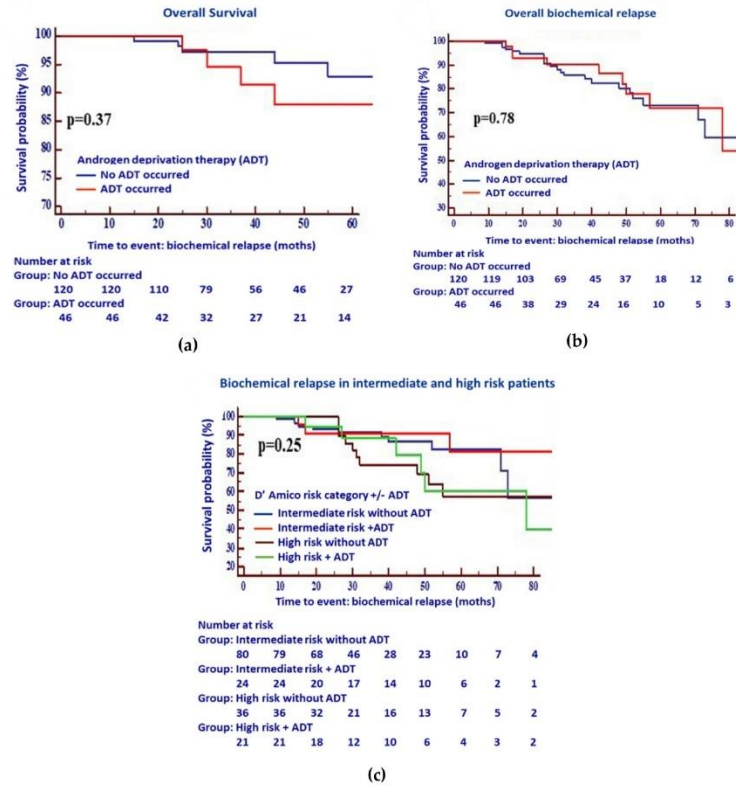


Figure 1. Kaplan–Meier estimates for (a) overall survival following RT with ADT ($n = 65$) or without ADT ($n = 138$), (b) the overall biochemical relapse of intermediate risk vs high risk PCa patients, and (c) the biochemical relapse in intermediate and high risk PCa patients following RT, with or without ADT. A multivariable Cox proportional hazards model did not show any statistically significant differences between the biochemical relapse of patients treated with ADT plus RT and those treated with RT alone.

Table 2. Gastrointestinal toxicity (GIT).

Side Effect		ADT		Total
		No	Yes	
Acute GIT Toxicity	No GIT	48	15	63
	Grade 1 or 2 GIT	65	29	94
Total		113	44	157

Table 3. Genitourinary toxicity (GUT).

Side Effect		ADT		Total
		No	Yes	
Acute GUT Toxicity	No GUT	17	2	19
	Grade 1 or 2 GUT	94	42	136
Total		111	44	155

One common issue between our retrospective study and other reported studies is the use of first-generation antiandrogens, such as bicalutamide or LHRH-analogue. Therefore, a possible explanation

for the lack of any significant benefit of the combination strategy could be such that ADT does not completely block the AR-axis.

2.2. Second-Generation Antiandrogens Enhance the Response of Prostate Cancer Cells to IR

Thus, we sought to explore the impact of combining second-generation antiandrogens to improve the ionizing radiation effect. To that end, androgen-sensitive LNCaP and castration-resistant C4-2B cells were exposed to IR with a dose of 2 Gy, after 24 h-incubation with two different concentrations of the second-generation antiandrogens; abiraterone acetate (Abi), enzalutamide (ENZA), or apalutamide (ARN509), and the effect on proliferation rate was measured.

In LNCaP, the second-generation antiandrogens alone exhibited similar growth-inhibiting effects (Figure 2a–c, upper panels), with a clear increase in doubling time (DT) in a dose-dependent manner (Figure 2a–c, lower panels). Irradiating the cells with 2 Gy alone reduced the cell growth to a similar extent as monotherapy with the respective antiandrogen, as illustrated by similar DTs. Interestingly, combining either of the indicated novel antiandrogens and 2 Gy further suppressed the growth rate of LNCaP, cells as exemplified by increased DTs of at least 1.5-fold for combination, with the lower concentration of antiandrogen and up to 2.3-fold with the therapeutic concentration, indicating a potential cooperative effect between these novel antiandrogens and IR.

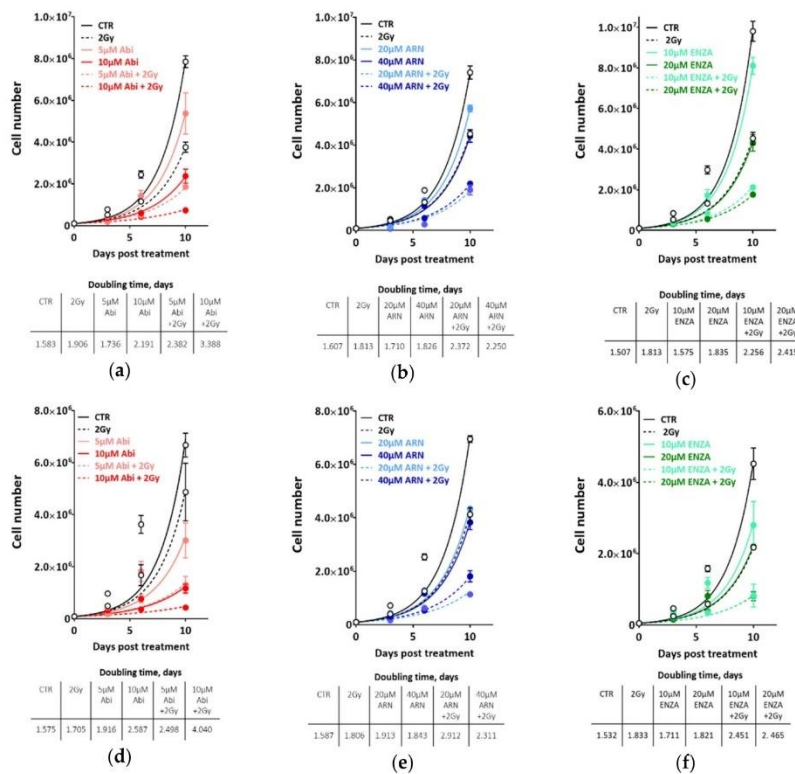


Figure 2. ADT potentiates the cytotoxicity of ionizing radiation in both hormone sensitive LNCaP and hormone resistant C4-2B cells. Cell number was determined in LNCaP (a–c) or C4-2B cells (d–f) on days 0, 3, 6 and 10 post treatment, with the indicated concentrations of abiraterone acetate (a,d), apalutamide (ARN) (b,e) or enzalutamide (ENZA) (d,f). Cell doubling time in days was calculated for each treatment, by fitting exponential growth curves using GraphPad Prism 7. Shown are means ±SEM of at least three independent experiments.

Strikingly, in castration-resistant C4-2B cells, we observed similar proliferation inhibitory effects (Figure 2d–f, upper panels) and increased DTs (Figure 2d–f, lower panels) as in androgen-sensitive LNCaP cells (Figure 2a–c). In order to consolidate these findings, castration-resistant 22-RV1 cell lines were employed, and the colony formation assay was used to assess the effect of the afore-mentioned combination therapy strategies on clonogenic cell survival. As illustrated in Figure 3a, the combination of antiandrogen with 2 Gy strongly inhibited the survival of 22R-V1 cells, despite the moderate effect of single therapy with either antiandrogens or 2 Gy alone (Figure 3a). In keeping with the radiosensitization idea, we reported a significant radiosensitizing effect on 22R-V1 cells, upon combining 5 μ M abiraterone acetate and different IR doses (Figure 3b). Importantly, this strong radio-sensitization effect was specific to the second-generation antiandrogens, while the first-generation of antiandrogen, bicalutamide (10 μ M), failed to further enhance the cytotoxic effects of IR compared to either bicalutamide or 2 Gy alone in 22R-V1 (Figure 3b), as well as in both LNCaP and C4-2B cells (Figure 3c,d). Notably, no difference was reported between the extents of radiosensitization mediated by the tested second-generation antiandrogens (Figure S1). Together, these data suggest that second-generation antiandrogens can more efficiently radiosensitize PCa cells, regardless of castration state.

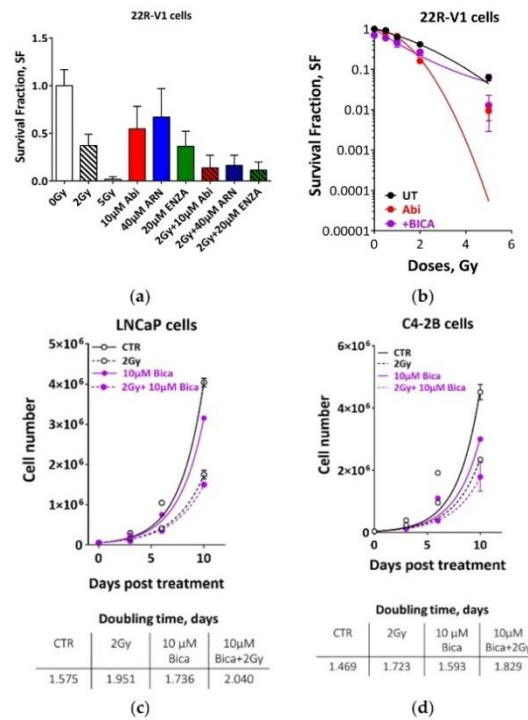


Figure 3. Second generation antiandrogen therapy but not bicalutamide potentiates the cytotoxicity of ionizing radiation in PCa cells. (a) 22R-V1 were treated with the indicated concentrations of second-generation antiandrogens and 2Gy either alone or combined and cell survivals were measured using colony forming assay. (b) 22R-V1 cells were treated with either 5 μ M abiraterone acetate or 10 μ M bicalutamide for 24 h before irradiated with the indicated doses, and the survival fractions (SFs) were measured using colony forming assay. (c,d) Upper panels: Cell number was determined in LNCaP (c) and C4-2B (d) cells on days 0, 3, 6 and 10 post treatment with 10 μ M bicalutamide and 2 Gy either individually or combined. Lower panels: Cell doubling time in days was calculated for each treatment by fitting exponential growth curves using GraphPad Prism 7. Shown are means \pm SEM of at least three independent experiments.

2.3. Second Generation Antiandrogens Escalate the IR Effect about 2 Times

The use of RT doses higher than the conventional IR doses of 70 to 72 Gy could increase the ability to sterilize and thereby cure PCa. However, additional RT doses would increase normal tissue toxicity, which limits this escalation strategy. Therefore, it is crucial to develop a strategy to intensify the effect of the IR without escalating the dose. Based on the previous investigation that ADT reduces the dose of RT required to control 50% of Shinonogi adenocarcinoma tumors [18], we compared the effect of escalating IR doses and the combination therapy with the second generation of antiandrogens. Therefore, we escalated the IR dose to 5 and 10 Gy, and compared the effect of these escalated radiation doses with the effect of combining 2 Gy with different concentrations of novel antiandrogens. As expected, a strong IR dose-dependent growth inhibition effect was found in both LNCaP and C4-2B cell lines (Figure S2). In both cell lines, the growth-inhibitory effect of combining 2 Gy and therapeutic concentrations of the utilized antiandrogens was similar to that of 5 Gy alone, as evidenced by (i) no, or at least, very little difference between the average of the inhibitory effects of both treatment settings, after 3 days, 6 days or 10 days (Figure 4a,b), and (ii) the similar increase in DTs (3.05 d, 2.8d, 2.9d and 2.7d for 5Gy, Abi+2 Gy, ARN+2 Gy and ENZA+2 Gy, respectively) (Figure 4c). In order to further verify this, LNCaP and C4-2B cells were treated with 5 μM abiraterone acetate and IR (0, 1, 2, 5, 10 Gy), either individually or combined, and effects on survival were analyzed using agarose CFA. Again, a radiosensitizing effect was reported upon pre-treatment with abiraterone acetate in both cell lines, and interestingly the effect of abiraterone + 2 Gy was similar to that of 5 Gy alone (Figure S2c,d). Again, bicalutamide failed to radiosensitize either LNCaP or C4-2B cells (Figure S2c,d). These data suppose a beneficial clinical outcome from the use of second-generation antiandrogens, either to (i) reduce IR doses, hence alleviating the adverse effects from higher IR doses, or (ii) to escalate the effect of the same RT dose.

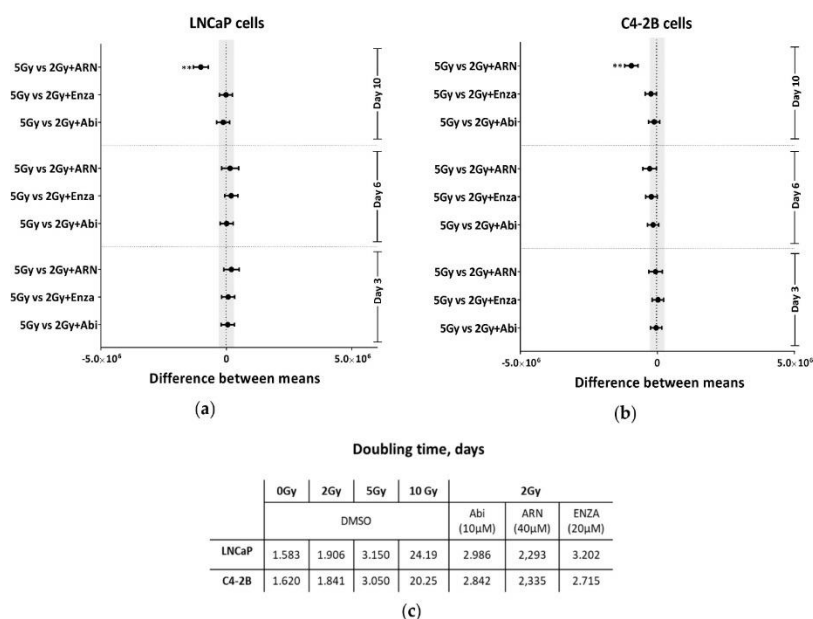


Figure 4. Second generation antiandrogen therapy enhances the IR effect at least 2-fold. Tukey’s multiple comparisons test was used to compare between the effect of 5 Gy and the different indicated treatments on the growth inhibition in (a) LNCaP and (b) C4-2B cells. Significance was measured using two-way ANOVA test. (c) Cell-doubling time in days was calculated for the indicated treatments by fitting exponential growth curves using GraphPad Prism 7. Shown are means ±SEM of at least three independent experiments. Significance is indicated as ** for $p < 0.001$.

2.4. Appropriate Choice of Antiandrogen to Maximize the Therapeutic Effect of IR in Acquired AHT-Resistant PCa Cells

The above data reveal that second-generation anti-androgens can efficiently radiosensitize even the CRPC cells. Since the CRPC is a very heterogeneous disease, and in order to more generalize our findings, we sought to employ PCa cell lines that had acquired resistance to therapeutic agents that target the AR axis [19,20], including (i) three subclones from the LNCaP cells which mimic hormone ablation-resistance (LNCaP-abl), are resistant to abiraterone acetate (LNCaP-Abi), or to apalutamide (LNCaP-ARN509) and (ii) one C4-2B subclone which is resistant to enzalutamide (C4-2B-ENZA).

Firstly, the resistant phenotypes of these cells were confirmed. In parental LNCaP cells, the cell growth rates were significantly inhibited with an approximately 2-fold increase in the DT in the presence of therapeutic concentrations of either of the antiandrogens. The resistant LNCaP sub-clones however, showed no effect on cell growth (Figure 5a–c, upper panels) and no difference in the DTs (Figure 5a–c, lower panels) when cultured in hormone-ablated medium (from 2.0 to 2.2 days), or treated with either 10 μM abiraterone acetate (from 3.836 to 4.132 days, Figure 5b) or 20 μM ARN509 (from 2.6 to 2.8 days, Figure 5c) for 10 days. Likewise, C4-2B-ENZA did not exhibit any significant change in the growth profile or DT (from 2.4 to 2.6 days) after treatment with 20 μM enzalutamide, while the proliferation of parental C4-2B cells was dramatically suppressed with a 1.7-fold increase in the DT (Figure 5d).

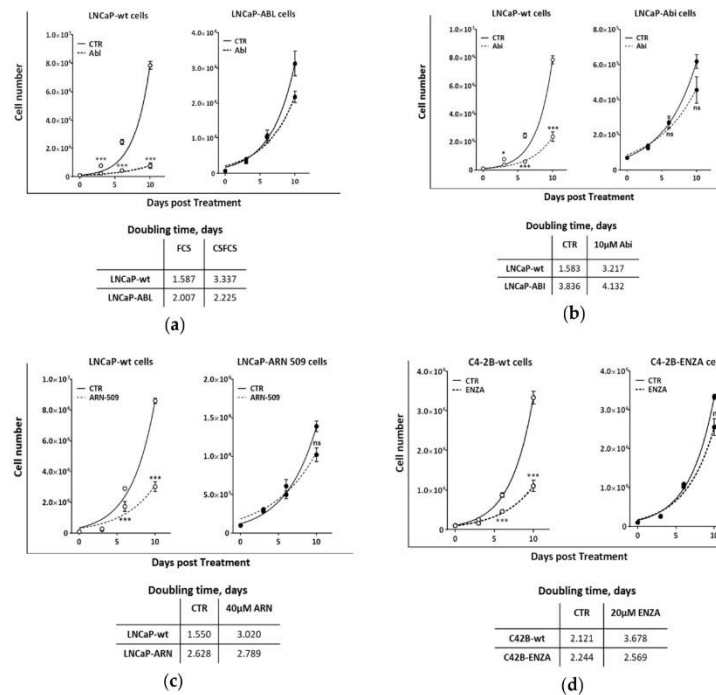


Figure 5. Resistance phenotype of ADT resistant PCa cells. Cell number was determined on days 0, 3, 6 and 10 post treatment with (a) hormone ablation, (b) 10 μM abiraterone acetate, (c) 40 μM apalutamide, or (d) 20 μM enzalutamide. Cells used are LNCaP (LNCaP-wt) cells, and their resistant sublines to: hormone ablation (LNCaP-abl), abiraterone acetate (LNCaP-abi), or apalutamide (LNCaP-ARN509), as well as wildtype C4-2B (C4-2B-wt) cells, or their resistant subclone to enzalutamide (C4-2B-ENZA). Cell-doubling time was calculated for each treatment by fitting exponential growth curves using GraphPad Prism 7. Shown are means ±SEM of at least three independent experiments. Significance is indicated as * for $p < 0.05$, and *** for $p < 0.0001$, ns: not significant.

Next, we investigated the effect of the different antiandrogens on the radiosensitivity of the resistant sublines. To that end, cells were treated with the indicated antiandrogens and 2 Gy either individually or combined, and the effect on cell growth was monitored by cell counting at 3, 6 and 10 days post treatment. As indicated in Figure 6a, in addition to the expected resistance to hormone ablation, LNCaP-abl cells were resistant to the other novel antiandrogens with no or very minor effect on DTs. However, combining 2 Gy with ARN509 or enzalutamide, but not abiraterone, significantly inhibited cell growth compared to the single use of antiandrogens or 2 Gy alone (Figure 5a). Enhanced radiosensitivity was also reported in LNCaP-abl cells grown in hormone-ablated medium with a 1.6-fold increase in DT compared to the same cells grown in hormone proficient medium (Figure 4a,e), indicating that ADT may radiosensitize even ADT-resistant cells. This was further confirmed in the other LNCaP-derived resistant subclones.

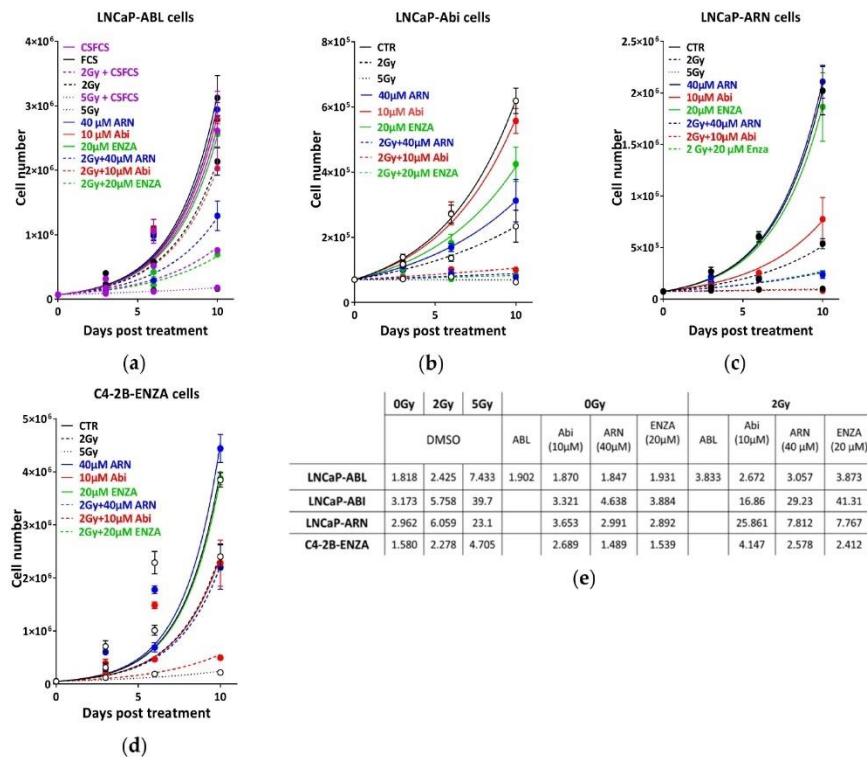


Figure 6. Second generation ADT potentiates the cytotoxicity of ionizing radiation in castration resistant PCa cells. Cell number was determined on days 0, 3, 6 and 10 post treatment with the indicated treatments in LNCaP resistant sublines, to either (a) hormone ablation (LNCaP-abl), (b) abiraterone acetate (LNCaP-abi), or (c) apalutamide (LNCaP-ARN509), as well as (d) enzalutamide resistant C4-2B subclone (C4-2B-ENZA). (e) Cell-doubling time was calculated for each treatment by fitting exponential growth curves using GraphPad Prism 7. Shown are means ±SEM of at least three independent experiments.

LNCaP-abi cells exhibited, as expected, no effect on cell growth upon treatment with 10 µM abiraterone, while enzalutamide and ARN509 slightly decreased the cell growth of these cells, as evidenced by increased DTs (from 3.173 days to 4.638 days and 3.884 days for ARN and ENZA, respectively). Strikingly, pre-treatment with any of the second generation antiandrogens, also including abiraterone, enhanced the cytotoxic effects of 2 Gy, as illustrated by compromised cell proliferation (Figure 6b) and a dramatic increase of DTs after combined treatments (2.9-fold, 5-fold and 7.2-fold after combination with abiraterone-acetate, apalutamide or enzalutamide, respectively)

(Figure 6e). LNCaP-ARN509 was resistant to both novel ARI ARN509 and enzalutamide, but could be radiosensitized upon treatment with the same drugs as well as abiraterone (Figure 6c,e).

While both ARN509 and enzalutamide showed no inhibitory effect on the proliferation of C4-2B-ENZA cells, abiraterone acetate treatment conferred a growth suppression similar to that caused by 2 Gy. Interestingly, these cells demonstrated an ultimate growth suppression when 10 μ M abiraterone acetate was combined with 2 Gy, with about 2-fold increase in DT (Figure 6d,e). Notably, bicalutamide showed contradictory effects on the radiosensitivity of the hormone resistant sub-clones. Bicalutamide treatment showed radioprotective activities on LNCaP-abi and LNCaP-ARN cells, by increasing the proliferation rate of these cells, as evidenced by decreasing the DTs of LNCaP-abi and LNCaP-ARN cells from 3.1 to 1.9 days and from 3.6 to 2.1 days, respectively (Figure S3a,b). This radio-protective effect can be explained by a previously described agonistic effect of bicalutamide on AR signaling [19], which might lead to the stimulation of the repair capacity. On the other hand, bicalutamide alone showed a stronger growth inhibitory effect on C4-2B-ENZA cells compared to IR alone. Combining bicalutamide and IR resulted in a slight increase in DT of C4-2B-ENZA cells from 2.3 to 2.6 days (Figure S3c). Collectively, these data further confirm that second generation antiandrogens can be used to efficiently potentiate the cytotoxic effects of IR, even in CRPC.

2.5. Second-Generation Antiandrogens Radiosensitize PCa Cells through the Inhibition of DSB Repair

DNA DSBs are considered the most lethal type of DNA damage induced by IR, and the DSB repair capacity of cells can determine their radiosensitivity, as well as the radiosensitizing effect of a specific treatment. To address whether the inhibition of DSB repair is the mechanism underlying the antiandrogen-mediated radiosensitization, DSBs were monitored using γ H2AX and 53BP1 in androgen-sensitive LNCaP and castration-resistant C4-2B cells after treatment with the individual anti-androgens and 2 Gy, either alone or combined (Figure 7).

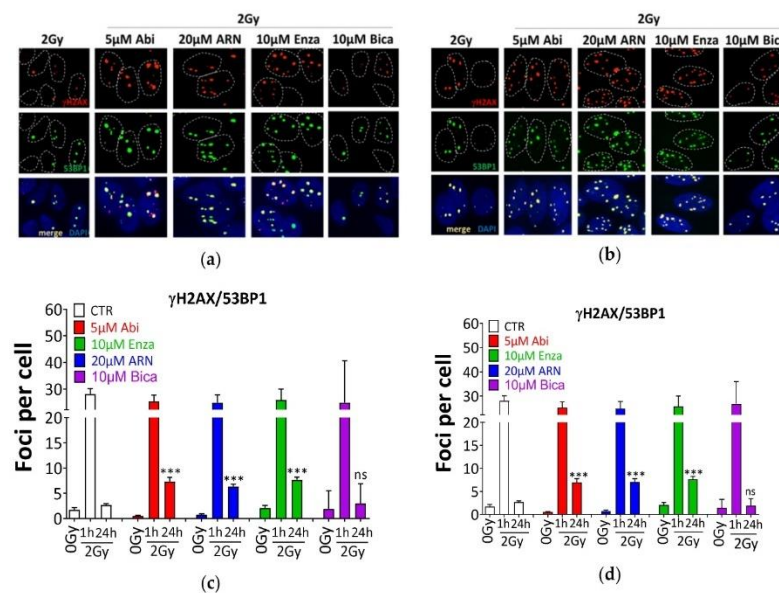


Figure 7. Second generation ADT inhibits the repair of ionizing radiation induced double strand breaks. Representative immunofluorescence micrographs for γ H2AX (red) and 53BP1 (green) foci at 24 h after 2Gy \pm the indicated antiandrogens in (a) LNCaP and (b) C4-2B cells. (c) and (d) Quantitation of colocalized γ H2AX/53BP1 foci of the experiments performed in A and C, respectively. At least 100 cells were analyzed. Shown are the means \pm SEM from at least three independent experiments. *p*-values were calculated using the Mann–Whitney U test. Significance is indicated as *** for *p* < 0.0001. ns: not significant.

Antiandrogens alone did not increase the number of γ H2AX or 53BP1 foci compared to untreated controls. The exposure to 2 Gy increased the number of γ H2AX and 53BP1 at 1 h (28.1 ± 2.1 foci/cell), and no further induction was observed 1 h post 2 Gy in addition to AHT. Remarkably, pretreatment of LNCaP cells with 5 μ M Abi, 10 μ M enzalutamide or 20 μ M ARN509 resulted in a significant increase in the number of individual (Figure S4a) and colocalized γ H2AX and 53BP1 foci (Figure 7a,c) at 24 h post 2 Gy ($p < 0.0001$), indicating a severe inhibition of DSB repair. Hence, LNCaP cells exposed to the novel antiandrogens were compromised in their ability to repair the IR-induced DSBs. These data were confirmed in C4-2B cells (Figure S4b and Figure 7b,d), showing again that antiandrogens exhibited no difference in the induction of DSBs, i.e. at 1 h post 2 Gy ($p = 0.2$), but significantly enhanced the number of residual γ H2AX/53BP1 foci at 24 h post 2 Gy ($p < 0.0001$). In agreement with the absence of bicalutamide induced radiosensitization, pretreating either LNCaP or C4-2B cells with 10 μ M bicalutamide did not increase the number of colocalized γ H2AX and 53BP1 foci (Figure 7) at 24 h post 2 Gy ($p = 0.74$ and $p = 0.80$, for LNCaP and C4-2B cells, respectively). Next, we sought to identify the repair pathway which is inhibited upon abiraterone treatment. In order to address this issue, LNCaP and C4-2B cells were treated with 5 μ M abiraterone acetate for 24 h, and then with either 5 μ M of either NU55933 (ATM inhibitor, ATMi) or NU7026 (DNAPK inhibitor, DNAPKi) for 2 h, before being irradiated with 2Gy, and subsequently, γ H2AX and 53BP1 foci were monitored at 1 h and 24 h post-IR. As illustrated in Figure S5a, combining ATMi and abiraterone did not further increase the number of residual γ H2AX/53BP1 compared to either ATMi or abiraterone. On the other hand, DNAPK inhibition increased the number of residual γ H2AX/53BP1 significantly more than abiraterone treatment alone. Furthermore, combining DNAPKi and abiraterone show a tendency of a synergistic increase in the number of residual unrepaired DSBs (Figure S5b). Together, these data indicate that abiraterone probably inhibits HR, but not NHEJ.

It is established that AR activity regulates the cell cycle and its inhibition causes a permanent G1 arrest [21]. Therefore, it was critical to assess whether the observed radiosensitization is cell cycle-dependent. To that end, the cell cycle profile was assessed in LNCaP (upper panel) and C4-2B (lower panel) after different time intervals post-combined treatment, and was compared to the effect of either IR or antiandrogens alone. As illustrated in Figure S6, irradiation arrested LNCaP cells in the S/G2 phase, which was resolved at later time points. Combining either of the novel antiandrogens with IR did not change the cell cycle profile compared to IR alone. Similar results were also reported in C4-2B cells. Furthermore, the analysis of apoptosis revealed no difference in apoptosis rates amongst the different treatment conditions (Figure S7). Together, this reveals that, regardless of castration state, the novel antiandrogens radiosensitize PCa cells through inhibition of DSB repair and independently of cell cycle redistribution or the induction of apoptosis.

2.6. Abiraterone but not Bicalutamide Reduces Repair Capacity of IR-Induced DSBs in Fresh Prostate Cancer Tissues

In order to further confirm the novel antiandrogen-mediated inhibition of DSB repair and hence the radiosensitization effect, we employed the previously described functional ex vivo assay, which enables monitoring DSB repair in fresh tumor tissues [22]. We obtained 26 fresh punch biopsies from 17 high-risk PCa patients undergoing radical prostatectomy at the Martini-Klinik Hamburg, Germany. Specimens were routinely examined by a pathologist, and only tissue samples with confirmed malignancy were included in this study. Cell viability and oxygenation were confirmed by monitoring EdU⁺ cells and pimonidazole staining as described [22]. Two patient samples were excluded from the analysis because they did not follow the previously described basic selection criteria [22]. The remaining punch biopsies were treated with 10 μ M abiraterone for 24 h before irradiation with 2 Gy. γ H2AX and 53BP1 foci were analyzed 1 h and 24 h later (Figure 8a).

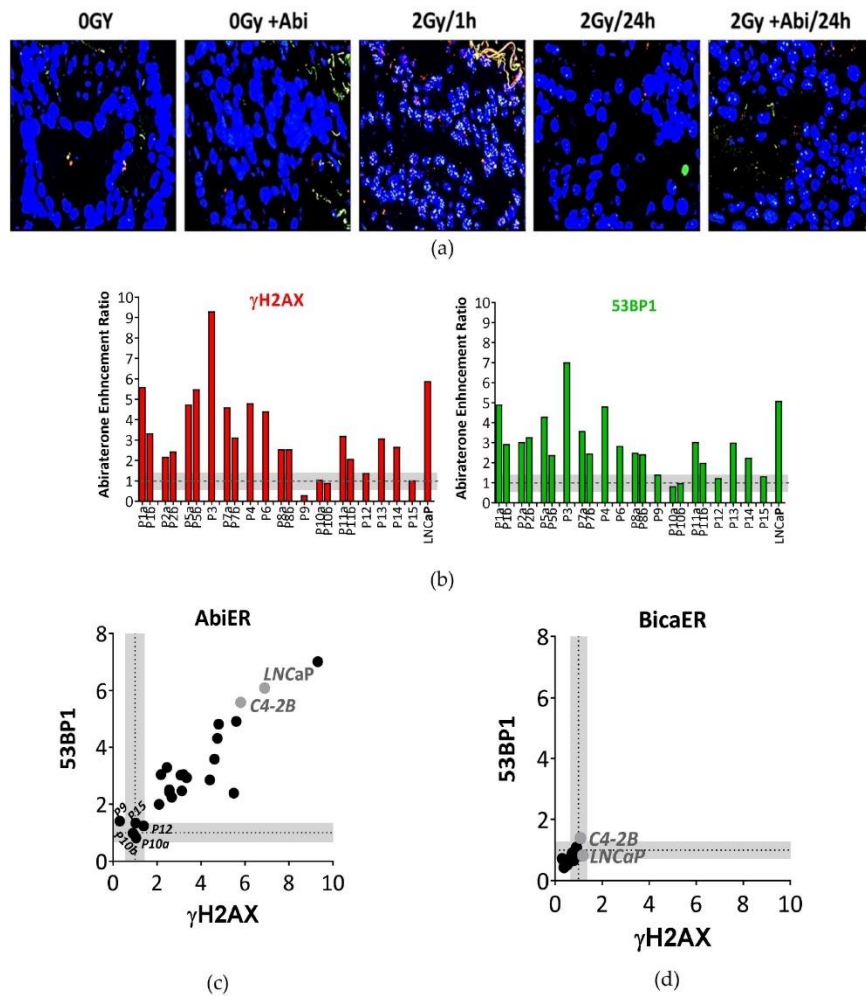


Figure 8. Abiraterone efficiently suppresses DSB repair in fresh PCa tissues after ex vivo irradiation. (a) Representative immunofluorescence micrographs for γ H2AX (red) and 53BP1 (green) foci after the indicated treatments in freshly collected tumor tissue from PCa patient P5. (b) Abiraterone-mediated enhancement ratio (AbiER) on γ H2AX (left panel) and 53BP1 (right panel) foci of 22 punch biopsies from 15 PCa patients. (c,d) Correlation between (C) AbiER or (D) BicaER on γ H2AX and 53BP1 foci. Threshold in grey was calculated as the mean standard error for each DSB marker in all samples.

As illustrated in Figure S9, the slices demonstrated no difference in the number of γ H2AX and 53BP1 upon treatment with abiraterone alone; however, this number increased upon irradiation with 2 Gy. Most tumor slices displayed significantly elevated numbers of residual γ H2AX and 53BP1 foci after 24 h of combined treatment with Abi and 2 Gy, compared to the single treatment. Analysis of the abiraterone acetate-induced radiosensitization enhancement ratio (AbiER) revealed that tumor samples from 13 out of 15 PCa patients (67%) showed at least a 2-fold increase in their AbiER index, with minor alterations between both γ H2AX (Figure 8a) and 53BP1 (Figure 8b) markers. Notably, two punch biopsies obtained from the same patient exhibited consistent results. Bicalutamide failed again to enhance the radiosensitivity in freshly collected prostate tumor tissues from 8 PCa patients (BicaER) (Figure 8d and Figure S8). The mean standard error of all samples was set as a threshold for each DSB marker. Together, this further confirms the finding that the novel antiandrogens, such as abiraterone acetate, radiosensitize PCa cells by suppressing DSB repair capacity.

3. Discussion

The combination of ADT and RT has been studied extensively in the clinical setting of localized PCa. Moreover, there is a strong rationale from preclinical models, highlighting a radiosensitizing effect of AR signaling inhibition. Clinically, the beneficial effect for an ADT plus RT combination depends on several factors, including the histopathological features of the tumor, tumor stage, PSA-level, and duration of ADT, among others. For low risk PCa patients treated with ADT plus RT, the RTOG 94-08 trial failed to show any significant improvement in disease control. There was, however, a significant decline in the biochemical failure rate, favoring the combined treatment approach [23]. Although a similar effect was observed in several other studies, the impact on OS for PCa patients receiving RT with ADT as compared with those receiving RT alone is less evident [24,25], except for high risk patients [16]. EORTC 22863 also showed a survival benefit for locally advanced PCa following combined treatment [26]; however, other studies could not recapitulate this benefit for locally advanced PCa patients [27,28]. RTOG 92-02 revealed no significant improvement in 10-year survival for PCa patients, except for those with a Gleason score of 8 or higher [28]. However, the Quebec L200 trial failed to recapitulate the results of these studies concerning biochemical failure rates [29]. Consequently, trial results are heterogeneous, which is at least, in part, ascribable to heterogeneous patient populations, end points and modalities of treatment applied, but a beneficial effect of ADT on RT activity seems highly likely. Therefore, concurrent ADT plus locally ablative RT has been adopted in clinical guidelines and routine care pathways, at least for intermediate and high risk localized PCa patients.

In the present study, a retrospective analysis of patients undergoing definitive radiotherapy for localized PCa at our institution confirmed a modest but insignificant improvement in biochemical failure-free survival of PCa receiving combined ADT and RT over RT alone. Assuming a correlation of impaired androgen signaling with enhanced radiosensitivity, and in view of the controversial clinical results, we opined that more effective AR signaling inhibition by second-generation antiandrogens would enhance the cytotoxicity of RT in pre-clinical models.

In the current study, we used the second generation antiandrogens abiraterone acetate, apalutamide and enzalutamide, all of which are FDA approved for clinical use in metastatic hormone-sensitive and castration-resistant prostate cancer (apalutamide in the latter setting only). The concentrations used for pre-clinical in vitro assessment are also in the range of clinically achievable steady state plasma concentrations (C_{max}) [30]. Indeed, the concentrations of the drugs intra-tumoral are basically much lower than the C_{max}. However, this study provides the evidence base for the clinical use of the aforementioned drugs as radiosensitizers in prostate cancer.

Taken together, our results revealed a stronger growth inhibition induced by combining one of the second generation antiandrogens: abiraterone acetate, enzalutamide or apalutamide, along with 2 Gy compared to antiandrogen or IR, alone or IR in combination with bicalutamide as a first-generation AR blocker. In fact, bicalutamide did not enhance RT-induced growth delay in our cell line models. In contrast, second generation antiandrogens profoundly intensified the effect of IR, as illustrated by a consistent increase in the DTs of irradiated PCa cells that had been treated with second-generation antiandrogens. We provide here proof-of-principle pre-clinical in vitro and ex vivo evidence to rationalize the clinical use of the second-generation antiandrogens to enhance the effect of IR as a potential strategy to improve the outcomes of PCa patients with localized disease who undergo ablative RT.

The inhibition of DNA DSB repair capacity was found to underlie the mediated radiosensitization effect of second-generation antiandrogens. This was evidenced by a significant increase in the number of both γ H2AX and 53BP1 foci remaining after 24 h post 2 Gy upon pretreating PCa cells, with either of the second-generation antiandrogens. Importantly, repair inhibition was further demonstrated in 22 freshly collected tumor tissue samples from 15 PCa patients treated with abiraterone acetate, before being ex vivo irradiated with 2 Gy. Previous studies reported a tight connection between DNA damage repair and AR signaling through hormone-mediated regulation of several DNA repair genes [31–34].

Another key conclusion in the current study is that the ADT-mediated radiosensitization was found to be independent of the hormone sensitivity state of the PCa cells. This was derived from the findings that (i) the castration-resistant C4-2B cells showed a similar radiosensitization effect upon treatment with any of the second-generation antiandrogens, compared to the hormone-sensitive prostate cancer (HSPC) LNCaP cells; (ii) the DT was increased similarly in both C4-2B and LNCaP cells, and furthermore, (iii) different specific ADT-resistant clones established from the HSPC cell line LNCaP were sensitized to IR by at least one of the second generation antiandrogens, interestingly including the ADT to which they are resistant. Notably, Goodwin et al. [35], reported—in contrast to our data—a smaller effect on IR sensitivity for the second-generation of antiandrogen, enzalutamide in the CRPC C4-2 cells. This discrepancy may be explained by the fact that they used a lower enzalutamide concentration to radiosensitize C4-2 cells. Another possible explanation could be that, given its dual role in inhibiting AR signaling [8,9], abiraterone might be a more potent radiosensitizing agent compared to enzalutamide and apalutamide. In keeping with this possibility, we showed here that abiraterone radiosensitized the hormone resistant cells more efficiently than enzalutamide and apalutamide.

IR is a local therapy with side effects restricted to tissues lacking AR and several second-generation ADT agents, such as abiraterone, apalutamide, enzalutamide and darolutamide; these are approved by the FDA for localized CRPC (M0 CRPC) [36], and this would rationalize the use of such drugs in combination with RT to control the localized HSPC, and probably prevent the progression to CRPC, with minimal side effects.

The STAMPEDE trial includes groups of PCa patients receiving a combination of either the first-generation ADT with RT, docetaxel and abiraterone acetate, or the first-generation ADT with enzalutamide and abiraterone acetate (NCT00268476). Although the data published so far demonstrated a benefit for the first combination arm, namely; abiraterone acetate + standard care treatment including RT over Abiraterone acetate + the standard care without RT, this data recommended the use of RT, but does not provide any clue for the radiosensitization effect of abiraterone. However, it provides the rationale for the use of abiraterone acetate in combination with RT as a treatment option. Additionally, the COUAA-31 trial (NCT00638690) reported that abiraterone acetate plus radiation was safely co-administered to patients with a perceived advantage in the palliative bone metastasis response. Abiraterone acetate with RT has been further tested in two separate phase 3 clinical trials, including ERA-223 (NCT02043678), and in the ongoing PEACE 1 trial as well [37]. Indeed, further randomized clinical trials are required to assess the effect of combining the second generation antiandrogens and RT for PCa patients.

The current study provides the rationale for this treatment regime for PCa patients, through combining second generation antiandrogens and RT for low risk/locally advanced PCa patients, which might prevent progression to CRPC.

4. Materials and Methods

4.1. Patients and Retrospective Study Design

A total of 166 patients (median age: 73 years, range 53–80) with localized prostate cancer underwent high dose-rate brachytherapy (HDR-BT), combined with subsequent external beam radiotherapy between 2008 and March 2016, at the Department of Radiotherapy and Radiooncology of the University Medical Center Hamburg-Eppendorf. Only patients who signed written informed consent and those with complete data sets were included in this analysis. HDR-BT was delivered with 9 Gy/fraction on days 1 and 8 with an iridium-192 source, while EBRT was administered with 1.8 Gy/fraction to a target dose of 50.4 Gy. Among these patients, 46 (27.7%) received neoadjuvant and/or concomitant ADT. Side effects were classified according to the toxicity criteria of the Radiation Therapy Oncology Group (RTOG) and the European Organization for Research and Treatment of Cancer (EORTC), as previously described [38].

4.2. Cell Culture, Drugs, and X-Irradiation

LNCaP and C4-2B prostate cancer cells (ATCC, Manassas, VA, USA) were grown in DMEM (Gibco, Invitrogen, Karlsruhe, Germany), supplemented with 10% fetal calf serum, 100 U/mL penicillin and 100 mg/mL streptomycin at 37 °C, with 10% CO₂. LNCaP-ARN509, LNCaP-abi, C4-2B-Enza cells (kindly provided by Prof. CP Evans, UC Davis School of Medicine, Sacramento, CA, USA) were maintained in media containing the corresponding drug to which they are resistant as previously described [17,18]. Abiraterone acetate and apalutamide were kindly provided by Janssen Cilag GmbH, Neuss, Germany. Bicalutamide and enzalutamide were purchased from Selleckchem, Germany. LNCaP-abl cells (a gift from Prof. Culig, Medical University Innsbruck, Austria) were grown in DMEM, supplemented with 10% Charcoal Stripped FBS (Sigma-Aldrich, Deisenhofen, Germany). All LNCaP-abl cells experiments were performed in poly-L-lysine coated 6-well culture plates. All cell lines tested negative for mycoplasma contamination. Irradiation was performed as previously described (200 kV, 15 mA, additional 0.5mm Cu filter at a dose rate of 0.8 Gy/min) [19]. To inhibit the kinase activity of ATM and DNAPK, 5 μM KU55933 (Selleckchem, Germany) and 5 μM NU7026 (Selleckchem, Germany) were used, respectively.

4.3. Proliferation Assay

Cells were plated in triplicate in 6-well plates, cultured in the appropriate growth media and allowed to attach overnight before treatment with the indicated drugs. For hormone ablation experiments with LNCaP-abl subclone, cells were seeded in FBS full medium for 18–24 h before changing to steroid-deprived medium (CS-FCS) for the indicated time points, with or without irradiation. To assess the effect of any treatment regimes, the cell number was determined via Beckman Coulter cell counter (Life Science, Krefeld, Germany) at 3, 6, and 10 days post-treatment. In all experiments, media with or without drugs were changed twice in the 10-day treatment course.

4.4. Colony Formation Assay

Cellular survival was determined via colony formation assay, as previously described [39,40]. Briefly, cells were plated at 200 cells per well in a 6-well plate, in the presence of 5 μM abiraterone acetate or 10 μM bicalutamide. After 24 h, cells were X-irradiated (RS225 research system, GLUMAY MEDICAL, UK at 200 kV, 15 mA) and maintained for 2–3 weeks. Colonies were thereafter fixed in 70% ethanol and stained in 0.1% crystal violet. Cellular survival was defined as the ability to form colonies containing at least 50 cells. For agarose CFA, cells were mixed in 0.3% agarose in DMEM with 10% FCS and plated at 10000 cells/well, onto 6-well plates containing a solidified bottom layer (0.6% agarose the same growth medium). After 14 days, colonies were stained with 0.5 mg/mL MTT (Sigma-Aldrich), and photo-graphed using REBEL Microscopy (ECHO, San-Diego, CA, USA). Colonies were then counted using Image-J. Surviving fractions (SF) were calculated by normalization to the plating efficiency of the un-irradiated control. DMSO was used as a control at the same concentration.

4.5. Immunofluorescence

Treated cells on coverslips were washed once with cold PBS and fixed with 4% para-formaldehyde/PBS for 10 min. Fixed cells were permeabilized with 0.2% Triton X-100/PBS on ice for 5 min and incubated for 1 h at room temperature with primary antibodies: Mouse monoclonal anti-phospho-S139-H2AX antibody (Millipore, Berlin, Germany), at a dilution of 1:500 and rabbit polyclonal anti-53BP1 antibody (Novus), at a dilution of 1:500. After being washed three times with cold PBS, the cells were incubated for 1h with secondary anti-mouse Alexa-fluor594 (Invitrogen), at a dilution of 1:500 or anti-rabbit Alexa-fluor488 (Invitrogen) at a dilution of 1:600. The nuclei were counterstained with 4'-6-diamidino-2-phenylindole (DAPI, 10 ng/mL). Slides were mounted in Vectashield mounting medium (Vector Laboratories).

Immunofluorescence of cultured tumor tissue was performed as previously described [22]. Fluorescence microscopy was performed using the Zeiss AxioObserver.Z1 microscope (objectives: x20, resolution 0.44 μm ; Plan Apo 63/1.4 Oil DICII, resolution 0.24 μm ; and filters: Zeiss 43, Zeiss 38, Zeiss 49). Z-stacks of semi-confocal images were obtained using the Zeiss Apotome, Zeiss AxioCam MRm and Zeiss AxioVision Software. For DSB analysis, fields of view were taken per time point or treatment with a minimum of 100 cells (xenograft) or 50 cells (primary tumor). All stainings were performed in duplicates. DSBs were analyzed using ImageJ and DAPI-based image masks, and normalized to single nucleus values [22].

4.6. Cell Cycle Analysis

For cell cycle analysis, treated cells were harvested and fixed with 80% cold ethanol ($-20\text{ }^{\circ}\text{C}$). After washing, the DNA was stained with propidium iodide solution containing RNase A. Cell cycle distribution was monitored by flow cytometry (FACS CANTO 2, BD Bioscience Systems, Heidelberg, Germany) and analyzed using Mod-Fit software (Verity Software House).

4.7. Apoptosis Quantification

Apoptosis was investigated by detection of caspase activity utilizing the FAMFLICA™ Poly Caspases Assay Kit (Immunochemistry Technologies, Bloomington, MN, USA), according to the manufacturer's instructions. Flow cytometric analysis was performed on a FACS Canto with FACS Diva Software (Becton Dickinson, Toronto, ON, Canada). Staurosporine (Sigma S6942) was used as a positive control with a final concentration of 1 μM for at least 12 h incubation.

4.8. Patient Sample Collection

Fresh PCa tissue was obtained from patients with high-risk PCa according to D'Amico risk stratification undergoing radical prostatectomy at Martini-Klinik, Prostate Cancer Center Hamburg, Germany. After resection, 1–2 punch biopsies were taken by the surgeon in palpable tumor areas. The biopsies were collected in culture media and immediately taken to the laboratory. Anonymized biopsies were processed within 30 minutes after resection. The laboratory received a final pathology report containing the Gleason score, PSA status and age of each anonymized patient for clinical analysis.

4.9. Tissue Slice Cultures

Tissue slice cultures were prepared as described [22]. Briefly, 300 μm slices were cut using the MacIrvine tissue chopper and placed on Millicell@cell culture inserts (0.4 μm , 30 mm diameter, Merck, Soden, Germany), which were inserted in 6 well dishes containing 1 mL Dulbecco's modified Eagle medium (DMEM; Gibco-Invitrogen), supplemented with 10% fetal calf serum (FCS) and incubated at 37 $^{\circ}\text{C}$. Prior to ex vivo treatment, the tissues slices were incubated for one day for recovery and re-oxygenation. To monitor proliferation, un-irradiated slice cultures were incubated with 5-ethynyl-20-deoxyuridine (EdU, 1:1000; Click-iT Assay Kit, Invitrogen) overnight for 16 h. All slices were additionally treated with pimonidazole (200 μM , Hypoxyprobe), 2 h before fixation, to monitor hypoxia. To analyse the effect of abiraterone or bicalutamide on IR, slices were treated with 5 μM abiraterone or 10 μM bicalutamide for 24 h before irradiation, using a Gulmay X-ray source (200 kV, 15 mA, additional 0.5 mm Cu filter, dose rate of 0.8 Gy/min).

4.10. Graphs and Statistics

Unless stated otherwise, experiments were independently repeated at least three times. Data points represent the mean \pm SEM of all individual experiments. Survival curves were deduced by means of the Kaplan–Meier method and comparisons were made by log-rank test. To estimate a hazard ratio (HR) of an occurring event, Cox proportional hazards regression model was applied (at a 95% confidence interval (CI)). A *p*-value of <0.05 was regarded statistically significant. Statistical analyses,

data fitting and graphics were performed with the GraphPad Prism 7.0 pro-program (GraphPad Software), SPSS Statistics 25 software (IBM Inc. SPSS Statistics, Armonk, NY, USA) and MedCalc 18.11 (MedCalc Software, Ostend, Belgium).

4.11. Ethical Approval

This study was in accordance with the World Medical Association Declaration of Helsinki, and the guidelines for experimentation with humans by the Chambers of Physicians of the State of Ham-burg (“Hamburger Ärztekammer”). All patients gave informed consent for their excised prostate specimens to be used for research purposes. All experiments were approved (Approval No. PV 7007) by the Ethics Committee of the Chambers of Physicians of the State of Hamburg (“Ham-burger Ärztekammer”).

5. Conclusions

We present a mechanistic rationale for the use of second-generation antiandrogens to radio-sensitize prostate tumors via the inhibition of DSB repair, interestingly regardless of castration state. The potential for the novel antiandrogens as standalone therapeutic agents seems to have plateaued for use in advanced PCa. It is far more likely that the next wave of therapeutic investigation will be focused on the combination of antiandrogen therapy, with other treatments such as radiotherapy and chemotherapy. The current study provides the proof-of-principle for the currently ongoing clinical trials, and paves the way to initiate additional ones.

Supplementary Materials: The following are available online at <http://www.mdpi.com/2072-6694/12/9/2467/s1>, Figure S1: Multiple comparisons between the combination of the indicated antiandrogens and IR. Figure S2: Second generation ADT therapy enhances the IR effect at least 2 fold. Figure S3: Quantitation of individual γ H2AX and 53BP1 foci. Figure S4: Second generation AHT does not affect cell cycle distribution after IR. Figure S5: Second generation AHT does not increase apoptosis after IR. Figure S6: Abiraterone acetate efficiently suppresses DSB-repair in fresh PCa tissues after ex-vivo irradiation. Figure S7: Second generation AHT does not increase apoptosis after IR. Figure S8: Bicalutamide does not inhibit DSB repair after IR. Figure S9: Abiraterone acetate efficiently suppresses DSB-repair in fresh PCa tissues after ex-vivo irradiation.

Author Contributions: Conceptualization, M.E.E. and W.M.; methodology, M.E.E., S.K., S.M. (Stefanie Meien), A.Z.; software, A.L., C.O., W.Y.M.; validation, M.E.E., S.M. (Sally Mutiara) and S.J.O.-H.; formal analysis, A.L. and C.O.; investigation, S.J.O.-H. and W.Y.M.; resources, K.R., R.S., H.H., D.T., C.P. and C.B.; data curation, K.R. and C.B.; writing—original draft preparation, M.E.E.; writing—review and editing, W.Y.M., S.J.O.-H., C.O., K.R., S.K., S.B.-R.; visualization, W.Y.M.; supervision, W.Y.M., K.R., C.P., and C.B.; project administration, W.Y.M.; funding acquisition, W.Y.M. and K.R. All authors have read and agreed to the published version of the manuscript.

Funding: This research was funded by BMBF (grants numbers 02NUK032 and 02NUK035B), Mildred Scheel Cancer Career Center HaTriCS4, Funding for pre-clinical Investigator Initiated Study (IIS) (Study ID: ARN-I-15-DEU-004) and the German Academic Exchange Service (DAAD).

Conflicts of Interest: The authors declare no conflict of interest.

References

1. Bray, F.; Ferlay, J.; Soerjomataram, I.; Siegel, R.L.; Torre, L.A.; Jemal, A. Global cancer statistics 2018: GLOBOCAN estimates of incidence and mortality worldwide for 36 cancers in 185 countries. *CA Cancer J. Clin.* **2018**, *68*, 394–424. [[CrossRef](#)] [[PubMed](#)]
2. Denis, L.J.; Griffiths, K. Endocrine treatment in prostate cancer. *Semin. Surg. Oncol.* **2000**, *18*, 52–74. [[CrossRef](#)]
3. Dal Pra, A.; Cury, F.L.; Souhami, L. Combining radiation therapy and androgen deprivation for localized prostate cancer—a critical review. *Curr. Oncol.* **2010**, *17*, 28–38. [[CrossRef](#)] [[PubMed](#)]
4. Sharifi, N.; Gulley, J.L.; Dahut, W.L. Androgen deprivation therapy for prostate cancer. *Jama* **2005**, *294*, 238–244. [[CrossRef](#)] [[PubMed](#)]
5. Huggins, C.; Stevens, R.A. The Effect of Castration on Benign Hypertrophy of the Prostate in Man11 This investigation was supported by a grant from the Committee on Research in Problems of Sex of the National Research Council. *J. Urol.* **1940**, *43*, 705–714. [[CrossRef](#)]

6. Knudsen, K.E.; Kelly, W.K. Outsmarting androgen receptor: Creative approaches for targeting aberrant androgen signaling in advanced prostate cancer. *Expert Rev. Endocrinol. Metab.* **2011**, *6*, 483–493. [[CrossRef](#)]
7. Petrylak, D.P. Current clinical trials in castrate-resistant prostate cancer. *Curr. Urol. Rep.* **2011**, *12*, 173–179. [[CrossRef](#)]
8. Soifer, H.S.; Souleimani, N.; Wu, S.; Voskresenskiy, A.M.; Collak, F.K.; Cinar, B.; Stein, C.A. Direct regulation of androgen receptor activity by potent CYP17 inhibitors in prostate cancer cells. *J. Biol. Chem.* **2012**, *287*, 3777–3787. [[CrossRef](#)]
9. Richards, J.; Lim, A.C.; Hay, C.W.; Taylor, A.E.; Wingate, A.; Nowakowska, K.; Pezaro, C.; Carreira, S.; Goodall, J.; Arlt, W.; et al. Interactions of abiraterone, eplerenone, and prednisolone with wild-type and mutant androgen receptor: A rationale for increasing abiraterone exposure or combining with MDV3100. *Cancer Res.* **2012**, *72*, 2176–2182. [[CrossRef](#)]
10. Helleday, T.; Lo, J.; van Gent, D.C.; Engelward, B.P. DNA double-strand break repair: From mechanistic understanding to cancer treatment. *DNA Repair* **2007**, *6*, 923–935. [[CrossRef](#)]
11. Michalski, J.M.; Pisansky, T.M.; Lawton, C.A.F.; Potters, L. Chapter 53—Prostate Cancer. In *Clinical Radiation Oncology*, 4th ed.; Gunderson, L.L., Tepper, J.E., Eds.; Elsevier: Philadelphia, PA, USA, 2016; pp. 1038–1095.e1018. [[CrossRef](#)]
12. Tarish, F.L.; Schultz, N.; Tanoglidis, A.; Hamberg, H.; Letocha, H.; Karaszi, K.; Hamdy, F.C.; Granfors, T.; Helleday, T. Castration radiosensitizes prostate cancer tissue by impairing DNA double-strand break repair. *Sci. Transl. Med.* **2015**, *7*, 312re311. [[CrossRef](#)] [[PubMed](#)]
13. Zagars, G.K.; Pollack, A.; von Eschenbach, A.C. Prognostic factors for clinically localized prostate carcinoma: Analysis of 938 patients irradiated in the prostate specific antigen era. *Cancer* **1997**, *79*, 1370–1380. [[CrossRef](#)]
14. D’Amico, A.V.; Matelski, H.; O’Leary, M.; Sussman, B. Prostate-specific antigen-producing cells in the bone marrow of a patient with early-stage prostate cancer. *Urology* **1997**, *49*, 279–282. [[CrossRef](#)]
15. Zietman, A.L. Overview. In *Clinical Radiation Oncology*, 4th ed.; Gunderson, L.L., Tepper, J.E., Eds.; Elsevier: Philadelphia, PA, USA, 2016; pp. 1035–1037. [[CrossRef](#)]
16. Joseph, D.J.; Lamb, D.S.; Denham, J.W.; Oldmeadow, C.; Attia, J.; Steigler, A. Ten year final results of the TROG 03.04 (RADAR) randomised phase 3 trial evaluating duration of androgen suppression ± zoledronate for locally advanced prostate cancer. *J. Clin. Oncol.* **2018**, *36*, 1. [[CrossRef](#)]
17. Nabid, A.; Garant, M.-P.; Martin, A.-G.; Bahary, J.-P.; Lemaire, C.; Vass, S.; Bahoric, B.; Archambault, R.; Vincent, F.; Bettahar, R.; et al. Duration of androgen deprivation therapy in high risk prostate cancer: Final results of a randomized phase III trial. *J. Clin. Oncol.* **2017**, *35*, 5008. [[CrossRef](#)]
18. Zietman, A.L.; Prince, E.A.; Nakfoor, B.M.; Park, J.J. Androgen deprivation and radiation therapy: Sequencing studies using the Shionogi in vivo tumor system. *Int. J. Radiat. Oncol. Biol. Phys.* **1997**, *38*, 1067–1070. [[CrossRef](#)]
19. Culig, Z.; Hoffmann, J.; Erdel, M.; Eder, I.E.; Hobisch, A.; Hittmair, A.; Bartsch, G.; Utermann, G.; Schneider, M.R.; Parczyk, K.; et al. Switch from antagonist to agonist of the androgen receptor bicalutamide is associated with prostate tumour progression in a new model system. *Br. J. Cancer* **1999**, *81*, 242–251. [[CrossRef](#)]
20. Nguyen, H.G.; Yang, J.C.; Kung, H.J.; Shi, X.B.; Tilki, D.; Lara, P.N., Jr.; DeVere White, R.W.; Gao, A.C.; Evans, C.P. Targeting autophagy overcomes Enzalutamide resistance in castration-resistant prostate cancer cells and improves therapeutic response in a xenograft model. *Oncogene* **2014**, *33*, 4521–4530. [[CrossRef](#)]
21. Knudsen, K.E.; Arden, K.C.; Cavenee, W.K. Multiple G1 regulatory elements control the androgen-dependent proliferation of prostatic carcinoma cells. *J. Biol. Chem.* **1998**, *273*, 20213–20222. [[CrossRef](#)]
22. Kocher, S.; Beyer, B.; Lange, T.; Nordquist, L.; Volquardsen, J.; Burdak-Rothkamm, S.; Schlomm, T.; Petersen, C.; Rothkamm, K.; Mansour, W.Y. A functional ex vivo assay to detect PARP1-EJ repair and radiosensitization by PARP-inhibitor in prostate cancer. *Int. J. Cancer* **2019**, *144*, 1685–1696. [[CrossRef](#)]
23. McGowan, D.G.; Hunt, D.; Jones, C.U.; Amin, M.; Leibenhaut, M.H.; Husian, S.M.; Rotman, M.; Souhami, L.; Sandler, H.; Shipley, W.U. Short-term Endocrine Therapy Prior to and during Radiation Therapy Improves Overall Survival in Patients with T1b-T2b Adenocarcinoma of the Prostate and PSA ≤ 20: Initial Results of RTOG 94-08. *Int. J. Radiat. Oncol. Biol. Phys.* **2010**, *77*, 1. [[CrossRef](#)]
24. D’Amico, A.V.; Chen, M.H.; Renshaw, A.A.; Loffredo, M.; Kantoff, P.W. Androgen suppression and radiation vs. radiation alone for prostate cancer: A randomized trial. *Jama* **2008**, *299*, 289–295. [[CrossRef](#)] [[PubMed](#)]
25. D’Amico, A.V.; Chen, M.H.; de Castro, M.; Loffredo, M.; Lamb, D.S.; Steigler, A.; Kantoff, P.W.; Denham, J.W. Surrogate endpoints for prostate cancer-specific mortality after radiotherapy and androgen suppression

- therapy in men with localised or locally advanced prostate cancer: An analysis of two randomised trials. *Lancet Oncol.* **2012**, *13*, 189–195. [[CrossRef](#)]
26. Bolla, M.; Gonzalez, D.; Warde, P.; Dubois, J.B.; Mirimanoff, R.O.; Storme, G.; Bernier, J.; Kuten, A.; Sternberg, C.; Gil, T.; et al. Improved survival in patients with locally advanced prostate cancer treated with radiotherapy and goserelin. *N. Engl. J. Med.* **1997**, *337*, 295–300. [[CrossRef](#)]
 27. Hanks, G.E.; Pajak, T.F.; Porter, A.; Grignon, D.; Brereton, H.; Venkatesan, V.; Horwitz, E.M.; Lawton, C.; Rosenthal, S.A.; Sandler, H.M.; et al. Phase III trial of long-term adjuvant androgen deprivation after neoadjuvant hormonal cyoreduction and radiotherapy in locally advanced carcinoma of the prostate: The Radiation Therapy Oncology Group Protocol 92-02. *J. Clin. Oncol.* **2003**, *21*, 3972–3978. [[CrossRef](#)]
 28. Horwitz, E.M.; Bae, K.; Hanks, G.E.; Porter, A.; Grignon, D.J.; Brereton, H.D.; Venkatesan, V.; Lawton, C.A.; Rosenthal, S.A.; Sandler, H.M.; et al. Ten-year follow-up of radiation therapy oncology group protocol 92-02: A phase III trial of the duration of elective androgen deprivation in locally advanced prostate cancer. *J. Clin. Oncol.* **2008**, *26*, 2497–2504. [[CrossRef](#)]
 29. Laverdiere, J.; Nabid, A.; de Bedoya, L.D.; Ebacher, A.; Fortin, A.; Wang, C.S.; Harel, F. The efficacy and sequencing of a short course of androgen suppression on freedom from biochemical failure when administered with radiation therapy for T2-T3 prostate cancer. *J. Urol.* **2004**, *171*, 1137–1140. [[CrossRef](#)]
 30. Liston, D.R.; Davis, M. Clinically Relevant Concentrations of Anticancer Drugs: A Guide for Nonclinical Studies. *Clin. Cancer Res.* **2017**, *23*, 3489–3498. [[CrossRef](#)]
 31. Al-Ubaidi, F.L.; Schultz, N.; Loseva, O.; Egevad, L.; Granfors, T.; Helleday, T. Castration therapy results in decreased Ku70 levels in prostate cancer. *Clin. Cancer Res.* **2013**, *19*, 1547–1556. [[CrossRef](#)]
 32. Asagoshi, K.; Tano, K.; Chastain, P.D., 2nd; Adachi, N.; Sonoda, E.; Kikuchi, K.; Koyama, H.; Nagata, K.; Kaufman, D.G.; Takeda, S.; et al. FEN1 functions in long patch base excision repair under conditions of oxidative stress in vertebrate cells. *Mol. Cancer Res.* **2010**, *8*, 204–215. [[CrossRef](#)]
 33. Kumar, R.; Horikoshi, N.; Singh, M.; Gupta, A.; Misra, H.S.; Albuquerque, K.; Hunt, C.R.; Pandita, T.K. Chromatin modifications and the DNA damage response to ionizing radiation. *Front. Oncol.* **2013**, *2*, 214. [[CrossRef](#)] [[PubMed](#)]
 34. Urbanucci, A.; Sahu, B.; Seppala, J.; Larjo, A.; Latonen, L.M.; Waltering, K.K.; Tammela, T.L.; Vessella, R.L.; Lahdesmaki, H.; Janne, O.A.; et al. Overexpression of androgen receptor enhances the binding of the receptor to the chromatin in prostate cancer. *Oncogene* **2012**, *31*, 2153–2163. [[CrossRef](#)]
 35. Goodwin, J.F.; Schiewer, M.J.; Dean, J.L.; Schrecengost, R.S.; de Leeuw, R.; Han, S.; Ma, T.; Den, R.B.; Dicker, A.P.; Feng, F.Y.; et al. A hormone-DNA repair circuit governs the response to genotoxic insult. *Cancer Discov.* **2013**, *3*, 1254–1271. [[CrossRef](#)] [[PubMed](#)]
 36. Rice, M.A.; Malhotra, S.V.; Stoyanova, T. Second-Generation Antiandrogens: From Discovery to Standard of Care in Castration Resistant Prostate Cancer. *Front. Oncol.* **2019**, *9*, 801. [[CrossRef](#)]
 37. Smith, M.; Parker, C.; Saad, F.; Miller, K.; Tombal, B.; Ng, Q.S.; Boegemann, M.; Matveev, V.; Piulats, J.M.; Zucca, L.E.; et al. Addition of radium-223 to abiraterone acetate and prednisone or prednisolone in patients with castration-resistant prostate cancer and bone metastases (ERA 223): A randomised, double-blind, placebo-controlled, phase 3 trial. *Lancet Oncol.* **2019**, *20*, 408–419. [[CrossRef](#)]
 38. Cox, J.D.; Stetz, J.; Pajak, T.F. Toxicity criteria of the Radiation Therapy Oncology Group (RTOG) and the European Organization for Research and Treatment of Cancer (EORTC). *Int. J. Radiat. Oncol. Biol. Phys.* **1995**, *31*, 1341–1346. [[CrossRef](#)]
 39. Mansour, W.Y.; Bogdanova, N.V.; Kasten-Pisula, U.; Rieckmann, T.; Kocher, S.; Borgmann, K.; Baumann, M.; Krause, M.; Petersen, C.; Hu, H.; et al. Aberrant overexpression of miR-421 downregulates ATM and leads to a pronounced DSB repair defect and clinical hypersensitivity in SKX squamous cell carcinoma. *Radiother. Oncol. J. Eur. Soc. Ther. Radiol. Oncol.* **2013**, *106*, 147–154. [[CrossRef](#)]
 40. Oing, C.; Tennstedt, P.; Simon, R.; Volquardsen, J.; Borgmann, K.; Bokemeyer, C.; Petersen, C.; Dikomey, E.; Rothkamm, K.; Mansour, W.Y. BCL2-overexpressing prostate cancer cells rely on PARP1-dependent end-joining and are sensitive to combined PARP inhibitor and radiation therapy. *Cancer Lett.* **2018**, *423*, 60–70. [[CrossRef](#)]



© 2020 by the authors. Licensee MDPI, Basel, Switzerland. This article is an open access article distributed under the terms and conditions of the Creative Commons Attribution (CC BY) license (<http://creativecommons.org/licenses/by/4.0/>).

Supplementary Material: Second-Generation Antiandrogen Therapy Radiosensitizes Prostate Cancer Regardless of Castration State Through Inhibition of DNA Double Strand Break Repair

Mohamed E. Elsesy, Su Jung Oh-Hohenhorst, Anastassia Löser, Christoph Oing, Sally Mutiara, Sabrina Köcher, Stefanie Meien, Alexandra Zielinski, Susanne Burdak-Rothkamm, Derya Tilki, Hartwig Huland, Rudolf Schwarz, Cordula Petersen, Carsten Bokemeyer, Kai Rothkamm and Wael Y. Mansour

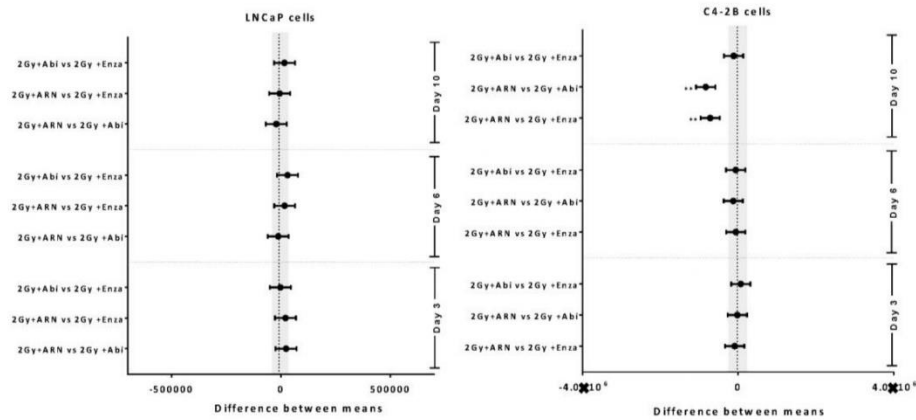


Figure S1. Multiple comparisons between the combination of the indicated antiandrogens and IR in (A) LNCaP and (B) C4-2B cells. Tukey’s multiple comparisons test was used to compare between the indicated treatments pairs in LNCaP or C4-2B cells. Significance was measured using two way ANOVA test. Significance is indicated as * for the $p < 0.05$, ** for $p < 0.001$ and *** for $p < 0.0001$. ns: not significant.

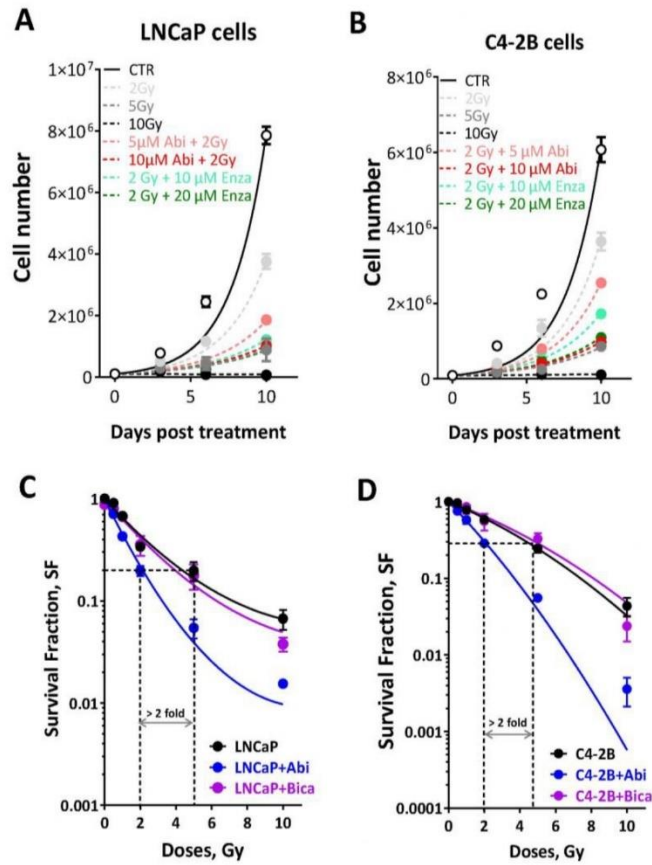


Figure S2. Second generation ADT therapy enhances the IR effect at least 2 fold. Cell numbers were determined in LNCaP (A) or C4-2B cells (B) on days 0, 3, 6 and 10 post treatment with the indicated second generation antiandrogens. (C,D) Survival fractions were measured using agarose CFA for LNCaP (C) and C4-2B (D) cells treated with 5 μ M abiraterone acetate or 10 μ M bicalutamide before irradiation with the indicated X-ray doses. Shown are means \pm SEM of at least three independent experiments.

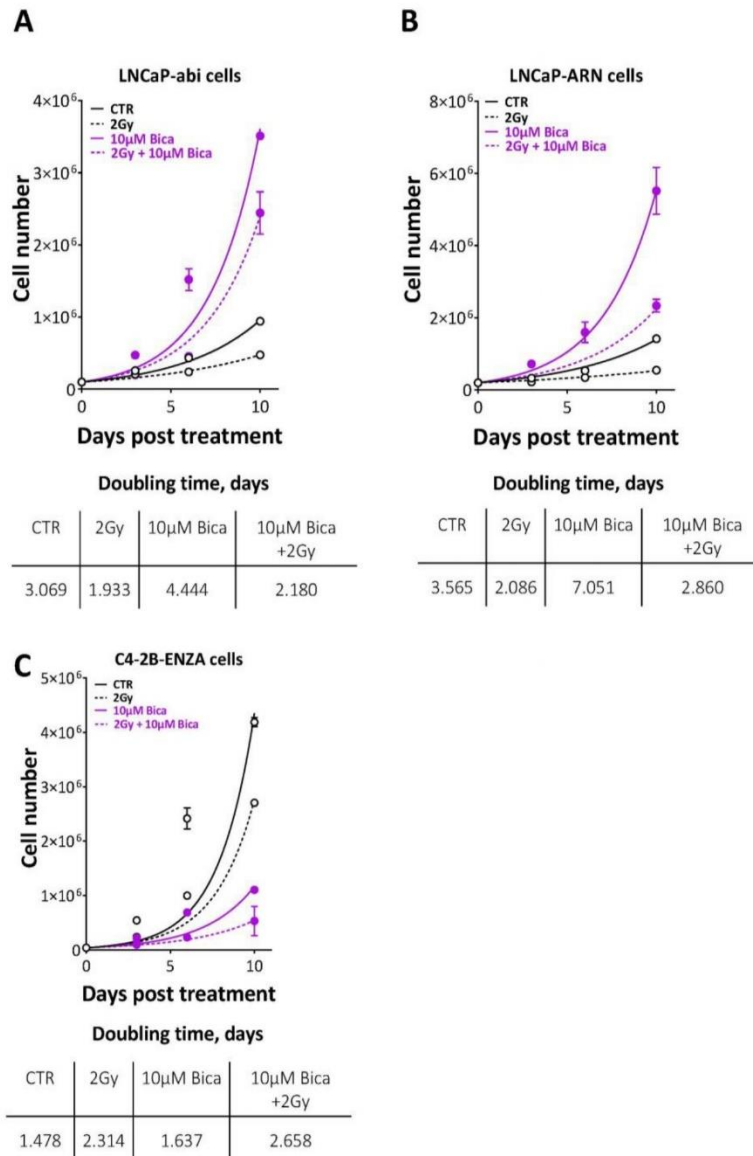


Figure S3 Bicalutamide showed contradictory effects on the cytotoxicity of ionizing radiation in hormone resistant cells. Cell number was determined in LNCaP-abi (A), LNCaP-ARN (B) or C4-2BENZA cells (C) on days 0, 3, 6 and 10 post treatment with 10 µM bicalutamide (Bica). Cell doubling time in days was calculated for each treatment by fitting exponential growth curves using GraphPad Prism 7. Shown are means ±SEM of at least three independent experiments.

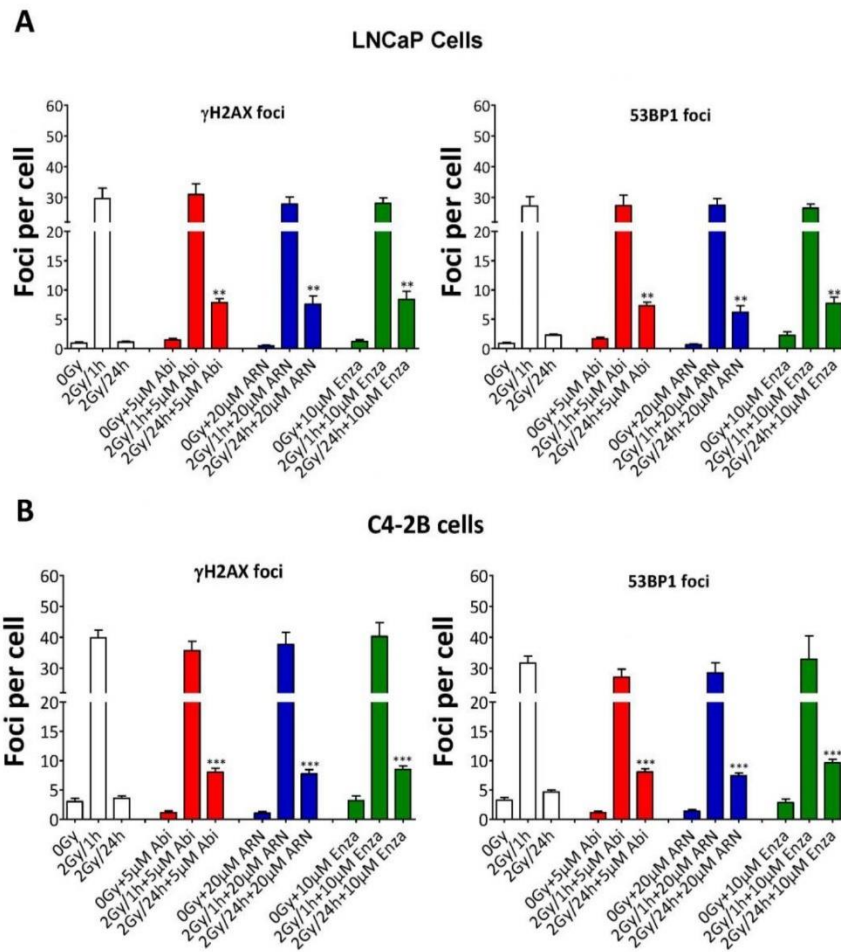


Figure S4. Quantitation of individual γ H2AX (left panel) and 53BP1 (right panel) foci of the experiments performed in Figure 7. in **(A)** LNCaP and **(B)** C4-2B cells. At least 100 cells were analyzed. Shown are the means \pm SEM from at least three independent experiments. p -values were calculated using the Mann-Whitney U test. Significance is indicated as * for the $p < 0.05$, ** for $p < 0.001$ and *** for $p < 0.0001$. ns: not significant.

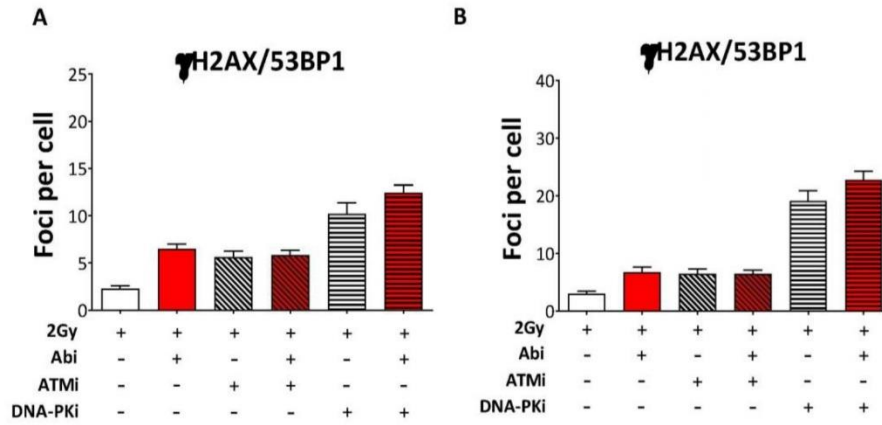


Figure S5. Quantitation of γ H2AX/53BP1 foci at 24h post 2Gy in (A) LNCaP and (B) C4-2B cells after treatment with 2.5 μ M ATM or 5 μ M DNA-PKcs inhibitor (2 h pre-IR) and 5 μ M abiraterone acetate (24 h-pre-IR) either individually or combined. At least 100 cells were analyzed. Shown are the means \pm SEM from at least three independent experiments.

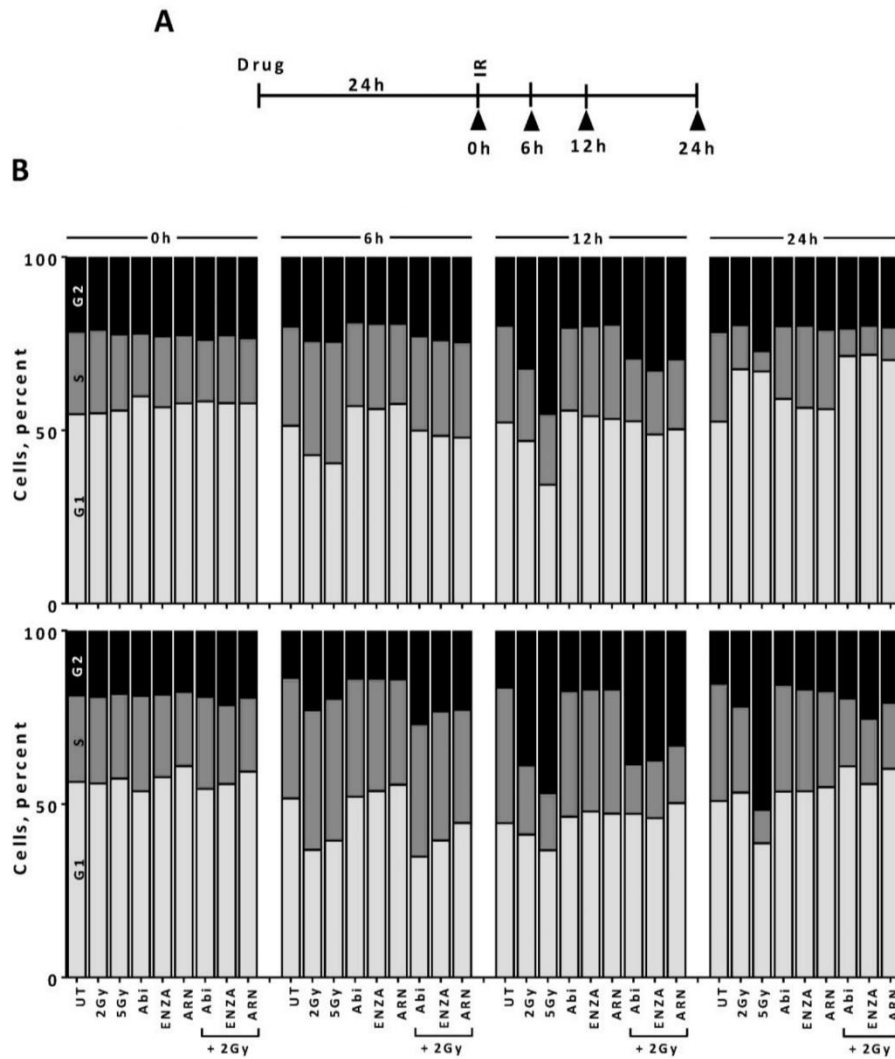


Figure S6. Second generation AHT does not affect cell cycle distribution after IR. **(A)** Schematic representation for the experiment flow. cells were treated with the indicated AHT for 24 hours before being irradiated with 2Gy and cell cycle profiles of LNCaP (upper panel) and C4-2B (lower panel) were determined by propidium iodide staining and flow cytometry at the indicated time points. **(B)** The percentage of cells from each treatment in G1 (light grey), S (dark grey) or G2 (black) phase are shown.

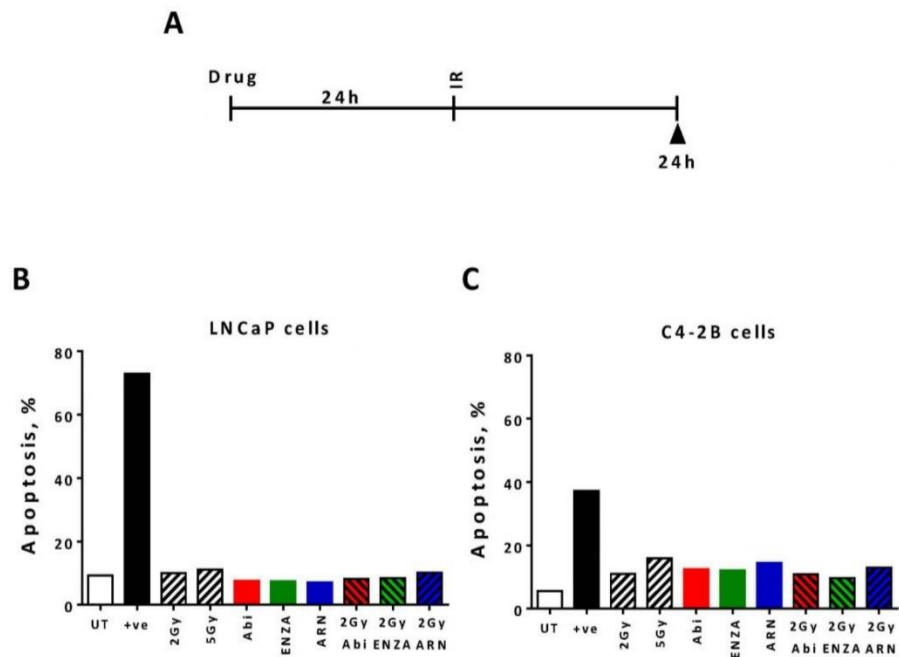


Figure S7. Second generation AHT does not increase apoptosis after IR. (A) Schematic representation for the experiment flow. Both LNCaP (B) and C4-2B (C) cells were treated the indicated antiandrogen for 24 hours before being irradiated with 2Gy and apoptosis were determined via caspase activity. As a positive control (+ve) for apoptosis induction, cells were treated with 1 μ M staurosporine for 12 h.

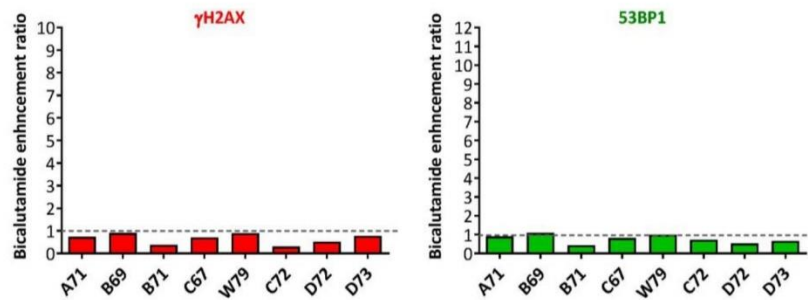


Figure S8. Bicalutamide does not inhibit DSB repair after IR. Bicalutamide-mediated enhancement ratio (BicaER) on gH2AX (left panel) and 53BP1 (right panel) foci of 8 punch biopsies from 8 PCA patients.

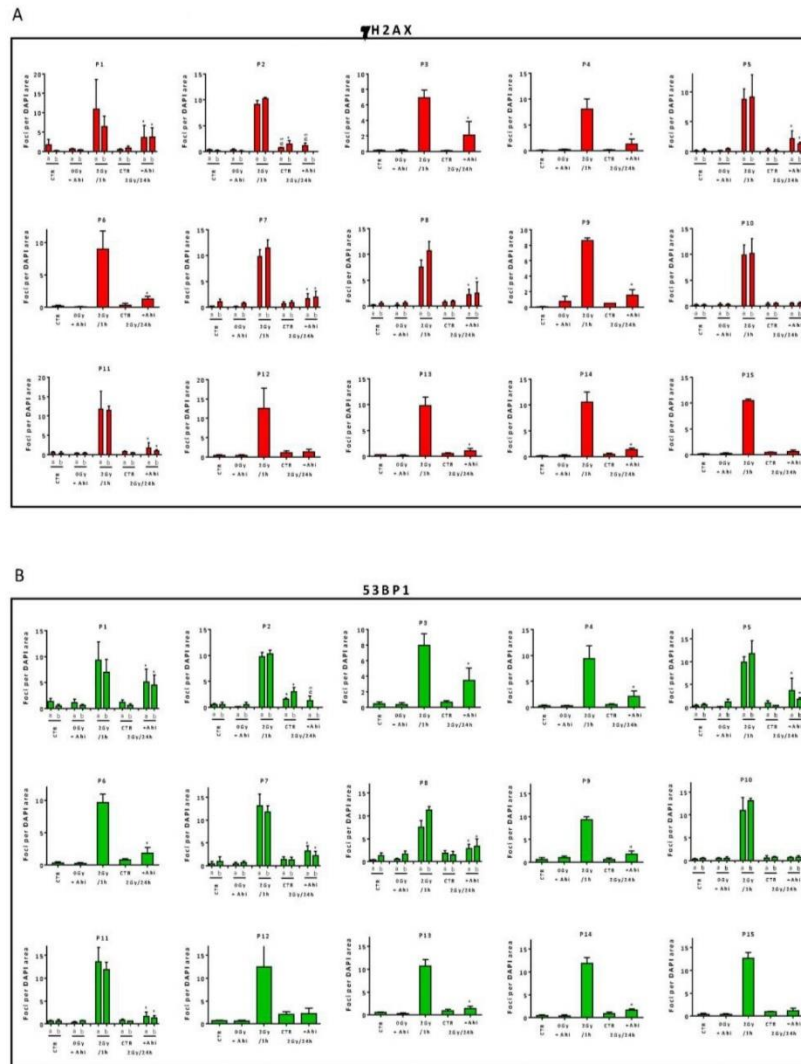


Figure S9. Abiraterone acetate efficiently suppresses DSB-repair in fresh PCa tissues after ex-vivo irradiation. Number of (A) yH2AX or (B) 53BP1 foci in 22 punch biopsies from the 15 PCa patients after the indicated treatments. Shown are the means \pm SEM from at least three independent experiments. *p*-values were calculated using the Mann-Whitney U test. Significance is indicated as * for the $p < 0.05$, ** for $p < 0.001$ and *** for $p < 0.0001$. ns: not significant.



© 2020 by the authors. Licensee MDPI, Basel, Switzerland. This article is an open access article distributed under the terms and conditions of the Creative Commons Attribution (CC BY) license (<http://creativecommons.org/licenses/by/4.0/>).

4.2. Publication 2

Preclinical patient-derived modeling of castration-resistant prostate cancer facilitates individualized assessment of homologous recombination repair deficient disease

Mohamed E. Elsesy^{1,2} , Su Jung Oh-Hohenhorst^{3,4}, Christoph Oing^{1,5} , Alicia Eckhardt^{1,6,7}, Susanne Burdak-Rothkamm^{1,8}, Malik Alawi⁹, Christian Müller^{1,9}, Ulrich Schüller^{6,10} , Tobias Maurer^{3,11}, Gunhild von Amsberg^{3,12}, Cordula Petersen¹, Kai Rothkamm¹ and Wael Y. Mansour^{1,5} 

- 1 Department of Radiotherapy and Radiooncology, University Medical Center Hamburg-Eppendorf, Germany
- 2 Department of Tumor Biology, National Cancer Institute, Cairo University, Giza, Egypt
- 3 Martini-Klinik Prostate Cancer Center, University Medical Center Hamburg-Eppendorf, Germany
- 4 Centre de Recherche du Centre Hospitalier de l'Université de Montréal (CRCHUM), QC, Canada
- 5 Mildred Scheel Cancer Career Center HaTriCS4, University Medical Center Hamburg-Eppendorf, Germany
- 6 Department of Pediatric Hematology and Oncology, University Medical Center Hamburg-Eppendorf, Germany
- 7 Research Institute Children's Cancer Center Hamburg, Germany
- 8 Department of Molecular & Clinical Cancer Medicine, University of Liverpool, UK
- 9 Bioinformatics Core, University Medical Center Hamburg-Eppendorf, Germany
- 10 Institute of Neuropathology, University Medical Center Hamburg-Eppendorf, Germany
- 11 Department of Urology, University Medical Center Hamburg-Eppendorf, Germany
- 12 Department of Oncology, University Cancer Center Hamburg Eppendorf, University Medical Center Hamburg-Eppendorf, Germany

Keywords

castration-resistant prostate cancer; *ex vivo* tumor cultures; homologous recombination; PARP inhibition; patient-derived organoids

Correspondence

W. Y. Mansour, Laboratory of Radiobiology and Experimental Radiooncology, Department of Radiotherapy and Radiation Oncology, University Medical Center Hamburg-Eppendorf, Martinistr. 52, 20251, Hamburg, Germany
 Fax: +49 40 7410 55139
 Tel: +49 40 7410 53831
 E-mail: w.mansour@uke.de

(Received 10 August 2022, revised 24 October 2022, accepted 23 January 2023)

doi:10.1002/1878-0261.13382

Abbreviations

Abi, abiraterone; ADT, androgen deprivation therapy; ARN, apalutamide; Bic, bicalutamide; CFA, colony formation assay; CisER, cisplatin-induced enhancement ratio; COSMIC, catalog of somatic mutations in cancer; CR, castration-resistant; CRPC, castration-resistant prostate cancer; CSS, charcoal-stripped serum; DAPI, 4'-6-diamidino-2-phenylindole; DMEM, Dulbecco's modified Eagle's medium; DSB, double strand break; DT, doubling time; EdU, 5-ethynyl-20-deoxyuridine; ENZA, enzalutamide; H&E, hematoxylin and eosin; HP, hormone-proficient; HRR, homologous recombination repair; mCRPC, metastatic castration-resistant prostate cancer; mHSPC, metastatic hormone-sensitive prostate cancer; MSI, microsatellite instability; MTT, 3-(4, 5-dimethylthiazolyl-2)-2, 5-diphenyltetrazolium bromide; PARPi, PARP inhibitors; PCa, prostate cancer; PDO, patient-derived tumor organoids; PIER, PARPi-induced enhancement ratio; RNA-SEQ, RNA-sequencing; SBS, single base substitutions; SF, surviving fraction; WGS, whole genome sequencing.

The use of mutation analysis of homologous recombination repair (HRR) genes to estimate PARP-inhibition response may miss a larger proportion of responding patients. Here, we provide preclinical models for castration-resistant prostate cancer (CRPC) that can be used to functionally predict HRR defects. *In vitro*, CRPC LNCaP sublines revealed an HRR defect and enhanced sensitivity to olaparib and cisplatin due to impaired RAD51 expression and recruitment. *Ex vivo*-induced castration-resistant tumor slice cultures or tumor slice cultures derived directly from CRPC patients showed increased olaparib- or cisplatin-associated enhancement of residual radiation-induced γ H2AX/53BP1 foci. We established patient-derived tumor organoids (PDOs) from CRPC patients. These PDOs are morphologically similar to their primary tumors and genetically clustered with prostate cancer but not with normal prostate or other tumor entities. Using these PDOs, we functionally confirmed the enhanced sensitivity of CRPC patients to olaparib and cisplatin. Moreover, olaparib but not cisplatin significantly decreased the migration rate in CRPC cells. Collectively, we present robust patient-derived preclinical models for CRPC that recapitulate the features of their primary tumors and enable individualized drug

screening, allowing translation of treatment sensitivities into tailored clinical therapy recommendations.

1. Introduction

Prostate cancer (PCa) is the most frequent malignant tumor in males; approximately one in six men will be diagnosed within their lifetime [1]. PCa is clinically variable, with often indolent and low-risk disease that will not pose a health threat over one's lifetime, but also aggressive phenotypes with rapid disease progression and treatment resistance. In the metastatic stage of disease, patients have no option for cure despite significant progress with new therapeutic treatment strategies. Androgen deprivation therapy (ADT) induces tumor regressions in the vast majority of patients with metastatic hormone-sensitive prostate cancer (mHSPC) and treatment intensification with docetaxel and/or androgen receptor (AR) pathway targeting agents has improved overall survival in randomized phase 3 clinical trials [2]. However, even at this early stage, the heterogeneity of the disease becomes obvious, with a nearly doubling of life expectancy in patients with metachronous development of metastases compared with patients with primary metastatic disease [3]. After systemic treatment initiation for mHSPC, virtually all patients progress to castration-resistant prostate cancer (CRPC) as a result of selection and/or acquired resistance [4]. CRPC carries a worse prognosis, with estimated median survival times of 16–18 months from the onset of CRPC progression [5–7]. Although additional treatments exist for such patients, including docetaxel, enzalutamide, abiraterone, radium-223, sipuleucel-T and cabazitaxel, these treatment successes are not long-lasting with only a modest overall survival benefit [8]. Comprehensive genomic characterization of CRPC identified frequent mutations in DNA repair genes, specifically those involved in homologous recombination repair (HRR) [9,10], with a frequency reaching in some studies to approximately 40% among patients with metastatic CRPC (mCRPC) [11]. Consequently, the paradigm of PARP inhibitors (PARPi)-mediated synthetic lethality or any other chemotherapy that targets HRR-deficient tumors expands the management options for mCRPC. However, not all HRR defects respond equally to PARP inhibition. This led, for example, to a restricted approval of olaparib in Europe to patients with BRCA1/2 alterations, since the pivotal PROFOUND trial revealed the highest PARP inhibitor efficacy for patients carrying these respective mutations. In

contrast, for alterations in other HRR genes, e.g. ATM, the effects were less convincing [12,13]. The story gets even more complicated when comparing two recent phase 3 trials on the efficacy of a combination of abiraterone/prednisone and olaparib (PROpel) or niraparib (MAGNITUDE). Whereas in the PROpel trial, presumably due to a BRCAness effect of abiraterone, a prolonged progression-free survival was also observed for the combination treatment in HRR wild-type patients, the MAGNITUDE trial did not show such an advantage [14,15]. This illustrates that we clearly do not yet comprehensively understand the molecular pathological processes of HRR in PCa. Furthermore, to date, HRR defects are basically detected by large-scale sequencing analysis, a costly process. Despite these comprehensive analyses, information on the actual effect of these alterations on HRR function in the tumor cell is limited, which highlights the need for valid assays to functionally detect HRR defects.

Preclinical and translational research into novel synthetic lethality concepts is, however, hampered by the lack of appropriate preclinical models for such disease. Various preclinical models have been introduced to advance CRPC research. Most studies relied on using immortalized cell lines grown in two-dimensional (2D) cultures or xenografts of such cell lines in immunocompromised animals. While these PCa cell lines are readily available and simple to use, only a limited number of cell lines are available and they are far from being authentic exemplars of CRPC due to their prolonged time in culture. In addition, the available cell lines fail to capture the various aspects of heterogeneity of PCa. Further, commonly used *in vitro* CRPC models, such as DU145 and PC3 cells, neither reflect the diversity of this disease, nor do they accurately predict patient sensitivity to treatment [16,17]. Although several genetically engineered mouse models exist [18], they fail to generally model clinical CRPC, as castration-resistant tumors in mice do not depend upon AR signaling mechanisms [19]. Therefore, three-dimensional (3D) culture models of PCa are currently gaining increasing attention as preclinical models that better mimic the *in vivo* tumor biology and microenvironment. *Ex vivo* culturing of freshly collected tumor slices as well as patient-derived organoids (PDOs) are considered promising 3D models. We and others have shown previously that tissue slice cultures show

comparability with the original tumor, preserving the tumor morphology and its microenvironment [20–23]. However, although the *ex vivo* assay allows a variety of functional analyses and biological readouts such as DSB repair and apoptosis, these do not include robust analysis of survival rates, one of the most important endpoints of drug sensitivity analysis.

Patient-derived tumor organoids are 3D tissue cultures that promise to enable the validation of preclinical drug testing in precision medicine and co-clinical trials by modeling tumors for predicting therapeutic responses with more reliable efficacy. Although there has also been a significant improvement in the generation of PDOs from PCa patients, their long-term propagation in culture has remained challenging. To the best of our knowledge, there are only a few studies reporting successful establishment of PDOs from PCa specimens [24–29], with a success rate of < 20%. Furthermore, the capacity for long-term maintenance of these PDOs is variable and limited [30]. In the current study, we provide different preclinical models derived from CRPC *in vivo* and the rationale for using these models to recapitulate and predict the response of individual CRPCs to PARP inhibitors, that is, olaparib and cisplatin.

2. Materials and methods

2.1. Cell culture, drugs and X-irradiation

LNCaP prostate cancer cells (ATCC, Manassas, VA, USA) were grown in Dulbecco's modified Eagle's medium (DMEM, Gibco, Paisley, UK) supplemented with 10% fetal calf serum (FCS), 100 U·mL⁻¹ penicillin and 100 mg·mL⁻¹ streptomycin at 37 °C with 10% CO₂. Novel antiandrogen-resistant sublines LNCaP-ARN509 and LNCaP-abi were generated by long-term treatment with apalutamide (ARN-509) (up to 40 μM) and abiraterone acetate (up to 10 μM), respectively, until acquiring androgen-independent growth feature [31]. C4-2B-Enza cells (kindly provided by Prof. C. P. Evans, UC Davis School of Medicine, Sacramento, CA, USA) were maintained in medium containing 20 μM enzalutamide. Abiraterone acetate, apalutamide and enzalutamide were kindly provided by Janssen Cilag GmbH, Neuss, Germany. LNCaP-abl cells (a gift from Prof. Z. Culig, Medical University Innsbruck, Austria) were grown in DMEM supplemented with 10% Charcoal Stripped FBS (Sigma-Aldrich, Taufkirchen, Germany) [32]. All cell lines tested negative for mycoplasma contamination. Irradiation was performed as previously described (200 kV, 15 mA, additional 0.5-mm Cu filter at a dose rate of 0.8 Gy·min⁻¹) [15].

2.2. Cell lines authentication

All cell lines used in the current study have been authenticated before executing the experiments. Authentication of cell lines used in the current study was performed in our laboratory. The profiles for all cell lines have been compared and matched with the STR profile database.

2.3. Proliferation assay

Proliferation assay was performed as previously described [31]. Briefly, cells were cultured in triplicate in 6-well plates before treatment. For LNCaP-abl subline, cells were seeded in CS-FCS-supplemented medium for 18–24 h before changing to the FBS full medium for the treatment. To assess the effect of any treatment regimes, the cell number was determined with a Beckman Coulter cell counter (Life Science, Beckman Coulter cell counter, Krefeld, Germany) at 3-, 6- and 10-days post-treatment. In all experiments, media with or without drugs were changed twice during the 10-day treatment course.

2.4. 3D colony formation assay

3D colony formation assay (CFA) for cell lines was performed by mixing cells in cold-reduced growth factor basement membrane extract (RGF BME) type 2 (R&D Systems, Minneapolis, MN, USA) and plated at 2000 cells per dome onto 24-well plates. For tumor organoids 3D CFA, tumor organoids were first harvested and sheared into single cells before being mixed in cold BME and plated at 4000 cells per dome. Upon completed gelation, different concentrations of olaparib or cisplatin as well as DMSO controls were added in triplicate in 500 μL of corresponding medium. After 3–4 weeks, colonies (tumoroids or 3D cell cultures) were stained with 0.5 mg·mL⁻¹ 3-(4,5-dimethylthiazolyl-2)-2, 5-diphenyltetrazolium bromide (MTT) for 1.5 h. For organoid colonies, medium was removed and BME domes were dissolved using Cultrex™ Organoid Harvesting Solution. MTT-stained 3D cellular colonies and tumoroids were photographed using REBEL Microscopy (ECHO, San Diego, CA, USA) and analyzed using IMAGE-J. Surviving fractions (SFs) were calculated by normalization to the plating efficiency of the untreated control. DMSO was used as a control at the same concentration.

2.5. Immunofluorescence

After treatment, cells cultured on coverslips were washed and fixed with 4% paraformaldehyde/PBS for 10 min.

Fixed cells were permeabilized with 0.2% Triton X-100/PBS on ice for 5 min and incubated for 1 h at room temperature with primary antibodies: mouse monoclonal anti-phospho-S139-H2AX antibody (Millipore, Darmstadt, Germany) at a dilution of 1 : 500 and rabbit polyclonal anti-53BP1 antibody (Novus, Braunschweig, Germany) at a dilution of 1 : 500 or rabbit polyclonal anti-RAD51 (Sigma Aldrich, Taufkirchen, Germany) at a dilution of 1 : 500. After being washed three times with cold PBS, the cells were incubated for 1 h with secondary anti-mouse Alexa Fluor 594 (Invitrogen) at a dilution of 1 : 500, and anti-rabbit Alexa Fluor 488 (Invitrogen) at a dilution of 1 : 600. The nuclei were counterstained with 4'-6-diamidino-2-phenylindole (DAPI, 10 ng·mL⁻¹). Slides were mounted in Vectashield mounting medium (Vector Laboratories, Newark, CA, USA). Immunofluorescence of cultured tumor tissue was performed as previously described [21]. Fluorescence microscopy was performed using the Zeiss AxioObserver.Z1 microscope (objectives: ×20, resolution 0.44 μm; Plan Apo 63/1.4 Oil DICII, resolution 0.24 μm; and filters: Zeiss 43, Zeiss 38, Zeiss 49, Göttingen, Germany). Z-stacks of semi-confocal images were obtained using the ZEISS APOTOME, ZEISS AXIO-CAM MRM and ZEISS AXIOVISION software. For DSB analysis, fields of view were taken per time point or treatment with a minimum of 100 cells (cell lines) or 50 cells (tumor tissue). All staining was performed in duplicate. DSBs were analyzed using IMAGE-J and DAPI-based image masks and normalized to single nucleus values [21].

2.6. Western blot

Whole cell lysates were subjected to western blot as previously described [33,34]. RAD51 immunoblot analysis was performed with the rabbit anti-RAD51 (Merck, Darmstadt, Germany, Cat#PC130). Beta-actin was immunoblotted by mouse anti-beta-actin (Sigma Aldrich, Taufkirchen, Germany, Cat#A1978) and used as a loading control. Goat-anti-mouse IgG-Alexa Fluor 594 (Molecular Probes, Sigma Aldrich, Taufkirchen, Germany, Cat#A11005) and goat-anti-rabbit IgG-AlexaFluor 488 (Molecular Probes, Cat#A11008) secondary antibodies were used. Membranes were developed and analyzed using LiCor Biosciences (Lincoln, NE, USA) at room temperature.

2.7. Patient sample collection

Fresh PCa tissue was obtained from patients with high-risk PCa according to D'Amico risk stratification, who underwent radical prostatectomy at Martini-Klinik, Prostate Cancer Center Hamburg, Germany between 2019 and 2022. Immediately after resection, one to two

punch biopsies were taken by the surgeon in palpable tumor areas. The biopsies were collected in culture media and immediately taken to the laboratory. Pseudonymized biopsies were processed within 30 min after resection. The laboratory received a final pathology report containing the Gleason score, PSA status and age of each pseudonymized patient for clinical analysis. The project was approved by the local ethics committee [Ethik-Kommission der Ärztekammer Hamburg] with the project number PV7007. The study methodologies conformed to the standards set by the Declaration of Helsinki. All experiments were undertaken with the understanding and written consent of each subject.

2.8. Tissue slice cultures

Ex vivo tissue slice cultures were prepared as previously described [20]. Briefly, 300-μm slices were cut using the MacIrvine tissue chopper and placed on Millicell® cell culture inserts (0.4 μm, 30 mm diameter, Merck), which were inserted in 6-well dishes containing 1 mL DMEM supplemented with 10% FCS and incubated at 37 °C. Prior to *ex vivo* treatment, the tissues slices were incubated for 1 day for recovery and re-oxygenation. To monitor proliferation, unirradiated slice cultures were incubated with 5-ethynyl-20-deoxyuridine (EdU, 1 : 1000; Click-iT Assay Kit, Invitrogen) overnight for 16 h. All slices were additionally treated with pimonidazole (200 μM, Hypoxyprobe, Burlington, MA, USA) 2 h before fixation to monitor tissue hypoxia.

2.9. Histology and imaging

PCa tumor tissues and PDOs were prepared as previously described [21]. Briefly, either tissues or tumoroids were fixed using 4% PFA (Merck) followed by washing in 25% sucrose twice each for 1 h. The samples were then frozen in TissueTek® (Sakura Finetek, Alphen aan den Rijn, Netherlands) and stored at -80 °C. Using the Cryo Star NX70 Microtome (Thermo Scientific) sectioning was performed to prepare cryoslices (5 μm). Histological analysis was performed by standard hematoxylin and eosin (H&E) staining and percentage of cancer cells and Gleason score were determined by an experienced PCa pathologist. Immunohistochemistry was performed using antibodies against AMACR (Thermo Scientific, Regensburg, Germany, PA5-82739, 1 : 250), and Ki67 (Abcam, Cambridge, UK, ab15580, 1 : 250). Images were acquired using ZEISS Axio Scan.Z1 Slide Scanner and photos were then processed using netScope® Viewer.

2.10. Prostate tumor tissue processing and organoid establishment

Organoid establishment and culture were adapted from Drost et al. [25] and Gao et al. [30]. Briefly, prostate tumor specimens from patients who underwent radical prostatectomy were received in adDMEM F12+++ [advanced DMEM F12 (Thermo Scientific) supplemented with 10 mM HEPES (Thermo Scientific), GlutaMAX (Thermo Scientific), and penicillin/streptomycin (Thermo Scientific)]. Tumor tissue samples were first washed three times with PBS and then placed in 3.5-cm culture dish where they underwent mechanical dissection into small pieces, which were then placed in 5 mg·mL⁻¹ Collagenase type II (Sigma-Aldrich) in adDMEM +++ with 10 μM ROCK inhibitor and incubated in a 37 °C shaker for 30–90 min for digestion. After tissue digestion, the suspension was passed through a 50-μm cell strainer (Sysmex) before being washed with adDMEM F12+++ and finally suspended in cold BME. Drops of BME cell suspension each 40 μL were allowed to solidify for 30 min at 37 °C onto a pre-warmed 24-well culture plate. After stabilization of Matrigel-containing cells, 500 μL of complete organoid medium (Table S1) was added. Fresh medium was replenished every 3–4 days during organoid growth. Organoids were passaged every 4–6 weeks. During passaging, the organoid droplets were mechanically sheared through P1000 pipet tip and incubated with TrypLE Express containing 10 μM ROCK inhibitor for a maximum of 5 min at 37 °C. The resulting cell clusters and single cells were washed and re-plated following the protocol described above.

2.11. *Ex vivo* induction of castration-resistant status

To induce castration-resistant phenotype *ex-vivo*, PCa tissues derived from naïve PCa patients were cultured in hormone-depleted condition (DMEM supplemented with CS-FBS containing 10 μM abiraterone). Each sample was cultured for up to 6 weeks in either hormone-proficient or -deficient conditions and the culture medium was refreshed every 3 days. The proliferative marker Ki67 was used to prove the attained castration-resistant phenotype through proliferative activity. The tumor tissue cultured in hormone-deficient condition that still showed Ki67 proliferative index similar to its counterpart slice cultured in hormone proficient medium, was considered a castration-resistant sample.

2.12. Migration assay

Chemotaxis assay was performed in 24-well Transwell plate using 8-μm pore-size (Corning® BioCoat®, 354578). Either LNCaP or LNCaP-ARN509 cells were harvested and re-suspended in FBS-free DMEM medium at concentrations of 2×10^5 cells in 0.2 mL, and then seeded into the upper chamber of a 24-well plate. The lower chambers were filled with 0.7 mL DMEM containing 10% FBS to act as an attractant. Cells were incubated for 36 h. At the end of the experiment, cells that migrated into the reverse side of the Transwell membrane were fixed with 70% ethanol, stained with 0.2% crystal violet, and then photographed using REBEL Microscopy and analyzed using IMAGE-J.

2.13. DNA methylation profiling

Total DNA was isolated from PCa cell lines, tissues or organoid cultures using Qiagen Kit (Qiagen, Hilden, Germany). The Illumina Human-Methylation450 BeadChip (450 K) arrays were used to analyze genome-wide DNA methylation patterns of tissues or organoids. Only sites covered by at least three reads were considered for analysis. For each sample, the percentage of methylation per site (beta value) was computed. Average hierarchical clustering of samples was performed by '1-Pearson's correlation coefficient' as distance measured on the $n = 10\,000$ CpG sites showing the highest standard deviation across the cohort. Several samples of the following datasets were included as a reference set: TCGA-BRCA, TCGA-Lung, TCGA-GBM, TCGA-PRAD, GSE112047, GSE38240, GSE83842 and glioblastoma samples (tissue and cell lines) and lung carcinoma samples were from UKE.

2.14. Whole genome sequencing (WGS)

WGS was performed by Novogene (Sacramento, CA, USA). WGS data analysis was performed by the Bioinformatics core facility at University Medical Center Hamburg-Eppendorf (UKE), Hamburg, Germany. Reads were aligned to the human genome assembly GRCh38 using bwa mem [35] and structural and short somatic mutations were labeled using Manta [36] and Strelka2 [37], respectively. Variants with a depth below 60 or presence in the Genome aggregation database (<https://gnomad.broadinstitute.org/>) were removed. Single base substitutions (SBS) – as defined by the Catalog of Somatic Mutations in Cancer (COSMIC) –

were identified using sigProfiler [38] and putative microsatellite instability (MSI) was determined using MANTIS [39]. The method HRDetect described by Davies et al. [40] for the identification of homologous recombination deficiency was applied using the R package signature.tools.lib [41].

2.15. RNA-sequencing (RNA-SEQ)

Total RNA was extracted from PCa cells using RNeasy Mini Kit (Qiagen, Hilden, Germany). RNA were then sent to Novogene for RNA-SEQ libraries preparation and sequencing. RNA-SEQ data analysis was performed by Novogene. Briefly, reads were aligned to the human reference genome GRCh37 using STAR [42] and differential expression analysis between LNCaP cells and their castration-resistant sublines was performed using R package EDGER [43]. Genes with a false discovery rate < 0.005 and an absolute log₂-fold-change > 1 were considered significant. Enrichment analysis of Gene ontology terms and pathway categories was carried out using R package CLUSTERPROFILER [44].

2.16. Graphs and statistics

Statistical analyses, data fitting and graphics were performed with the GRAPHPAD PRISM 9.0 program (GraphPad Software, Boston, MA, USA). The IDAT files of the samples were loaded, filtered and normalized with the package LIMMA (version 3.40.0) in R (version 3.6.0). By using multiple datasets containing different numbers of CpG sites, our samples were reduced to 450 k sites. In addition, a correction was made for possible batch effects related to chip size using the LIMMA package.

3. Results

3.1. Castration-resistant cells are more radiosensitive than hormone-sensitive cells due to impaired DSB repair

Previously, we reported that DSB repair in CRPC cells is less efficient than in hormone-sensitive cells [31]. Since DSB repair capacity is a determinant factor for cellular radiosensitivity [45], we sought to analyze radiosensitivity in CRPC cells. To that end, LNCaP cells and their castration-resistant sublines (LNCaP-abl, LNCaP-abi, C4-2B, and C4-2B-ENZA) were treated with different IR doses and the effect on cell growth was monitored by cell counting at 3-, 6- and 10-days post-irradiation. A remarkable irradiation-related decrease in cell growth was observed in the resistant clones compared with the parental cells (Fig. 1A). Consistently, IR resulted in a

significant increase in doubling times (DT) in resistant clones compared with their parental cell lines (Fig. 1B), indicating an enhanced radiosensitivity in CRPC sublines. In keeping with this idea, using Matrigel-based 3D-culturing, we identified a significant radiosensitivity in all CRPC clones compared with their sensitive parental cells using colony forming assay (Fig. 1C). To analyze DSB repair efficiency, androgen-sensitive LNCaP and castration-resistant sublines were exposed to IR with a dose of 2 Gy, and γ H2AX and 53BP1 foci were quantified after 1 and 24 h post-irradiation (Fig. 1D). Although we observed no difference in the number of γ H2AX/53BP1 between sensitive and resistant cells at the 1-h time point post-2 Gy, the exposure to 2 Gy significantly increased the number of residual γ H2AX/53BP1 foci (threefold) at 24 h in all resistant sublines compared with sensitive LNCaP cells, pointing at impaired double-strand break repair capacity (Fig. 1E).

3.2. Impaired HR in castration-resistant cells due to lower RAD51 expression and loading

To unveil the mechanism underlying the impaired DSB repair in castration-resistant cells, we compared the transcription profile of LNCaP cells and their castration-resistant sublines using RNA-SEQ in biological duplicates. We then pooled all resistant clones and compared the commonly expressed genes with those in their parental hormone-sensitive LNCaP cells. More than 4500 genes were found to be significantly differentially expressed in the resistant clones, 2413 genes of which were downregulated in pooled resistant clones (Fig. 2A). Interestingly, gene ontology analysis (Fig. 2B) revealed that the most differentially repressed molecular pathways were DNA damage-response pathways including DNA replication, cell cycle and HRR. Among the HR repressed genes, RAD51 was significantly downregulated in resistant sublines (<https://www.ebi.ac.uk/ena/browser/view/PRJEB55017>). Given that the level of RNA is not necessarily always correlated with protein levels, we analyzed RAD51 protein levels in LNCaP cells and their castration-resistant sublines as well as in 22-RV1, DU145 and PC3 cell lines, which have been established from xenografts or metastatic lesions of patients with CRPC. Except for the 22-RV1 cells, twofold lower RAD51 protein levels were detected in resistant LNCaP sublines as well as in other castration-resistant cells than in hormone-sensitive LNCaP cells (Fig. 2C), indicating impaired HR in castration-resistant cells. To recapitulate this, LNCaP cells and their resistant sublines were irradiated with 2 Gy and RAD51 colocalized with γ H2AX foci were monitored at 3 and 24 h post-irradiation (Fig. 2D,

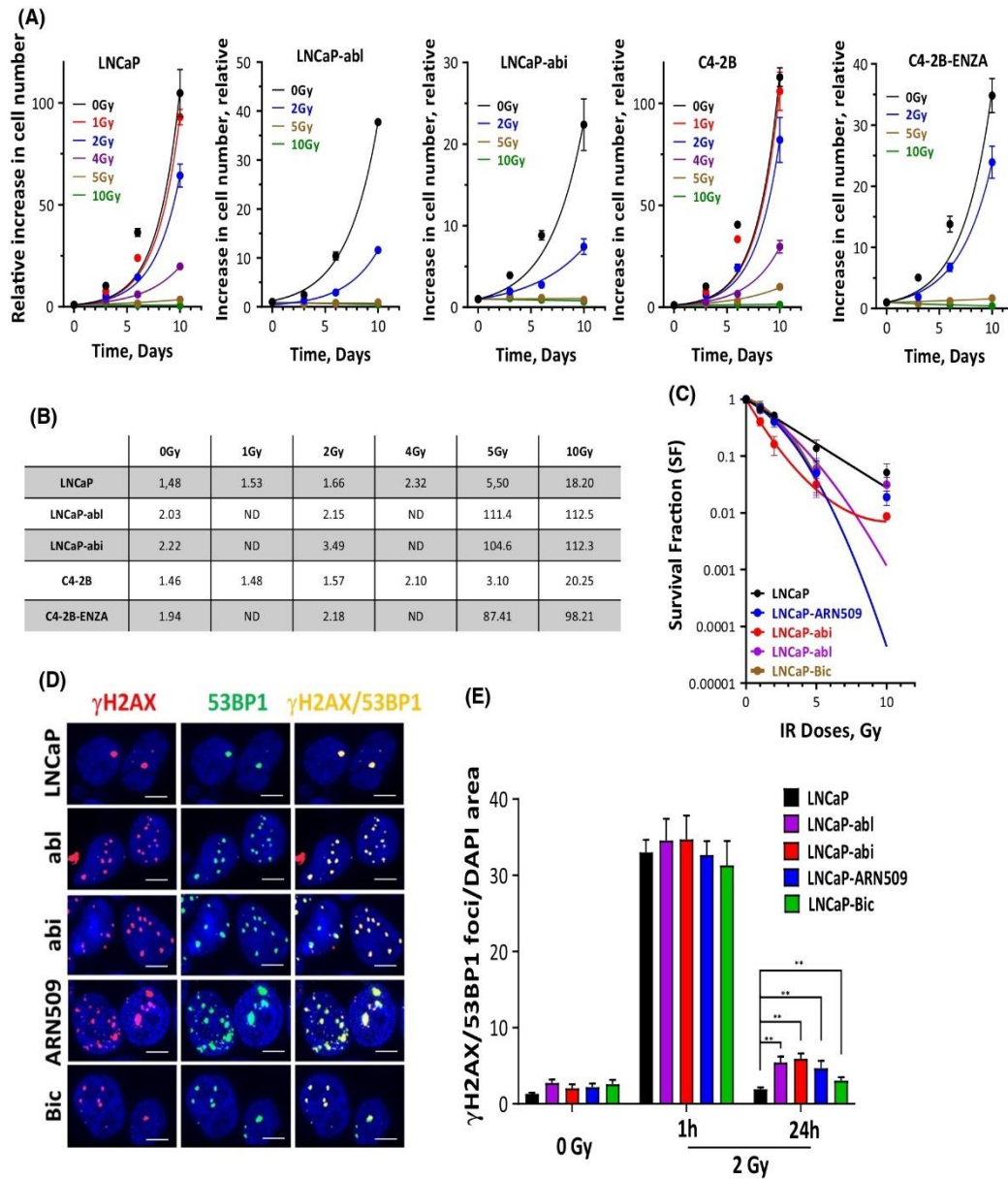


Fig. 1. Castration-resistant cells are more radiosensitive than the parental hormone-sensitive cells. (A) Cell number was determined in LNCaP, LNCaP-abl, LNCaP-abl, C4-2B and C4-2B-ENZA cells on days 0, 3, 6 and 10 post-irradiation with the indicated doses. (B) Cell doubling time in days was calculated for each treatment by fitting exponential growth curves using GRAPHPAD PRISM 9. Shown are means \pm SEM of three independent experiments. (C) Radiosensitivity of the indicated cells was analyzed by colony formation assay to calculate survival fractions after different irradiation doses. Shown are means \pm SEM of four independent experiments. (D) Representative micrographs of γ H2AX/53BP1 foci (Scale bar: 100 μ m) in the indicated cells 24 h after irradiation with 2 Gy and (E) quantifications of γ H2AX/53BP1 foci in the indicated cells before and 1 and 24 h after irradiation with 2 Gy. Shown are means \pm SEM of three independent experiments. Significance was calculated using the Mann-Whitney *U*-test: ***P* < 0.01 vs. control.

upper panel). As illustrated in the lower panel of Fig. 2D, the number of RAD51/ γ H2AX foci was significantly lower (twofold) in resistant clones than in

sensitive LNCaP cells (*P* = 0.003). Together, these data indicate that HRR may be impaired during transition to a castration-resistant phenotype.

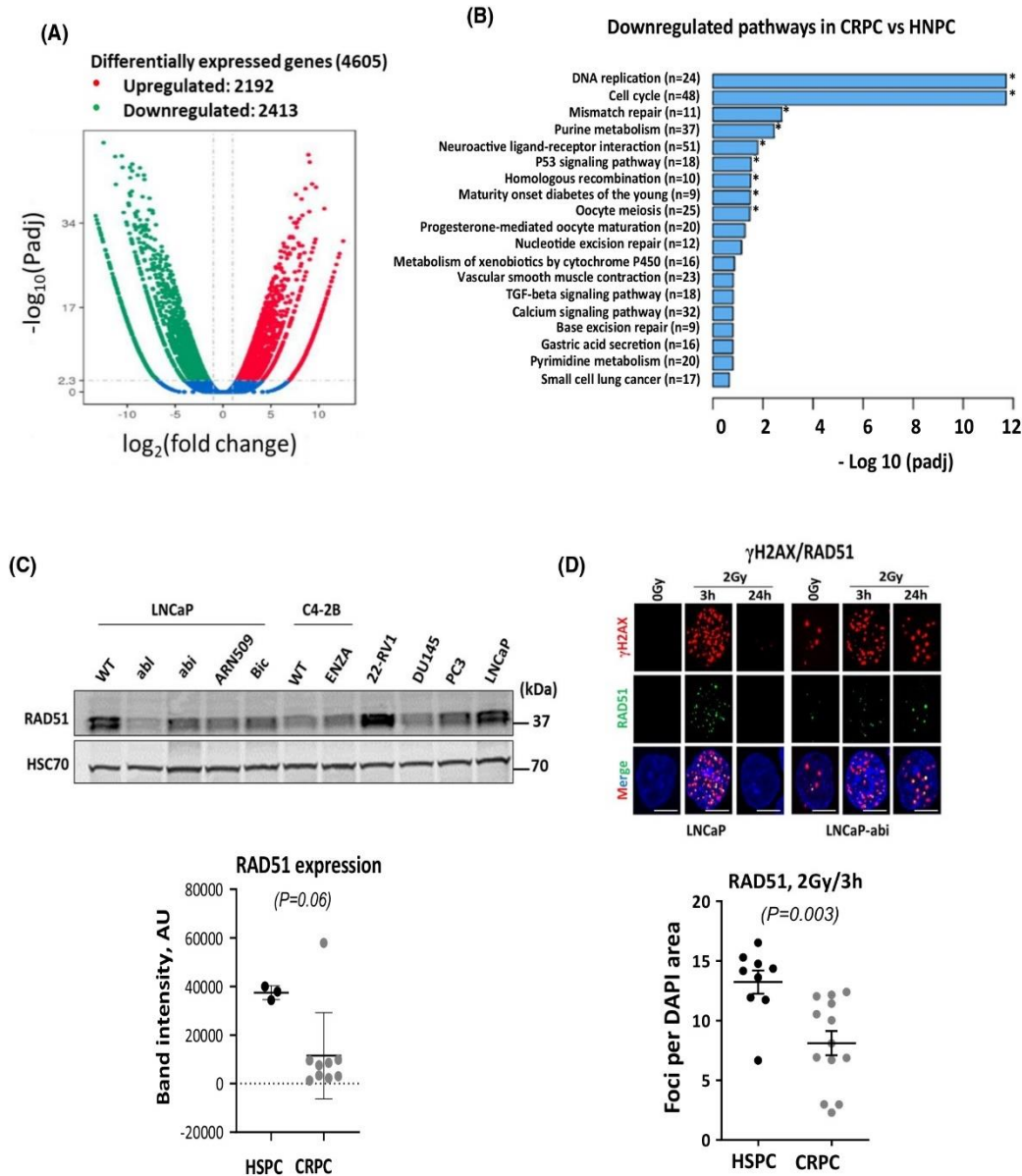


Fig. 2. Castration-resistant cells show a HRR deficiency due to RAD51 downregulation. (A) Volcano plot showing differentially expressed genes in polled castration-resistant sublines ($n = 4$) vs. hormone-sensitive LNCaP cells ($n = 2$), measured by RNA-SEQ. (B) Gene ontology (GO) enrichment analysis of the significantly downregulated pathways [$-\log_{10}$ (adjusted P value)] in castration-resistant cells. Significance: $*P < 0.05$. (C) Upper panel: Western blotting showing the expression of RAD51 protein in LNCaP cells (WT), castration-induced LNCaP sublines (abl, abi, ARN509, Bic), *in vivo* induced castration-resistant C4-2B cells and their enzalutamide-resistant subline (Enza), as well as 3 castration-resistant cell lines (22-RV1, DU145, and PC3). HSC70 was used as a loading control. Lower panel: band intensities were calculated from three independent blots. (D) Upper panel: Representative immunofluorescence images of γ H2AX and RAD51 foci (Scale bar: 100 μ m) detected after 3 and 24 h post-irradiation with 2 Gy. DAPI counterstain was used to visualize nuclei. Lower panel: Quantification of RAD51 foci numbers induced at 3 h post irradiation with 2 Gy. Shown are means \pm SEM of three independent experiments. Significance was calculated using the Mann-Whitney U -test vs control.

3.3. Castration-resistant cells are more sensitive to olaparib or cisplatin

A direct association between the response to PARPi or cisplatin and non-functional HRR pathway was reported [19,32]. We therefore investigated the sensitivity of castration-resistant cells to PARP inhibition with olaparib. To this end, the effect of 1 μ M olaparib on the proliferation of castration-resistant cells was measured. Although olaparib did not reduce the cell growth in the hormone-sensitive LNCaP cells (Fig. 3A), it significantly decreased the proliferation rate in LNCaP-abl (Fig. 3B), LNCaP-abi (Fig. 3C) and LNCaP-ARN509 (Fig. 3D), as exemplified by an increase in DT (1.3-, 2.6- and 2.3-fold, respectively; Fig. 3E). To further verify this, LNCaP and resistant sublines were treated with different concentrations of olaparib (0, 0.5, 1, 2, 5 and 10 μ M) and effects on survival were analyzed using 3D Matrigel CFA (Fig. 3F). To ensure better visualization and counting of living cells, MTT was used to stain living cells within 3D cultures pre-harvesting. Again, a significantly enhanced sensitivity to olaparib was observed in castration-resistant sublines compared with parental LNCaP cells (Fig. 3G). Similar results were obtained for cisplatin (Fig. 3G).

Since CRPC is a very heterogeneous disease, we sought to analyze the genome profile of the CR LNCaP sublines to elucidate whether they carry the alterations found in CRPC *in vivo*. WGS data reported no big structural differences in CRPC sublines compared with their hormone naïve parental cells (Fig. S1A). Mutational signatures analysis revealed that single base substitutions (SBS) – as defined by the Catalog of Somatic Mutations in Cancer (COSMIC) – detected in the CR samples included age-related signatures SBS1 and SBS5 but also SBS44, which is associated with defective DNA mismatch repair (Fig. S1B). In fact, all CR samples had high MSI scores (LNCaP-ARN509: 0.69, LNCaP-abi: 0.72, LNCaP-abl: 0.69, LNCaP-bic: 0.73), indicating genomic instability in the derived CRPC sublines. No mutation signature for HRR defect was detected in CR cells, despite showing a functional HRR deficiency associated with lower RAD51 expression at the transcriptional level. Possibly, CRPC sublines did not have enough time during establishment of resistance phenotype to accumulate genetic aberrations to show the HRR defect signature.

3.4. *Ex vivo* induction of castration resistance as an approach to study the sensitivity of CRPC to olaparib or cisplatin

The above results may imply that HRR is compromised during the development of castration resistance.

To further confirm this hypothesis, we used an approach to *ex vivo* induction of a castration-resistant phenotype in primary hormone naïve prostate cancer tumor specimens (Fig. 4A). Briefly, tumor slices from three patients with hormone naïve prostate cancer were cultured *ex vivo* for up to 6 weeks in androgen-depleted medium supplemented with charcoal-stripped serum (CSS) in the presence of abiraterone to induce a CRPC state. Ki67 IHC staining was used to confirm the development of the androgen-independency of the cultured primary tumor samples. Tumor slices showing no change in Ki67 index after culturing under castration-resistant (CR) conditions were considered to be CRPC. As a control, tumor slices from the same three patients were cultured under hormone-proficient (HP) conditions, i.e. in normal medium containing FCS plus DHT for the same period. We assessed this approach with 12 PCa samples from individual eight PCa patients, but only three samples from three patients showed no difference in the Ki67 index upon hormone-depleted culturing conditions (Fig. 4B). Next, we compared the radiosensitization effect mediated by either olaparib or cisplatin in PCa tissue slices cultured under either HP or CR conditions. To that end, slice cultures from more than six tumor punch biopsies collected from 3 PCa patients were irradiated *ex vivo* with 3 Gy in the presence or absence of either olaparib or cisplatin. γ H2AX and 53BP1 foci were then analyzed 1 and 24 h later (Fig. 4C). No change was observed in the number of foci at the 1-h time point between the slices cultured under either condition. However, tumor slices cultured in CR conditions demonstrated an increased number of residual γ H2AX and 53BP1 at 24 h post-IR (Fig. S2A,B). Further, the radiosensitization enhancement ratio mediated by olaparib (PiER) or cisplatin (CisER) was evaluated using the mean standard error of all samples set as a threshold for each DSB marker. Data clearly showed that the PiER of tumor slices cultured under CR but not HP rose above the threshold, with minor alterations between both markers (Fig. 4D). This confirms the findings in Fig. 3 that HRR is compromised in the induced CR models.

3.5. Olaparib increases the cytotoxicity of ionizing radiation in castration-resistant but not hormone naïve prostate cancer tissues

To further validate the above findings and the applicability of the presented preclinical CRPC models, we sought to recapitulate the data from Fig. 4, using tumor biopsies collected from CRPC patients. A total of 13 tumor biopsies from nine PCa patients (CRPC; $n = 5$ and HSPC; $n = 4$) were collected and irradiated

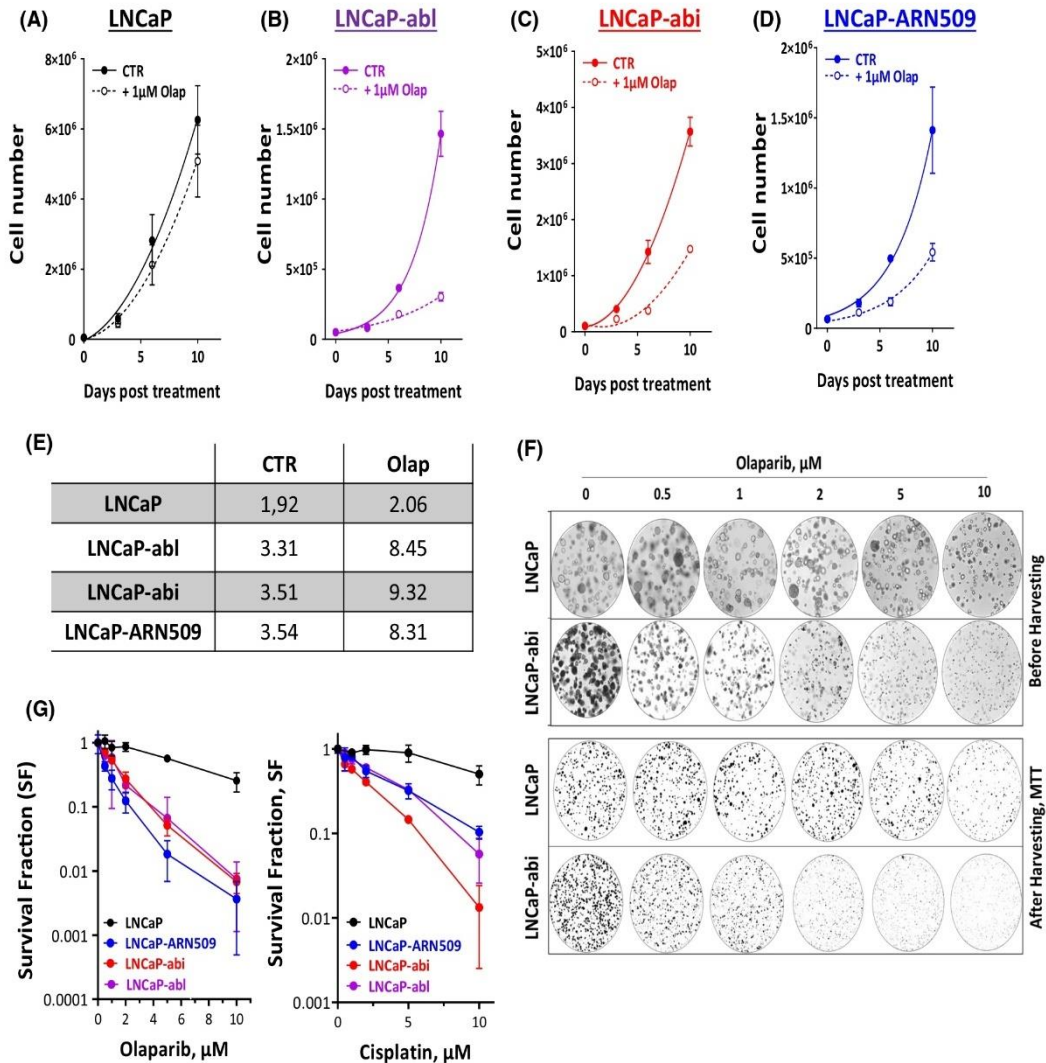


Fig. 3. Olaparib is more toxic for castration-resistant cells than for the parental hormone-sensitive cells. Cell number was determined in LNCaP (A), LNCaP-abl (B), LNCaP-abi (C) and LNCaP-ARN509 (D) cells on days 0, 3, 6 and 10 post treatment with 1 μ M of the PARP inhibitor olaparib. (E) Cell doubling time in days was calculated for each treatment by fitting exponential growth curves using GRAPHPAD PRISM 9. Shown are means \pm SEM of four independent experiments. (F) Representative images of 3D-cultures of the LNCaP and LNCaP-abl cells treated with the indicated concentrations of olaparib before (upper panel) and after (lower panel) harvesting and staining with MTT. (G) Survival fractions measured by colony forming assay after treating the indicated cells with different concentrations of olaparib (left panel) or cisplatin (right panel). Shown are means \pm SEM of three independent experiments.

ex vivo with 3 Gy after treatment with either olaparib or cisplatin. The impact of irradiation on the number of γ H2AX/53BP1 foci was then analyzed 1 and 24 h later (Fig. 5A) and the PiER and CisER were assessed. Ultimately, 10 punch biopsies from seven patients fulfilled all the previously described requirements [21] and were therefore used for further analysis. Again, no difference was observed in the number of γ H2AX/53BP1 foci at 1 h post-3 Gy between CRPC and HSPC

biopsies; however, tumor biopsies from CRPC patients showed a distinct increase at 24 h for both γ H2AX and 53BP1 markers upon pretreatment with olaparib (Fig. S3A,B). Consistently, PiER of all biopsies from CRPC clearly increased above the threshold, again with minor alterations between both DSB markers (Fig. 5B). Similar results were obtained using cisplatin (Fig. S3A,B, Fig. 5C). Together these findings reveal the plausibility of the preclinical models of CRPC to

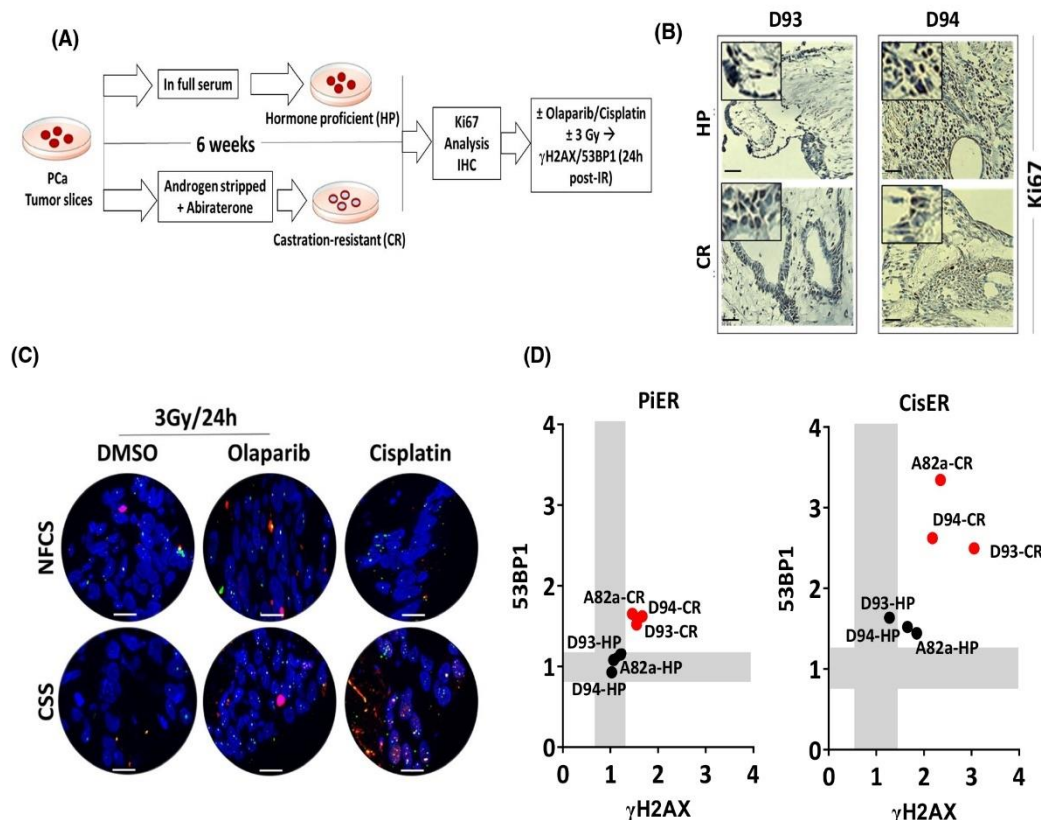


Fig. 4. *Ex vivo* induction of castration resistance in prostate cancer increases cytotoxicity to olaparib and cisplatin via impairing double strand break repair efficiency. (A) Schematic representation of castration resistance induction in *ex vivo* cultures of prostate cancer (PCa) specimens which had shown no signs of castration resistance *in vivo*. Briefly, PCa slices were cultured for up to 6 weeks in either androgen-stripped serum containing medium in the presence of abiraterone (10 μ M) or in full serum containing medium. Ki67 expression was monitored by immunohistochemical staining. Only tumor slices showing a similar Ki67 index under castration resistance culturing conditions were included in the next experiments. (B) Representative images of Ki67 staining (Scale bar: 100 μ m) in two tumor slices from two PCa patients (D93 and D94) cultured under hormone-proficient (HP) or castration resistance-inducing (CR) conditions. High magnification images (magnification, 80 \times) of ROI are shown. (C) Representative micrographs of γ H2AX (red) and 53BP1 (green) foci 24 h after treatment with olaparib plus 3 Gy or cisplatin alone in PCa slices from patient #D93. Scale bar: 100 μ m. (D) Plots showing the correlation between PARP inhibitor (PARPi) enhancement ratio (PIER, left panel) or cisplatin enhancement ratio (CisER, right panel) of residual γ H2AX (X-axis) and 53BP1 (Y-axis) at 24 h post treatment; three independent experiments for each tumor slice. Black and red dots represent tumor slices cultured under hormone-proficient and castration resistance conditions, respectively.

detect DSB repair defect, sensitivity to cisplatin and radiosensitization effect of olaparib.

3.6. Establishment and characterization of patient-derived organoids cultures from PCa patients

Twelve long-term PDO cultures from four naïve and four CRPC patients were established using a modified protocol from Gao et al. [30]. We obtained a success rate of more than 60%. All established PDOs were successfully expanded and maintained under the same

culturing conditions for > 12 passages with no obvious morphological changes (data not shown) and were frozen down to create an organoid biobank. Clinical information and pathological parameters showed similarities between the established patient-derived organoids and their donors (Table S2). The histological features of each of the established PDOs were of similar appearance to their matched primary tumors (Fig. 6A), with a strong AMCAR immunohistochemistry staining (Fig. 6A). We also evaluated CpG-rich methylation in PDOs on a genome-wide scale using Illumina HumanMethylation450 Bead Chip (450 K) arrays [46]. The

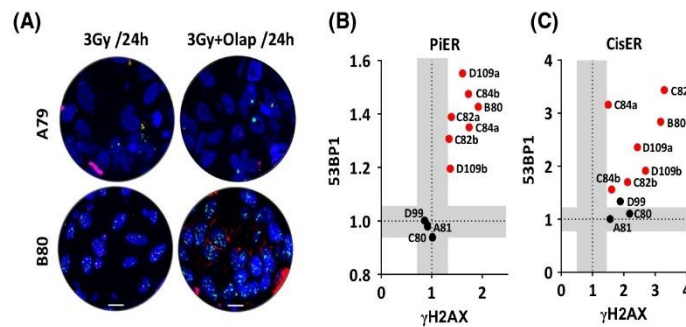


Fig. 5. Olaparib or cisplatin increases cytotoxic effects of IR in castration-resistant PCa. (A) Representative micrographs of γ H2AX (red) and 53BP1 (green) foci 24 h after treatment with olaparib plus 3 Gy in tumor biopsies from a castration-resistant PCa patient #B80. Scale bar: 100 μ m. (B) PIER of residual γ H2AX (X-axis) and 53BP1 (Y-axis) foci at 24 h post 3 Gy. (C) Cisplatin-enhancement ratio (CisER) of residual γ H2AX (X-axis) and 53BP1 (Y-axis) at 24 h. Shown are mean \pm SEM of three independent experiments. Black and red dots represent data from hormone naïve and castration-resistant PCa, respectively.

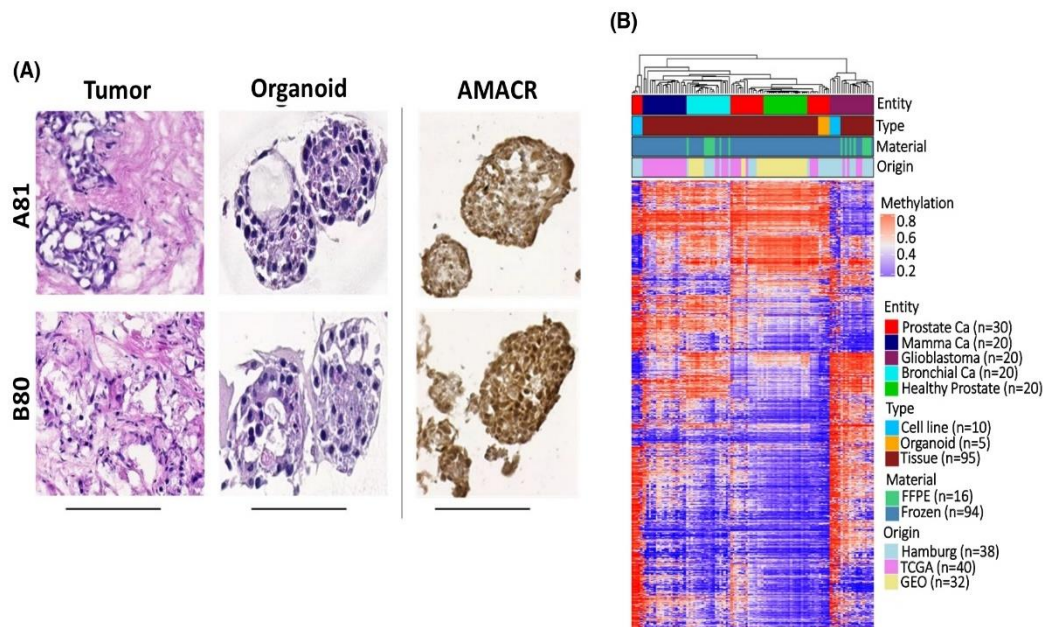


Fig. 6. Establishment and characterization of patient-derived organoid cultures from prostate cancer (PCa) patients. (A) Representative images of the established organoids and their corresponding primary tumors with H&E and immunohistochemical staining for AMACR. Scale bar: 50 μ m. (B) Genome-wide DNA methylation cluster analysis of the established organoids showing clustering with PCa but not with normal prostate or other tumor entities using a cohort of 110 samples.

PDOs models were found to cluster with PCa but not with normal prostate or other tumor entities based on DNA methylation profiling (Fig. 6B). Interestingly, the methylation profile of the PDOs did not cluster with that of the established cell lines, indicating that the PDOs more appropriately represent the patients' *in vivo* tumor. Altogether, this confirms that the established PDOs represent the PCa *in vivo* and can therefore serve as preclinical models for PCa research.

3.7. Olaparib and cisplatin are more toxic for organoids established from CRPC than hormone naïve patients

The advantage of using PDOs as preclinical models is that they not only allow DSB repair monitoring but also enable the analysis of the effect of olaparib or cisplatin on clonogenic survival by colony formation assay. Briefly, PDOs were treated with different

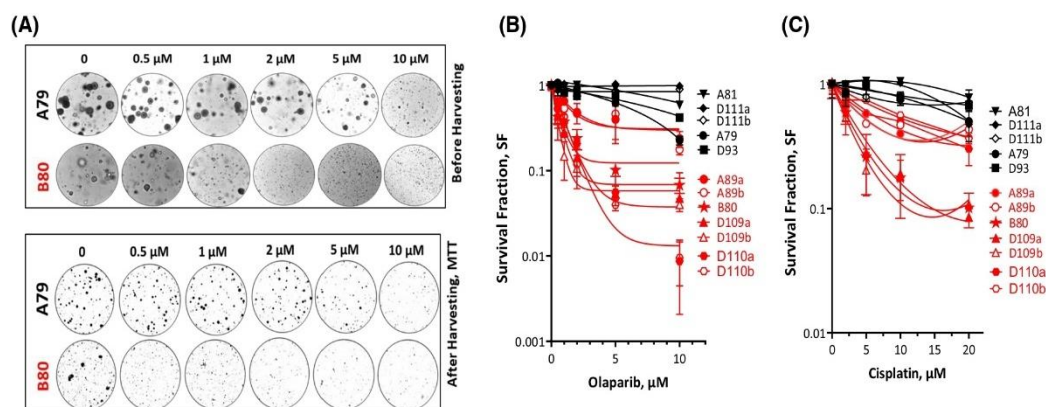


Fig. 7. Olaparib is more toxic for castration-resistant organoids than for the hormone-sensitive PCa organoids. (A) Representative images of organoid cultures of a hormone naïve (A79) and castration-resistant (B80) PCa organoid treated with the indicated concentrations of olaparib before (upper panel) and after (lower panel) harvesting and staining with MTT. (B,C) Survival fractions measured by colony forming assay after treatment of organoids established from hormone naïve (black) or castration-resistant (red) PCa patients with different concentrations of olaparib (B) or cisplatin (C). Shown are means \pm SEM of four independent experiments (except for hormone naïve patients, where $n = 3$).

concentrations of either olaparib (0, 0.5, 1, 2, 5 and 10 μM) or cisplatin (0, 2, 5 10 and 20 μM) and CFA was used to quantify the survival fractions in 3D settings. To ensure the better visualization and counting of living cells, MTT was used to stain living cells within individual organoids pre-harvesting (Fig. 7A). Compared with hormone-sensitive ones, CRPC organoids were found to be clearly more sensitive to olaparib (Fig. 7B) and cisplatin (Fig. 7C), which indeed rationalizes the use of either olaparib or cisplatin as effective drugs in CRPC patients.

3.8. Enhanced pro-metastatic signaling and migration in castration-resistant cells

To date, metastatic CRPC remains incurable and the prognosis for these patients is poor. Therefore, it is important to have preclinical models to facilitate the identification of other treatment options for this disease setting. RNA-SEQ analysis revealed more than 2000 upregulated genes in pooled castration-resistant LNCaP sublines compared with the parental LNCaP cells (Fig. 2A). Interestingly, when gene ontology analysis was performed (Fig. 8A), we found that despite the fact that LNCaP cells were originally established from metastatic PCa, the most differentially upregulated molecular pathways in the resistant sublines were those related to metastatic progress, dissemination, including ECM receptor interaction, focal and cell adhesion molecules. This indicates that the metastatic potential might be further stimulated in the CR sublines. To investigate this issue, we monitored the ability of castration-

resistant clones to scatter outside the clones using a cell scattering assay. As illustrated in Fig. 8B, compared with the parental LNCaP cells, LNCaP-ARN509, LNCaP-abi and LNCaP-abl cells displayed the typical scattering phenotype characterized by the loss of cell-to-cell contacts and drastic cellular elongation in both 2D and 3D culture settings. In contrast, DU145 cells, which are known to have a lower metastatic potential, showed no signs of cell scattering. Analysis of cell migration – an integral part of the metastatic cascade – using a chamber assay confirmed the enhanced invasive properties in the castration-resistant LNCaP-ARN509 cells compared with their hormone-sensitive parental LNCaP cells as evidenced by a significantly higher number (two-fold) of migrating cells in LNCaP-ARN509 (346 ± 50.7 vs. 724.3 ± 188.4 migrated cells per field, $P = 0.01$). Interestingly, pretreatment with 1 μM olaparib significantly decreased the migrating cells both in LNCaP and LNCaP-ARN509 castration-resistant cells ($P = 0.001$) (Fig. 8C,D). In contrast, pretreatment with 2 μM cisplatin failed to reduce migration in LNCaP-ARN509 cells. Notably, no change was seen in the proliferation or growth rate upon treatment with either olaparib or cisplatin for the entire 36 h of this experiment in either LNCaP or LNCaP-ARN509 cells (Fig. S4). Together, these data reflect the ability of olaparib but not cisplatin to inhibit the metastatic behavior of CRPC cells.

4. Discussion

Compared with other tumor entities, translational research in PCa has lagged behind due to a lack of

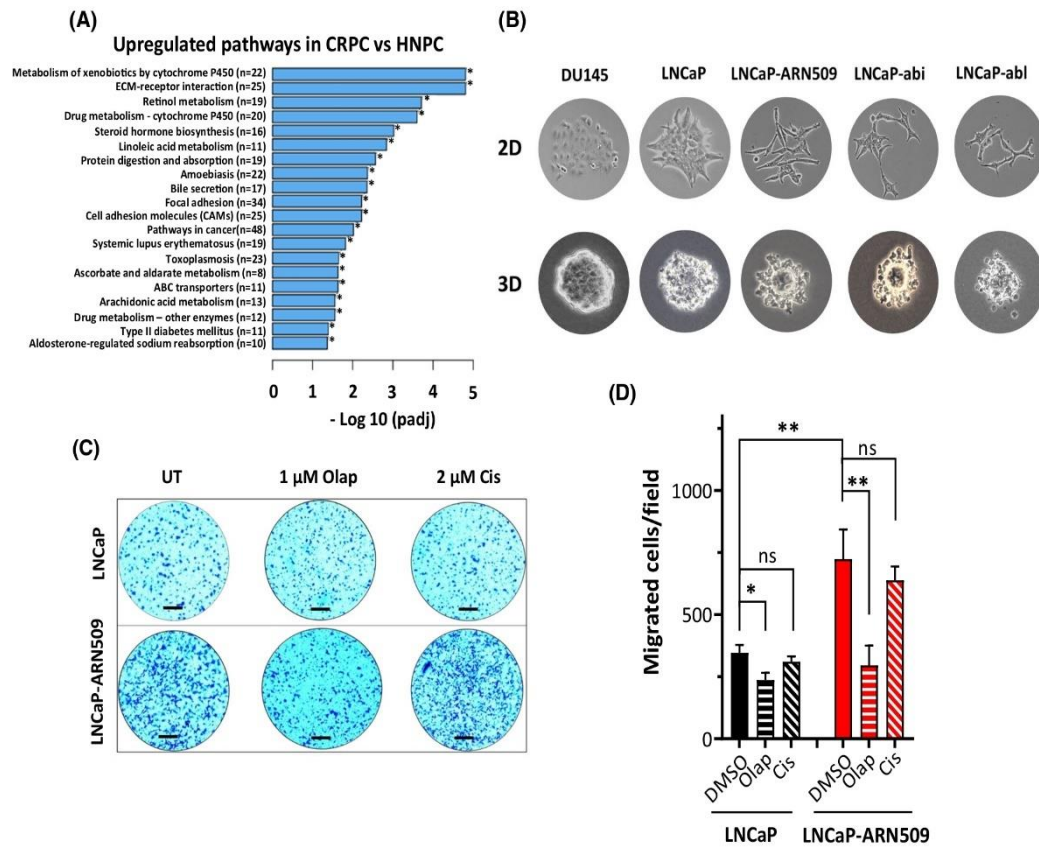


Fig. 8. Pro-metastatic pathways and migration are enhanced in castration-resistant cells. (A) Gene ontology enrichment analysis of the significantly upregulated pathways [$-\log_{10}$ (adjusted P -value)] in castration-resistant cells showing upregulation in pro-metastatic pathways. Significance: $*P < 0.05$. (B) Cell colony scattering assays were performed with the indicated cells by seeding cells at a low density and allowing them to form colonies in 2D or 3D cultures. Light microscopy images of the colonies were taken at random for each cell line. (C) Transwell migration assay: representative microscopic images of the indicated cells that migrated through the Transwell in the migration assay after treatment with 1 μ M olaparib or 2 μ M cisplatin for 36 h. UT, untreated control. Crystal violet was used to visualize cells. Scale bar: 200 μ m. (D) Quantification of the experiments performed in (C). Shown are means \pm SEM of four independent experiments ($n = 3$ for cis). Significance was calculated using the Mann-Whitney U -test: $*P < 0.05$, $**P < 0.01$ vs. control. ns, not significant.

appropriate preclinical models. Few preclinical models accurately reflect the clinical and molecular variability seen in PCa patients, impeding the rational development of molecularly derived tailored treatment options. The techniques and models described in the current study are essential tools not only for bolstering the understanding of the drivers behind oncogenesis and how this affects the clinical course, but also to provide a rationale for alternative therapeutic targets for individual PCa patients.

Among the commonly used human PCa cancer models are cancer cell lines that are established from cancer patients. However, these do not represent PCa *in vivo*. Here we employed our previously reported CRPC-induced sublines from the hormone-sensitive

PCa cell line LNCaP [31] and revealed compromised DSB repair efficiency and increased radiosensitivity in the hormone-resistant clones than in the parental cells. WGS analysis did not show any evidence of genetic mutations in DSB genes. RNA-SEQ demonstrated a different transcriptome in CRPC sublines with decreased expression of several HRR-related genes such as *RAD51*. A lower *RAD51* protein expression was also reported in the CRPC cells, resulting in HRR deficiency. In line with this finding, *RAD51* foci recruitment at IR-induced DSB sites was decreased twofold in CR sublines. These data pinpoint the HRR deregulation in CRPC and rationalize the use of PARPi for this subtype of the disease. In fact, the efficacy of different PARPi has been or is being tested for

the treatment of mCRPC patients in several clinical trials. Most of these studies revealed that PARPi significantly improve tumor response in terms of disease control and overall survival for mCRPC patients with HRR mutations. Recently, nine clinical trials using PARPi in mCRPC have been analyzed in a meta-analysis to test the benefit of PARPi in mCRPC patients [47]. The trials demonstrated that the magnitude of benefits from PARPi varies greatly between different HR-defect subgroups, showing the most vigorous efficacy for PARPi in BRCA-mutation carriers compared with patients who harbored no BRCA mutations. Furthermore, this analysis reported that BRCA2 mutations are likely the most effective mutations that predict the response to PARPi in PCa. Interestingly, a significant benefit in BRCA wild-type tumors was observed, supporting the view that besides BRCA mutations, other non-BRCA HRR-related gene aberrations may also be used to predict the antitumor activity of PARPi. Hence, only using BRCA mutational status as a marker for PARPi sensitivity is inadequate, and it may miss a potentially larger proportion of responding patients. Following large-scale cancer sequence analysis, mutations in other HR-related genes such as CDK12, ATM and PALB2 were commonly found in mCRPC [11,48,49], and these non-BRCA DNA repair genes could be used as alternative biomarkers to predict the sensitivity of PARPi. TOPARP-A and B clinical studies by Mateo et al. [50,51] provided evidence that mCRPC patients with other mutations in genes related to the HRR machinery also appear to benefit from PARP inhibitors.

A deep sequencing of all PCa patients would facilitate identifying the common genetic alterations with HRR to predict the benefit from PARPi. Despite the latest advances in the field of large-scale sequencing analysis, it is still difficult to apply it in regular routine clinical work, as it is very costly and more importantly requires a previous knowledge about the role of each gene in HRR. In fact, there is only limited knowledge of the functional consequences of these mutations on HRR. Moreover, it is ultimately unclear why alterations in the same gene lead to a therapy response in one patient but not in another.

Here we present, in addition to the aforementioned *in vitro* cell lines, *ex vivo* preclinical models (*ex vivo* tumor slice and organoid cultures) that may help in detecting functional HRR defects to predict the response to PARPi. Furthermore, we present the rationale for the use of platinum-based therapy such as cisplatin, which so far has not been routinely used in the treatment of CRPC but which has been reported to have some activity, especially in patients harboring

HRR defects. This is in line with the previously published multicenter retrospective analysis showing anti-tumor activity for treatment with platinum-based therapies in the cohort of CRPC patients with tumors harboring DNA repair gene aberrations [52]. Importantly, we believe that this is the first work that shows that olaparib but not cisplatin is able to impair the metastatic potential of PCa. Previously, we reported a functional *ex vivo* assay that enables the analysis of DSB formation and repair directly in tumor slice cultures from individual PCa patients [21]. Compared with tumor slices from HSPC patients, we clearly demonstrated here, in the CRPC slice cultures, an increase in the number of residual and thus unrepaired IR-induced γ H2AX and 53BP1 foci upon pretreatment with olaparib or cisplatin as evidenced by increased PiER and CisER indices, respectively. This was further confirmed using a modified approach to induce a CR phenotype through growing hormone-sensitive tumor sample slices for several weeks in androgen-depleted medium supplemented with CSS and abiraterone. Of note, there are some concerns about the applicability of the CR-induction *ex vivo* approach in the clinical settings because of the relatively limited success rate in inducing CR (< 40% in our study) and the uncertainty as to whether the CR induction process represents the *in vivo* situation. Despite these concerns, this model confirmed the benefits of olaparib in patients pretreated with anti-hormone therapy, especially abiraterone, which is in line with the results from the PROpel phase III study showing prolonged progression-free survival for olaparib + abiraterone compared with abiraterone alone, irrespective of HRR status [53]. As a patient-derived preclinical model, we further present here a very robust protocol for establishing organoids from PCa patients. Attempts to establish PCa organoids have been performed by other laboratories, but with lower overall success rates for longer/indefinite propagation and expansion. We could increase the success rate for the establishment of PCa organoids to 60–70% irrespective of hormone sensitivity state (HSPC and CRPC). This increased rate could be attributed to several factors such as ROCK inhibitor and epithelial growth factors, which enable the cells to adapt very quickly/more efficiently from tissue to culture conditions without inducing senescence as previously described in many studies [25,26,30]. Another explanation for our high success rate might be the efficient logistics, which enables the timely transport of freshly collected samples immediately from the operating theater to the lab, avoiding delays which may affect the efficiency of the lab-based organoid formation. Tumor cell content has been confirmed in our

established PCa PDO cultures by histopathological analysis. Also, PDOs have consistent IHC-positive staining of the well-established tumor marker AMACR and show histological similarities to their original primary tumors. In addition, evaluation of CpG-rich global methylation revealed clustering of the organoids with other *in vivo* PCa datasets but not with other tumor entities or with normal prostate tissues. Given that PDOs enable the measurement of the direct effect on survival fractions, we demonstrated the increased sensitivity of CRPC organoids to olaparib or cisplatin compared with the organoids established from HSPC patients. Together, these data confirm a HRR-deficient state of CRPC patients irrespective of distinct genomic alternations in known key players of HRR. It is important to note, however, that there is still space for future improvement for the PDO system presented here. For example, it is important to establish conditions that allow the establishment of micro-environmental elements such as blood vessels, immune cells and other stroma cells.

5. Conclusion

In conclusion, we present reliable preclinical models that allow for rapid functional testing and comparison of multiple individual drugs prior to *in vivo* analysis for example testing the presence of HRR deficiency in CRPC and response prediction to olaparib or cisplatin. This individual assessment of HRR functional capacity will enable us to improve future patient selection for personalized treatment approaches and thus increase the likelihood of response to PARP inhibitor therapy.

Acknowledgements

This work was supported by BMBF grants 02NUK032 & 02NUK035B, the German Academic Exchange Service (DAAD) and Milderd-Scheel Cancer Career Center, HaTRiCs4 program.

Conflict of interest

The authors declare no conflict of interest.

Author contributions

ME and WM designed the study concept and the experiments and wrote the paper. GvA, SJO-H, CO, TM, AE, US, CP and KR collected and analyzed the clinical data. AE and US examined the methylome and performed the corresponding analysis; CM and MA performed the bioinformatics for WGS and

RNA-SEQ. SB-R performed the pathological analyses of tumor and organoid samples SJO-H provided drug-resistant cell lines. ME and WM did artwork. All authors reviewed and edited the paper and have approved its final version.

Peer review

The peer review history for this article is available at <https://publons.com/publon/10.1002/1878-0261.13382>.

Data accessibility

Sequence data have been deposited in the European Nucleotide Archive (ENA) at EMBL-EBI under accession number PRJEB55017 (<https://www.ebi.ac.uk/ena/browser/view/PRJEB55017>). Generated raw data supporting the findings of this study are available from the corresponding author (WM) on request.

References

- Bray F, Ferlay J, Soerjomataram I, Siegel RL, Torre LA, Jemal A. Global cancer statistics 2018: GLOBOCAN estimates of incidence and mortality worldwide for 36 cancers in 185 countries. *CA Cancer J Clin*. 2018;**68**:394–424. <https://doi.org/10.3322/caac.21492>
- Sayegh N, Swami U, Agarwal N. Recent advances in the management of metastatic prostate cancer. *JCO Oncol Pract*. 2022;**18**:45–55. <https://doi.org/10.1200/op.21.00206>
- Finianos A, Gupta K, Clark B, Simmens SJ, Aragon-Ching JB. Characterization of differences between prostate cancer patients presenting with de novo versus primary progressive metastatic disease. *Clin Genitourin Cancer*. 2017;**16**:85–9. <https://doi.org/10.1016/j.clgc.2017.08.006>
- Grasso CS, Wu YM, Robinson DR, Cao X, Dhanasekaran SM, Khan AP, et al. The mutational landscape of lethal castration-resistant prostate cancer. *Nature*. 2012;**487**:239–43. <https://doi.org/10.1038/nature11125>
- Harris WP, Mostaghel EA, Nelson PS, Montgomery B. Androgen deprivation therapy: progress in understanding mechanisms of resistance and optimizing androgen depletion. *Nat Clin Pract Urol*. 2009;**6**:76–85. <https://doi.org/10.1038/nepuro1296>
- Marques RB, Dits NF, Erkens-Schulze S, van Weerden WM, Jenster G. Bypass mechanisms of the androgen receptor pathway in therapy-resistant prostate cancer cell models. *PLoS One*. 2010;**5**:e13500. <https://doi.org/10.1371/journal.pone.0013500>
- Sun S, Sprenger CC, Vessella RL, Haugk K, Soriano K, Mostaghel EA, et al. Castration resistance in human

- prostate cancer is conferred by a frequently occurring androgen receptor splice variant. *J Clin Invest.* 2010;**120**:2715–30. <https://doi.org/10.1172/jci41824>
- 8 Ruch JM, Hussain MH. Evolving therapeutic paradigms for advanced prostate cancer. *Oncolo Gy (Williston Park).* 2011;**25**(496–504):508.
 - 9 Beltran H, Yelensky R, Frampton GM, Park K, Downing SR, MacDonald TY, et al. Targeted next-generation sequencing of advanced prostate cancer identifies potential therapeutic targets and disease heterogeneity. *Eur Urol.* 2013;**63**:920–6. <https://doi.org/10.1016/j.eururo.2012.08.053>
 - 10 Leongamornlert D, Mahmud N, Tymrakiewicz M, Saunders E, Dadaev T, Castro E, et al. Germline BRCA1 mutations increase prostate cancer risk. *Br J Cancer.* 2012;**106**:1697–701. <https://doi.org/10.1038/bjc.2012.146>
 - 11 Robinson D, Van Allen EM, Wu YM, Schultz N, Lonigro RJ, Mosquera JM, et al. Integrative clinical genomics of advanced prostate cancer. *Cell.* 2015;**161**:1215–28. <https://doi.org/10.1016/j.cell.2015.05.001>
 - 12 De Bono JS, Matsubara N, Penel N, Mehra N, Kolinsky MP, Bompas E, et al. Exploratory gene-by-gene analysis of olaparib in patients (pts) with metastatic castration-resistant prostate cancer (mCRPC): PROfound. *J Clin Oncol.* 2021;**39**:126–6. https://doi.org/10.1200/JCO.2021.39.6_suppl.126
 - 13 Hussain M, Mateo J, Fizazi K, Saad F, Shore N, Sandhu S, et al. Survival with olaparib in metastatic castration-resistant prostate cancer. *N Engl J Med.* 2020;**383**:2345–57. <https://doi.org/10.1056/NEJMoa2022485>
 - 14 Chi KN, Rathkopf DE, Smith MR, Efsthathiou E, Attard G, Olmos D, et al. Phase 3 MAGNITUDE study: first results of niraparib (NIRA) with abiraterone acetate and prednisone (AAP) as first-line therapy in patients (pts) with metastatic castration-resistant prostate cancer (mCRPC) with and without homologous recombination repair (HRR) gene alterations. *J Clin Oncol.* 2022;**40**:12–2. https://doi.org/10.1200/JCO.2022.40.6_suppl.012
 - 15 Clarke Noel W, Armstrong Andrew J, Thierry-Vuillemin A, Oya M, Shore N, Loreda E, et al. Abiraterone and olaparib for metastatic castration-resistant prostate cancer. *NEJM Evid.* 2022;**1**:EVIDoa2200043. <https://doi.org/10.1056/EVIDoa2200043>
 - 16 Sobel RE, Sadar MD. Cell lines used in prostate cancer research: a compendium of old and new lines--part 1. *J Urol.* 2005;**173**:342–59. <https://doi.org/10.1097/01.ju.0000141580.30910.57>
 - 17 Sobel RE, Sadar MD. Cell lines used in prostate cancer research: a compendium of old and new lines--part 2. *J Urol.* 2005;**173**:360–72. <https://doi.org/10.1097/01.ju.0000149989.01263.dc>
 - 18 Arriaga JM, Abate-Shen C. Genetically engineered mouse models of prostate cancer in the postgenomic era. *Cold Spring Harb Perspect Med.* 2019;**9**:a030528. <https://doi.org/10.1101/cshperspect.a030528>
 - 19 Zhang M, Lin YH, Sun YJ, Zhu S, Zheng J, Liu K, et al. Pharmacological reprogramming of fibroblasts into neural stem cells by signaling-directed transcriptional activation. *Cell Stem Cell.* 2016;**18**:653–67. <https://doi.org/10.1016/j.stem.2016.03.020>
 - 20 De-Colle C, Yaromina A, Hennenlotter J, Thames H, Mueller AC, Neumann T, et al. Ex vivo gammaH2AX radiation sensitivity assay in prostate cancer: inter-patient and intra-patient heterogeneity. *Radiother Oncol.* 2017;**124**:386–94. <https://doi.org/10.1016/j.radonc.2017.08.020>
 - 21 Kocher S, Beyer B, Lange T, Nordquist L, Volquardsen J, Burdak-Rothkamm S, et al. A functional ex vivo assay to detect PARP1-EJ repair and radiosensitization by PARP-inhibitor in prostate cancer. *Int J Cancer.* 2019;**144**:1685–96. <https://doi.org/10.1002/ijc.32018>
 - 22 Menegakis A, De Colle C, Yaromina A, Hennenlotter J, Stenzl A, Scharpf M, et al. Residual gammaH2AX foci after ex vivo irradiation of patient samples with known tumour-type specific differences in radio-responsiveness. *Radiother Oncol.* 2015;**116**:480–5. <https://doi.org/10.1016/j.radonc.2015.08.006>
 - 23 Menegakis A, von Neubeck C, Yaromina A, Thames H, Hering S, Hennenlotter J, et al. gammaH2AX assay in ex vivo irradiated tumour specimens: a novel method to determine tumour radiation sensitivity in patient-derived material. *Radiother Oncol.* 2015;**116**:473–9. <https://doi.org/10.1016/j.radonc.2015.03.026>
 - 24 Drost J, Clevers H. Organoids in cancer research. *Nat Rev Cancer.* 2018;**18**:407–18. <https://doi.org/10.1038/s41568-018-0007-6>
 - 25 Drost J, Karthaus WR, Gao D, Driehuis E, Sawyers CL, Chen Y, et al. Organoid culture systems for prostate epithelial and cancer tissue. *Nat Protoc.* 2016;**11**:347–58. <https://doi.org/10.1038/nprot.2016.006>
 - 26 Elbadawy M, Abugomaa A, Yamawaki H, Usui T, Sasaki K. Development of prostate cancer organoid culture models in basic medicine and translational research. *Cancers (Basel).* 2020;**12**:777. <https://doi.org/10.3390/cancers12040777>
 - 27 Gleave AM, Ci X, Lin D, Wang Y. A synopsis of prostate organoid methodologies, applications, and limitations. *Prostate.* 2020;**80**:518–26. <https://doi.org/10.1002/pros.23966>
 - 28 Puca L, Bareja R, Prandi D, Shaw R, Benelli M, Karthaus WR, et al. Patient derived organoids to model rare prostate cancer phenotypes. *Nat Commun.* 2018;**9**:2404. <https://doi.org/10.1038/s41467-018-04495-z>
 - 29 Richards Z, McCray T, Marsili J, Zenner ML, Manlucu JT, Garcia J, et al. Prostate stroma increases

- the viability and maintains the branching phenotype of human prostate organoids. *iScience*. 2019;**12**:304–17. <https://doi.org/10.1016/j.isci.2019.01.028>
- 30 Gao D, Vela I, Sboner A, Iaquina PJ, Karthaus WR, Gopalan A, et al. Organoid cultures derived from patients with advanced prostate cancer. *Cell*. 2014;**159**:176–87. <https://doi.org/10.1016/j.cell.2014.08.016>
 - 31 Elsesy ME, Oh-Hohenhorst SJ, Löser A, Oing C, Mutiara S, Köcher S, et al. Second-generation antiandrogen therapy radiosensitizes prostate cancer regardless of castration state through inhibition of DNA double Strand break repair. *Cancers (Basel)*. 2020;**12**:2467. <https://doi.org/10.3390/cancers12092467>
 - 32 Culig Z, Hoffmann J, Erdel M, Eder IE, Hobisch A, Hittmair A, et al. Switch from antagonist to agonist of the androgen receptor bicalutamide is associated with prostate tumour progression in a new model system. *Br J Cancer*. 1999;**81**:242–51. <https://doi.org/10.1038/sj.bjc.6690684>
 - 33 Bakr A, Oing C, Kocher S, Borgmann K, Dornreiter I, Petersen C, et al. Involvement of ATM in homologous recombination after end resection and RAD51 nucleofilament formation. *Nucleic Acids Res*. 2015;**43**:3154–66. <https://doi.org/10.1093/nar/gkv160>
 - 34 Kasten U, Borgmann K, Burgmann P, Li G, Dikomey E. Overexpression of human Ku70/Ku80 in rat cells resulting in reduced DSB repair capacity with appropriate increase in cell radiosensitivity but with no effect on cell recovery. *Radiat Res*. 1999;**151**:532–9.
 - 35 Li H, Durbin R. Fast and accurate long-read alignment with burrows-wheeler transform. *Bioinformatics*. 2010;**26**:589–95. <https://doi.org/10.1093/bioinformatics/btp698>
 - 36 Chen X, Schulz-Trieglaff O, Shaw R, Barnes B, Schlesinger F, Källberg M, et al. Manta: rapid detection of structural variants and indels for germline and cancer sequencing applications. *Bioinformatics*. 2016;**32**:1220–2. <https://doi.org/10.1093/bioinformatics/btv710>
 - 37 Kim S, Scheffler K, Halpern AL, Bekritsky MA, Noh E, Källberg M, et al. Strelka2: fast and accurate calling of germline and somatic variants. *Nat Methods*. 2018;**15**:591–4. <https://doi.org/10.1038/s41592-018-0051-x>
 - 38 Bergstrom EN, Huang MN, Mahto U, Barnes M, Stratton MR, Rozen SG, et al. SigProfilerMatrixGenerator: a tool for visualizing and exploring patterns of small mutational events. *BMC Genomics*. 2019;**20**:685. <https://doi.org/10.1186/s12864-019-6041-2>
 - 39 Kautto EA, Bonneville R, Miya J, Yu L, Krook MA, Reeser JW, et al. Performance evaluation for rapid detection of pan-cancer microsatellite instability with MANTIS. *Oncotarget*. 2017;**8**:7452–63. <https://doi.org/10.18632/oncotarget.13918>
 - 40 Davies H, Glodzik D, Morganella S, Yates LR, Staaf J, Zou X, et al. HRDetect is a predictor of BRCA1 and BRCA2 deficiency based on mutational signatures. *Nat Med*. 2017;**23**:517–25. <https://doi.org/10.1038/nm.4292>
 - 41 Degasperi A, Amarante TD, Czarnecki J, Shooter S, Zou X, Glodzik D, et al. A practical framework and online tool for mutational signature analyses show inter-tissue variation and driver dependencies. *Nat Cancer*. 2020;**1**:249–63. <https://doi.org/10.1038/s43018-020-0027-5>
 - 42 Dobin A, Davis CA, Schlesinger F, Drenkow J, Zaleski C, Jha S, et al. STAR: ultrafast universal RNA-seq aligner. *Bioinformatics*. 2013;**29**:15–21. <https://doi.org/10.1093/bioinformatics/bts635>
 - 43 Robinson MD, McCarthy DJ, Smyth GK. edgeR: a Bioconductor package for differential expression analysis of digital gene expression data. *Bioinformatics*. 2010;**26**:139–40. <https://doi.org/10.1093/bioinformatics/btp616>
 - 44 Yu G, Wang LG, Han Y, He QY. clusterProfiler: an R package for comparing biological themes among gene clusters. *Omic*. 2012;**16**:284–7. <https://doi.org/10.1089/omi.2011.0118>
 - 45 Dikomey E, Borgmann K, Brammer I, Kasten-Pisula U. Molecular mechanisms of individual radiosensitivity studied in normal diploid human fibroblasts. *Toxicolo Gy*. 2003;**193**:125–35.
 - 46 Capper D, Jones DTW, Sill M, Hovestadt V, Schrimpf D, Sturm D, et al. DNA methylation-based classification of central nervous system tumours. *Nature*. 2018;**555**:469–74. <https://doi.org/10.1038/nature26000>
 - 47 Wu K, Liang J, Shao Y, Xiong S, Feng S, Li X. Evaluation of the efficacy of PARP inhibitors in metastatic castration-resistant prostate cancer: a systematic review and meta-analysis. *Front Pharmacol*. 2021;**12**:777663. <https://doi.org/10.3389/fphar.2021.777663>
 - 48 The molecular taxonomy of primary prostate cancer. *Cell*. 2015;**163**:1011–25. <https://doi.org/10.1016/j.cell.2015.10.025>
 - 49 Pritchard CC, Mateo J, Walsh MF, De Sarkar N, Abida W, Beltran H, et al. Inherited DNA-repair gene mutations in men with metastatic prostate cancer. *N Engl J Med*. 2016;**375**:443–53. <https://doi.org/10.1056/NEJMoa1603144>
 - 50 Mateo J, Carreira S, Sandhu S, Miranda S, Mossop H, Perez-Lopez R, et al. DNA-repair defects and olaparib in metastatic prostate cancer. *N Engl J Med*. 2015;**373**:1697–708. <https://doi.org/10.1056/NEJMoa1506859>

- 51 Mateo J, Porta N, Bianchini D, McGovern U, Elliott T, Jones R, et al. olaparib in patients with metastatic castration-resistant prostate cancer with DNA repair gene aberrations (TOPARP-B): a multicentre, open-label, randomised, phase 2 trial. *Lancet Oncol.* 2020;**21**:162–74. [https://doi.org/10.1016/s1470-2045\(19\)30684-9](https://doi.org/10.1016/s1470-2045(19)30684-9)
- 52 Schmid S, Omlin A, Higano C, Sweeney C, Martinez Chanza N, Mehra N, et al. Activity of platinum-based chemotherapy in patients with advanced prostate cancer with and without DNA repair gene aberrations. *JAMA Netw Open.* 2020;**3**:e2021692. <https://doi.org/10.1001/jamanetworkopen.2020.21692>
- 53 Saad F, Armstrong AJ, Thiery-Vuillemin A, Oya M, Loredó E, Procopio G, et al. PROpel: phase III trial of olaparib (Ola) and abiraterone (abi) versus placebo (pbo) and abi as first-line (1L) therapy for patients (pts) with metastatic castration-resistant prostate cancer (mCRPC). *J Clin Oncol.* 2022;**40**:11–1. https://doi.org/10.1200/JCO.2022.40.6_suppl.011

Supporting information

Additional supporting information may be found online in the Supporting Information section at the end of the article.

Fig. S1. Whole genome profile differences between castration-resistant cells and their parental sensitive counterpart LNCaP.

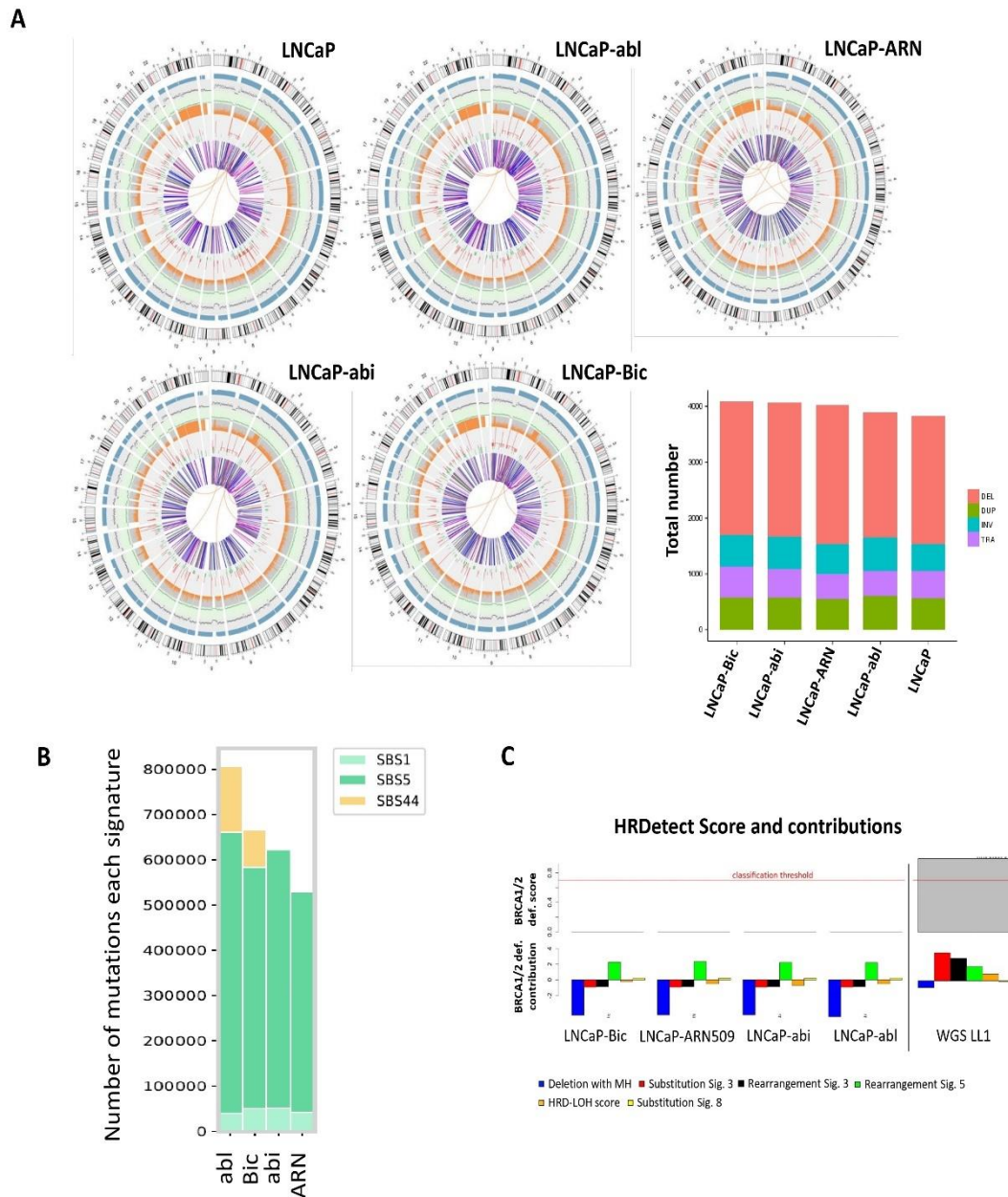
Fig. S2. Effect of olaparib or cisplatin on DSB-repair in CR-induced *ex vivo* PCa cultures.

Fig. S3. Effect of olaparib or cisplatin on DSB-repair in freshly collected tumor tissues from hormone naïve or castration-resistant PCa patients.

Fig. S4. Effect of 1 μ M olaparib or 2 μ M cisplatin on cell survival.

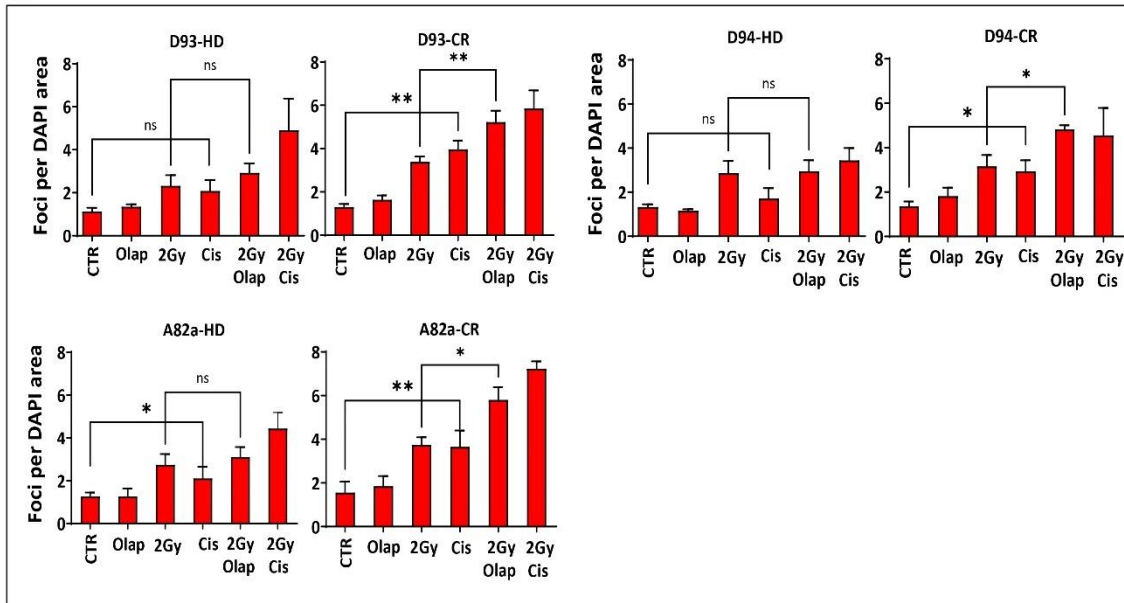
Table S1. Culture medium components for human prostate organoids.

Table S2. Clinical information and pathological parameters of donors for the established patient-derived organoids.

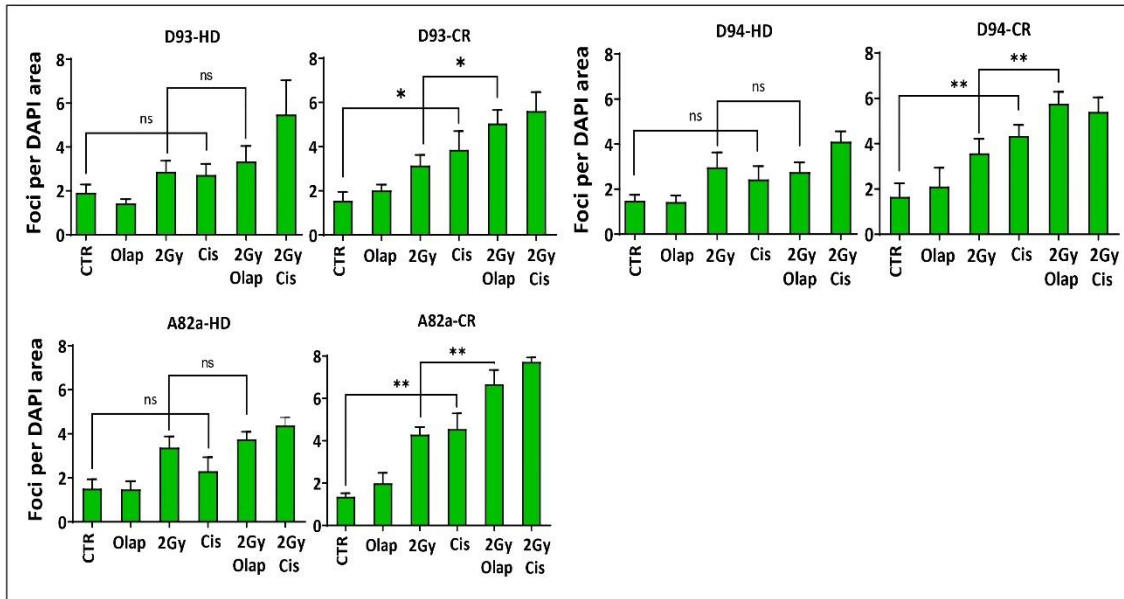


Supplementary Figure S1 Whole genome profile differences between Castration-resistant cells and their parental sensitive counterpart LNCaP. (A) Circos plots from outermost rings heading inwards: (i) The outer circle (the first circle) is chromosome information. (ii) The second ring represents the read coverage in histogram style. A histogram is the average coverage of a 0.5Mbp region. (iii) The third ring represents indel density in scatter style. A black dot is calculated as indel number in a range of 1Mbp. (iv) The fourth ring represents snp density in scatter style. A green dot is calculated as snp number in a range of 1Mbp. (v) The fifth ring represents the proportion of homozygous SNP (orange) and heterozygous SNP (grey) in histogram style. A histogram is calculated from a 1Mbp region. (vi) The sixth ring represents the CNV inference. Red means gain, and green means loss. (vii) The most central ring represents the SV inference in exonic and splicing regions. TRA (orange), INS (green), DEL (grey), DUP (pink) and INV (blue). The size of genomic regions affected by CNVs in each sample. The x-axis represents samples, and the y-axis represents the total size of genomic regions affected by gains or losses (Mb). (B) Different single base substitutions (SBS) reported in the indicated CR sublines compared to their parental naïve cell line. (C) HRDetect scores measured by the BRCAness probability score on the y-axis and contributions by different mutational signatures for CR sublines compared to their parental naïve cell line. Publicly available data from a breast cancer cell line (HCC1395, HCC1395BL) and a matched control from the same patient were used as a positive control (WGS LL1). Signatures contributing to the HRDetect score were proportion of deletions with microhomology (blue), number of SBS3 (red) and SBS8 (yellow) mutations, number of mutations for rearrangement signatures 3 (black) and 5 (green) and loss of heterozygosity score (orange). The contributions are the normalized values of the features multiplied for the corresponding HRDetect logistic model coefficient. A BRCAness probability score > 0.7 was used to identify HRD.

A

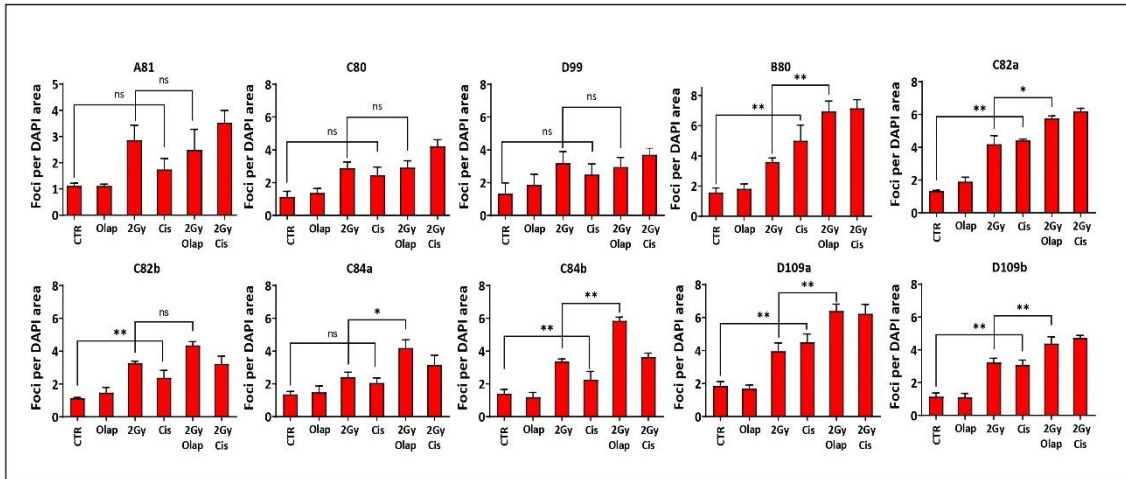


B

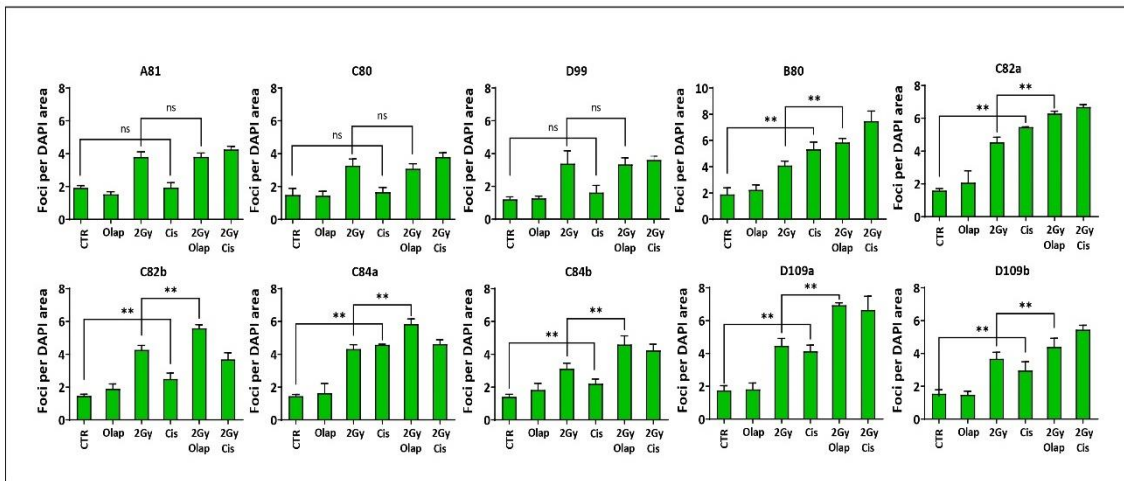


Supplementary Figure S2. Effect of Olaparib or Cisplatin on DSB-repair in CR-induced ex vivo PCa cultures. Number of (A) γ H2AX or (B) 53BP1 foci were monitored in tumor slices cultured under hormone-dependent (HD) or castration resistance (CR) conditions 24h after the indicated treatments. Shown are the means \pm SEM from at least three independent experiments. P-values were calculated using the Mann-Whitney U test. Significance is indicated as * for the $P < 0.05$, ** for $P < 0.001$ and ns: not significant.

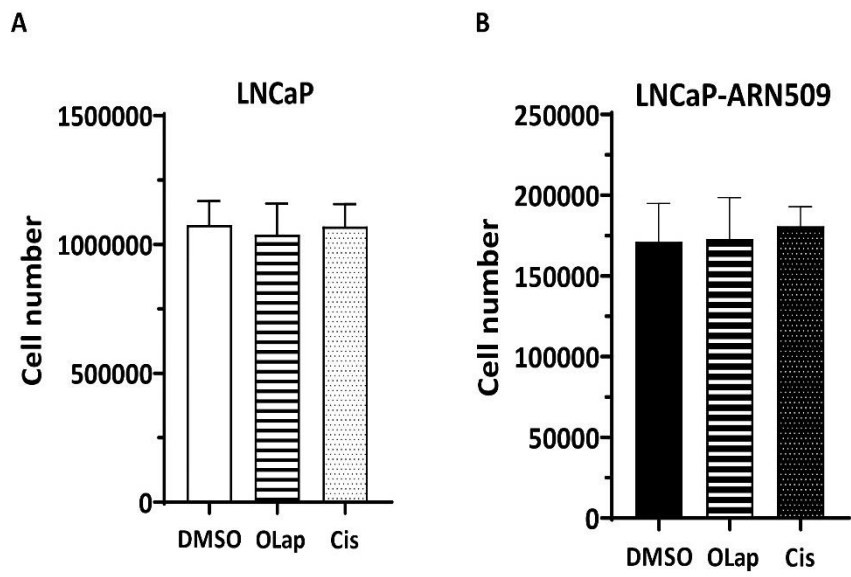
A



B



Supplementary Figure S3. Effect of Olaparib or Cisplatin on DSB-repair in freshly collected tumor tissues from hormone naïve or castration resistant PCa patients. Number of (A) γ -H2AX or (B) 53BP1 foci in tumor slices cultures 24h after the indicated treatments. Shown are the means \pm SEM from at least three independent experiments. P-values were calculated using the Mann-Whitney U test. Significance is indicated as * for the $P < 0.05$, ** for $P < 0.001$ and ns: not significant.



Supplementary Figure S4 Effect of 1 μ M Olaparib or 2 μ M cisplatin on cell survival. Cells were suspended in in FBS-free DMEM medium at concentrations of 2×10^5 cells for (A) LNCaP and (B) LNCaP-ARN509. Seeded cells were then treated with DMSO, 1 μ M Olaparib (olap) or 2 μ M cisplatin (cis) and incubated for 36h before being counted.

Table S1 Culture medium components for human prostate organoids

Compound	Supplier	Catalog #	Concentration
Glutamax	Thermo Sci	35050061	1x
HEPES	Thermo Sci	15630080	10 mM
Pen/Strep	Thermo Sci	15140122	1x
B27 supplement	Thermo Sci	17504044	1x
N-acetylcysteine	Sigma	A9165-5G	1.25 mM
EGF	PeproTech	AF-100-15	5 ng/mL
Noggin	PeproTech	120-10C	100 ng/mL
R-spondin 1	Conditioned medium		10%
A83-01	Sigma	SML0788	500 nM
FGF10	PeproTech	100-26	20 ng/mL
FGF-7 (KGF)	PeproTech	100-19	5 ng/mL
Prostaglandin E2	Sigma	P0409	1 μ M
Nicotinamide	Sigma	N0636	5 mM
SB202190	Sigma	S7067	500 nM
Y-27632 (ROCK inhibitor)	Miltenyi	130-106-538	10 μ M
DHT	Sigma	A8380	0.1nM for CRPC samples, 1nM for hormone-sensitive samples

Publication list

Table S2. Clinical information and pathologic parameters of donors for the established patient-derived organoids

Organoid ID	Age* (years)	iPSA (ng/ml)	Neoadj. ADT	Tumor stage	Lymph node invasion	Surgical margin	Gleason score		CRPC feature**
							1ry Tumor	Organoid	
A79	59	7.9	No	pT3b	pN1 (1/6)	positive	4+5	4+5	No
A81	54	7.48	Yes	pT3a	pN0 (0/8)	positive	3+4	4+4	No
A82	63	8.4	No	pT3a	pN1 (3/19)	negative	4+3 with minor 5		No
A89	63	53,6	Yes	pT3b	pN1 (8/36)	positive	5+4	4+5	Yes
B80	60	41.5	No	pT3b	pN0 (0/12)	positive	4+3	4+3	Yes
C80	57	29	Yes	pT3b	pN0 (0/23)	negative	3+4 with minor 5		No
C82	68	11.9	Yes	pT3b	pN1(1/8)	positive	4+5		Yes
C84	58	106	No	pT3b	pN1 (12/26)	positive	5+4		Yes
D93	63	10.0	No	pT2c	pN0 (0/18)	negative	3+4	4+4	No
D94	71	92.12	Yes	pT3b	pN1 (2/12)	negative	4+5 with minor 3		Less sensitive to LHRH, sensitive to apalutamid
D99	66	49.7	Yes	pT3b	pN1 (2/27)	negative	4+5		No
D109	69	9.1	Yes	pT3b	pN0 (0/22)	negative	4+5 with minor 3	4+5	Yes
D110	68	142	Yes	pT3b	pN0 (0/29),	negative	4+3 with minor 5	4+4	Yes
D111	73	76,3	Yes	pT3a	pN1 (1/19),	positive	5+4	4+5	Sensitive to apalutamid

All tumor tissues are adenocarcinoma. Highlighted are patients from which organoids were established. iPSA: initial PSA at the time of tumor diagnosis by biopsy. ADT: Androgen deprivation therapy. * at the time of surgery ** testosterone > 20 ng/dL (0.7 nmol/L), inadequate PSA decrease or rapid clinical progress under (neoadjuvant) ADT

5. Zusammenfassung

Trotz großer Fortschritte in der Behandlung des Prostatakarzinoms ist eine metastasierte Erkrankung weiterhin nicht heilbar und die Behandlungsoptionen im Stadium der Kastrationsresistenz begrenzt. Es besteht daher unmittelbarer Bedarf an neuen zielgerichteten Therapien, um die Behandlungsergebnisse und die Prognose zu verbessern. In der vorgestellten Arbeit haben wir zwei Strategien verfolgt, um die Behandlung des fortgeschrittenen Prostatakarzinoms zu verbessern.

Strategie 1:

Publizierte prä-klinische Studien zeigen einen Einfluss des Androgenrezeptor-Signalwegs auf die DNA-Reparatur-Maschinerie durch Regulation der Expression verschiedener DNA-Reparaturgene. Ionisierende Strahlen wirken zytotoxisch durch die Induktion von DNA-Doppelstrangbrüchen. Gegenstand der ersten Publikation (Elsesy et al., 2020) war die Untersuchung der Auswirkung einer ADT auf die Strahlensensibilität von Prostatakarzinomzellen. Wir konnten zeigen, dass Antiandrogene der zweiten Generation potente *Radiosensitizer* sind, die die Reparatur strahleninduzierter Doppelstrangbrüche hemmen und die Zytotoxizität der Bestrahlung verstärken. Dieses Ergebnis beruht auf folgenden Beobachtungen:

- Die Kombination aus Bestrahlung plus einem Zweitgenerationsantiandrogen, Abirateron Acetat, Apalutamid bzw. Enzalutamid, reduzierte das Zellwachstum und verlängerte die Verdopplungszeiten signifikant verglichen mit einer alleinigen Bestrahlung.
- Die Radiosensitivierung beruht auf einer Hemmung der DNA-Reparaturkapazität, was durch eine signifikante Erhöhung residueller γ H2AX/53BP1-Reparaturfoci nach kombinierter Behandlung versus Bestrahlung allein belegt ist.
- Interessanterweise war der Radiosensitivierungseffekt der Zweitgenerationsantiandrogene unabhängig von der Hormonsensitivität (Androgen-abhängig versus Kastrations-resistent), da sich die Einschränkung der DNA-Reparaturkapazität sowohl in hormon-abhängigen LNCaP Zellen, als auch in induzierten hormon-unabhängigen LNCaP-Sublinien ((i) kompletter Androgenentzug (LNCaP-abl), (ii) Abirateron Acetat (LNCaP-abi), (iii) Apalutamid (LNCaP-ARN509), (iv) Enzalutamid (C4-2B-ENZA) zeigte.

- Der radiosensitivierende Effekt der vorgenannten Antiandrogene zeigte sich zusätzlich an *ex-vivo* kultivierten Prostatakarzinomgeweben von 22 Patienten. Auch hier zeigte sich nach kombinierter Behandlung mit Bestrahlung und Zweitgenerationsantiandrogenen eine signifikante Zunahme residueller γ H2AX/53BP1-Reparaturfoci gegenüber der alleinigen Bestrahlung.

Die Ergebnisse liefern wichtige funktionelle Hinweise für einen Einsatz dieser Kombinationsbehandlung zur Verbesserung der klinischen Wirksamkeit einer Strahlentherapie bei Patienten mit lokalisiertem Prostatakarzinom.

Strategie 2:

Für die prä-klinische und translationale Forschung besteht weiterhin großer Bedarf an robusten Prostatakarzinommodellen, die die Biologie der Erkrankung patientennäher reflektieren als die wenigen verfügbaren Zelllinienmodelle. Aus diesem Grund haben wir prä-klinische Modelle basierend auf frischem Tumorgewebe von Prostatakarzinompatienten entwickelt, die die Untersuchung funktioneller Defekte in der homologen Rekombination (HR) erlauben. Ziel war es Patienten mit defizienter HR auf Basis der Wirksamkeit von PARP-Inhibitoren bzw. Cisplatin zu identifizieren (Elsesy et al., 2023). Diese Form der individuellen Behandlungssensitivitätstestung erlaubt eine unmittelbare Translation in maßgeschneiderte klinische Therapiekonzepte basierend auf der Sensitivität individueller Tumoren.

Die wichtigsten Ergebnisse werden wie folgt zusammengefasst:

- Durch eine *ex-vivo* Kultivierung von Prostatakarzinomgewebeproben lässt sich anhand der Untersuchung von residuellen HR-induzierten γ H2AX/53BP1-Reparaturfoci die Wirkung von Olaparib und Cisplatin bei Patienten mit kastrationsresistenter Erkrankung analysieren.
- Wir haben zudem ein Modellsystem zur Kultivierung von Tumor-Organoiden aus primärem Prostatakarzinomgewebe (*patient-derived organoids*, PDOs) entwickelt. Die Organoiden rekapitulieren die morphologische Struktur des Originaltumors und das DNA-Methylierungsmuster der Organoiden ist vergleichbar mit dem primärer Prostatakarzinome und nicht normalem Prostatagewebe oder anderen Tumorentitäten.

Zusammenfassung

- Die Behandlung der PDOs mit Olaparib oder Cisplatin erlaubt wie die vorgenannte *ex-vivo* Kultivierung die Analyse von DNA-Reparaturfoci und PDOs kastrationsresistenter Tumore sind empfindlicher gegenüber dieser Behandlung als PDOs hormonsensitiver Tumore.
- Verglichen mit der *ex-vivo* Gewebekultur repräsentieren PDOs ein robusteres Modell für prä-klinische translationale Forschung.

Die entwickelten prä-klinischen Modelle (*ex-vivo* Gewebekultur und PDOs) erlauben eine individuelle Analyse der HR-Kapazität von Prostatakarzinomen und können für eine Tumorgewebe-basierte Selektion von Patienten für eine Behandlung mit PARP-Inhibitoren und/oder Cisplatin in der Klinik herangezogen werden.

6. Summary

Despite huge improvement in prostate cancer treatment, advanced PCa is still associated with poor outcomes, with CRPC being an incurable disease with limited treatment options. This highlights the urgent need for more tailored therapy that improve the survival of PCa patients. In the current study, we followed two strategies to help improve the treatment of advanced PCa.

Strategy 1:

Previously published pre-clinical data highlight the role of AR-signaling in fuelling the DNA repair machinery, through regulating the expression of several DNA repair genes. Given that IR kills cells by inducing DSBs, we sought in Publication 1 to test the use of ADT to enhance the radiosensitivity of PCa cells (Elsesy et al., 2020). We demonstrate that second generation antiandrogens are potent radiosensitisers that inhibit DSB repair and increase the cytotoxic effect of IR. This conclusion was derived from the following key findings:

- Only the second-generation antiandrogens abiraterone acetate, apalutamide or enzalutamide significantly suppressed cell growth and increased the doubling times upon combination with IR compared to IR alone.
- The radiosensitising effect was attributed to inhibition of DNA repair capacity as evidenced by significantly increased numbers of residual γ H2AX and 53BP1 foci after combined therapy vs. single treatment.
- Interestingly, the second-generation antiandrogen-mediated radiosensitising effect was found to be castration-independent, as it was observed in both hormone-responsive LNCaP cells and in sublines resistant to (i) hormone ablation (LNCaP-abl), (ii) abiraterone acetate (LNCaP-abi), (iii) apalutamide (LNCaP-ARN509), (iv) enzalutamide (C4-2B-ENZA).
- Further validation of this radiosensitization was performed using tumour slice cultures from 22 PCa patients. Again, regardless of their castration status, a significant increase in the number of residual γ H2AX and 53BP1 foci was monitored after combined therapy of IR and abiraterone acetate.

Translated into clinical practice, our results may help to find additional strategies to improve the effectiveness of RT in localized PCa, paving the way for a clinical trial.

Strategy 2:

Currently, there is an urgent need to develop robust pre-clinical models for PCa that are closer to the tumour in-vivo to allow better bench-to bed-side research. In Strategy 2, it was sought to develop pre-clinical models from naive and castration resistant PCa patients that can be used to functionally detect HRR-defects and better stratify PCa patients according to their response to drugs such as PARPi or cisplatin (Elsesy et al., 2023). This individualized drug screening allows immediate translation of treatment sensitivities into tailored clinical therapy recommendations.

Key findings can be summarized as follows:

- Using *ex vivo* tumour slice cultures, a substantial benefit was observed for CRPC patients from olaparib and cisplatin, as evidenced by a significantly increased number of residual IR-induced γ H2AX/53BP1 foci.
- A robust detailed protocol for PDO cultures driven from CRPC-patients was provided. This protocol maintains the morphological structure of the original tumours in the established PDOs.
- The methylome profiling analysis revealed that PDOs are clustered with PCa but not with normal prostate or other tumour entities.
- Employing these PDOs, patients who would benefit from olaparib or cisplatin were identified, validating the results obtained from *ex-vivo* tumour slice cultures.
- Compared to *ex-vivo* tumour slice cultures, PDOs present a more robust pre-clinical cancer model for better translational research, as they allow more functional analyses for survival.

These pre-clinical models allow individualized functional assessment of HRR deficient disease and provide immediate use to select PCa patients for the treatment with the aforementioned drugs in the clinical settings.

7. Erklärung des Eigenanteils an den Publikationen

Name of doctoral candidate: Mohamed E. Elsesy

Publication 1 (Second-Generation Antiandrogen Therapy Radiosensitizes Prostate Cancer Regardless of Castration State through Inhibition of DNA Double Strand Break Repair; **Mohamed E. Elsesy**, Su Jung Oh-Hohenhorst, Anastassia Löser, Christoph Oing, Sally Mutiara, Sabrina Köcher, Stefanie Meien, Alexandra Zielinski, Susanne Burdak-Rothkamm, Derya Tilki, Hartwig Huland, Rudolf Schwarz, Cordula Petersen, Carsten Bokemeyer, Kai Rothkamm and Wael Y. Mansour; *Cancers* (Basel). 2020 Aug 31;12(9):2467. doi: 10.3390/cancers12092467).

My personal contribution in publication 1 includes:

Development and conception of research project, methodology, validation of the data, and writing the original draft of the manuscript.

Publication 2 (Preclinical patient-derived modeling of castration-resistant prostate cancer facilitates individualized assessment of homologous recombination repair deficient disease; **Mohamed E. Elsesy**, Su Jung Oh-Hohenhorst, Christoph Oing, Alicia Eckhardt, Susanne Burdak-Rothkamm, Malik Alawi, Christian Müller, Ulrich Schüller, Tobias Maurer, Gunhild von Amsberg, Cordula Petersen, Kai Rothkamm and Wael Y. Mansour; *Mol Oncol*. 2023 Jan 24. doi: 10.1002/1878-0261.13382).

My personal contribution in publication 2 includes:

Concept/planning of the study, methodology, and writing the original draft of the manuscript.

Mohamed Elsayed Elsesy



Hamburg, 14.04.2023

8. Acknowledgement

In the name of Allah, The Most Gracious and The Most Merciful. First and foremost, thanks to the God, the Almighty, for supporting and blessing me to complete this work successfully.

At the beginning, I would like to express my sincere thanks and gratitude to my supervisor: Prof. Dr. Kai Rothkamm, you have been a tremendous advisor for me. I would like to thank you for encouraging my research and for allowing me to grow as a research scientist.

I would like to express my special appreciation and thanks to my mentor PD. Dr. Wael Mansour for the continuous support of my Ph.D study and related research, for his patience, motivation, and immense knowledge. I am so grateful to him for his sincere efforts and guidance through the entire work.

I thank the German academic exchange service (DAAD) for providing me the scholarship and giving me the opportunity to accomplish my PhD in Germany.

I would like to extend my appreciation and thankfulness also to the whole lab staff, especially Dr. Christoph Oing and Dr. Sabrina Köcher for their sincere help, advice, and wholehearted support through fruitful discussions in lab meetings.

Last but not least, I would like to thank and dedicate this work to my father and my mother for all of the sacrifices that they've made on my behalf. A deep special thanks to my beloved wife and my daughters for giving me all the love and wholehearted support to continue.

9. Curriculum Vitae (CV)

Mohamed Elsayed Elsesy

Date of birth: 05/06/1986 | **Nationality:** Egyptian | **Gender:** Male | **Phone number:** (+20) 1008976520 (Mobile) |

Phone number: (+49) 15205722401 (Work) | **Email address:** mohamed.elsesy@nci.cu.edu.eg | **Email address:** m.elsesy@uke.de |

Address: Department of Radiotherapy and Radiation Oncology, Center for Oncology, UKE, 20246 , Hamburg, Germany (Work)

● WORK EXPERIENCE

06/2016 – CURRENT Egypt

ASSISTANT LECTURER CANCER BIOLOGY DEPARTMENT, NATIONAL CANCER INSTITUTE, CAIRO UNIVERSITY

1-Teaching different subjects in Pharmacology to Nursing students in the National Cancer Institute:

- General (Basic) Pharmacology (Introduction to Pharmacology).
- Drugs affecting the Autonomic Nervous System.
- Drugs affecting the Cardiovascular System.
- Chemotherapeutic Drugs.
- Analgesic Antipyretic Anti-inflammatory Drugs.

Language of instruction: English.

2-Drug monitoring for Cancer Patients using (Viva-E Drug Testing System) (SIEMENS).

3-Using HPLC-UV/VIS and LC- MS/MS in the analysis of different molecules.

4-Screening for anti-cancer agents using different tissue culture techniques.

Address Kasr EL-Aini Street-Fom EL- Khalig, 11796, Cairo, Egypt | **Website** <http://www.nci.cu.edu.eg>

06/2009 – 06/2016 Egypt

TEACHING ASSISTANT (DEMONSTRATOR) CANCER BIOLOGY DEPARTMENT, NATIONAL CANCER INSTITUTE, CAIRO UNIVERSITY

Address Cairo, Egypt

● EDUCATION AND TRAINING

09/2013 – 09/2015 Lincoln, United Kingdom

MASTER'S DEGREE IN PHARMACEUTICAL SCIENCES (PHARMACOLOGY) EQUALISED BY THE SUPREME COUNCIL OF UNIVERSITIES IN EGYPT Master's in Forensic Science (Biology) , College of Science, University of Lincoln

Address Lincoln, United Kingdom | **Final grade** Distinction

2011 – 2012 Cairo, Egypt

PASSED THE MASTER'S GENERAL & SPECIAL COURSES IN PHARMACEUTICAL SCIENCES WITH THE GENERAL GRADE "EXCELLENT". Pharmacology And Toxicology Dep., Faculty of Pharmacy, Ain Shams University

Address Cairo, Egypt

2009 – 2010 Cairo, Egypt

PASSED THE PRE-MASTER COURSE WORK (GENERAL & SPECIALIZED COURSES) IN PHARMACEUTICAL SCIENCES WITH CUMULATIVE GPA 3.5/4 . Pharmacology And Toxicology Dep., Faculty of Pharmacy, Cairo University

Address Cairo, Egypt

Curriculum Vitae

2003 – 2008 6th of October, Egypt

BACHELOR'S DEGREE IN PHARMACEUTICAL SCIENCES WITH GENERAL GRADE "EXCELLENT WITH HONORS" 90.8% Faculty of Pharmacy- Misr University for Science & Technology

Address 6th of October, Egypt

20/11/2012 – 22/11/2012 Darmstadt, Germany

ADVANCED TRIPLE QUAD LC/MS/MS TRAINING (THEORETICAL & PRACTICAL) AB SCIEX
Germany GmbH

Address Darmstadt, Germany

● LANGUAGE SKILLS

Mother tongue(s): **ARABIC**

Other language(s):

	UNDERSTANDING		SPEAKING		WRITING
	Listening	Reading	Spoken production	Spoken interaction	
ENGLISH	C1	C1	B2	B2	C1
GERMAN	B1	B1	B2	B2	B1

Levels: A1 and A2: Basic user; B1 and B2: Independent user; C1 and C2: Proficient user

● ADDITIONAL INFORMATION

PUBLICATIONS

[Preclinical patient-derived modelling of castration-resistant prostate cancer facilitates individualized assessment of homologous recombination repair deficient disease](#)

– 2023

[The natural isoflavone Biochanin-A synergizes 5-fluorouracil anticancer activity in vitro and in vivo in Ehrlich solid-phase carcinoma model.](#)

– 2022

[Second-Generation Antiandrogen Therapy Radiosensitizes Prostate Cancer Regardless of Castration State through Inhibition of DNA Double Strand Break Repair.](#)

– 2020

[Improved chemo-photothermal therapy of hepatocellular carcinoma using chitosan-coated gold nanoparticles.](#)

– 2018

[Anticancer potentiality of lignan rich fraction of six Flaxseed cultivars.](#) – 2018

NETWORKS AND MEMBERSHIPS

Memberships Associate member of American Association Cancer Research. AACR ID: 341082

CONFERENCES AND SEMINARS

27/09/2021 – 29/09/2021 – Online-Konferenz

Deutschen Gesellschaft für Biologische Strahlenforschung (DeGBS)

27/08/2021 – 28/08/2021 – Online-Konferenz

XIII. UCCH Research Retreat 2021

24/06/2021 – 26/06/2021 – Online-Konferenz

27. Jahrestagung der DEGRO

Curriculum Vitae

30/08/2019 – 31/08/2019 – Tagungshotel, Jesteburg (Germany)

XI. UCCH Research Retreat 2019

03/04/2013 – 05/04/2013 – Grand Hyatt hotel, Cairo (Egypt)

NCI 45 Years Against Cancer in Egypt, Updates on Breast and GIT Cancer

23/10/2009 – 27/10/2009 – Grand Hyatt hotel, Cairo (Egypt)

The 15th Annual Multidisciplinary Symposium on Breast Diseases and the First International Breast Health Education Program

HONOURS AND AWARDS

Honours and awards

- Erasmus Mundus Scholar European Commission EACEA (Education, Culture and Audiovisual Executive Agency) 2013
- DAAD scholarship 2017

ACKNOWLEDGMENTS

Acknowledgments

Hany A. Omar and Mai F. Tolba. **Caffeic Acid Phenethyl Ester Guards against Benign Prostate Hypertrophy in Rats: Role of IGF 1R/Protein Kinase-B (Akt)/b-Catenin Signaling.** IUBMB Life, 2018. Acknowledged by the authors for the contribution in the practical part.

SOCIAL ACTIVITIES

Social Activities

- Teaching Arabic to Non-Arabic Speakers in the Arabic School, Lincoln, United Kingdom, 2014.
- Attended Spanish language and culture course, 11 September to 26 October 2013, Cordoba University, Cordoba, Spain.

Place, Date:

Hamburg, 14.04.2023

Signature:



10. Eidesstattliche Erklärung

Ich versichere ausdrücklich, dass ich die Arbeit selbständig und ohne fremde Hilfe verfasst, andere als die von mir angegebenen Quellen und Hilfsmittel nicht benutzt und die aus den benutzten Werken wörtlich oder inhaltlich entnommenen Stellen einzeln nach Ausgabe (Auflage und Jahr des Erscheinens), Band und Seite des benutzten Werkes kenntlich gemacht habe.

Ferner versichere ich, dass ich die Dissertation bisher nicht einem Fachvertreter an einer anderen Hochschule zur Überprüfung vorgelegt oder mich anderweitig um Zulassung zur Promotion beworben habe.

Ich erkläre mich einverstanden, dass meine Dissertation vom Dekanat der Medizinischen Fakultät mit einer gängigen Software zur Erkennung von Plagiaten überprüft werden kann.

Unterschrift: Abdullah G. Alres